

Acknowledgments

I would like to express my sincere thanks and deep gratitude to my supervisors **Prof. Dr. Sabah M. Juma** and **Dr. Fatin Abdul Jalil Al-Moudarris** for supervising the present work and for their support and encouragement throughout the research.

I am most grateful to the Dean of College of Science and the staff of the Department of Physics at Al-Nahrain University, particularly **Dr. Azhaar Jawad Dawood** for their valuable support and cooperation.

The assistance given by the staff of the library of the College of Science at Baghdad University is highly appreciated.

Finally, I most grateful to my **parents**, my brothers **Haider, Mohammed,** and **Ahmad,** and my sisters **Shaima'a, Suiroor,** and **Shahad** for their patience and encouragement throughout this work, and to my friends **Shereen Abdul-Qadir, Itab Fadhil, Basma Hussain,** and **Rana Abid Hamza,** for their encouragement, and to **Ammar Al-Rawi, Wesam Fawzi,** and **Sadeem Abbaas** for their support.

Isra'a

Certification

We certify that this thesis entitled “**Computations on the Optical Properties of a Triplet Electrostatic Quadrupole Lens**” is prepared by **Miss Isra'a Lateef Mohammad Al-Omairi** under our supervision at the College of Science of Al-Nahrain University in partial fulfillment of the requirements for the degree of **Master of Science in Physics**.

Supervisor: Prof. Dr. Sabah M. Juma

Supervisor: Dr. Fatin Abdul Jalil

Al-Moudarris

Date: / / 2005

Date: / / 2005

In view of the recommendations, we present this thesis for debate by the examination committee.

Dr. Ahmad K. Ahmad

Head of Physics Department

Date: / / 2005

Examination Committee Certification

We certify that we have read the thesis entitled **Computations on the Optical Properties of a Triplet Electrostatic Quadrupole Lens**, and as an examination committee, examined the student **Miss. Isra'a Lateef Mohammad Al-Omairi** on its contents, and that in our opinion it is adequate for the partial fulfillment of the requirements for the degree of **Master of Science in Physics**.

Signature:

Name: Dr. Ayad A. Al-Ani

Title: (Chairman)

Date: / / 2005

Signature:

Name: Dr. Ahmad K. Ahmad

Title: (Member)

Date: / / 2005

Signature:

Name: Prof. Dr. Sabah M. Juma

Title: Professor (Supervisor)

Date: / / 2005

Signature:

Name: Dr. Sameer Khedhir Al-Ani

Title: (Member)

Date: / / 2005

Signature:

Name: Dr. Fatin Abdul Jalil

Al-Moudarris

Title: (Supervisor)

Date: / / 2005

Approved by the University Committee of Postgraduate Studies

Signature:

Name: Dr. Laith A. Al-Ani

Title:

Dean of College of Science

Date: / / 2005

1. ELECTROSTATIC QUADRUPOLE LENSES

1.1 Electrostatic Lenses

Electrostatic lenses are finding increasing applications in many areas and technology, because of their versatility and the rapid development of modern instrumentation. With the aid of electrostatic lenses, ion probes are employed in ion implantation to change the local properties of semiconductors. Electron probes are widely utilized in industry to fabricate miniature semiconductor devices by electron lithography. Electrostatic lenses have the following most important features (**Szilagyi 1988, Hawkes and Kasper 1989**):-

(a) For the non-relativistic cases the focusing properties as well as the aberrations are independent of the charge-to-mass quotient of the particles. Therefore, electrostatic lenses may be used for focusing various ions.

(b) Potential ratios have influence on the lens properties. Therefore, if particles of the opposite sign have to be focused, the signs of all electrode potentials must be reversed to arrive at the same properties. The particles trajectory remains the same if both the sign of the particles charge and the electrode potentials are reversed.

(c) Electrostatic lenses are characterized by their simple electrodes fabrication, alignment, small size, and relatively light weight. Furthermore, their low power requirements suggest the need of lighter and more stable power supplies. The major manufacturing problems are electric breakdown and accumulation of charges on the insulating surfaces. Under vacuum

pressure of about 10^{-6} torr the electrodes must be separated from each other so that the maximum field strength does not exceed 15 kV/mm (**Szilagyi 1988, Hawkes and Kasper 1989**).

1.2 Quadrupole Lenses

There are many electron and ion optical instruments and devices in which there are advantages in using quadrupole lenses rather than round lenses, such as instruments where strong focusing or astigmatic properties are needed. Among these are accelerators, cathode-ray tubes, and devices for correcting aberrations. For example, in electron and mass spectrometers containing sector magnets or electrostatic cylindrical analyzers which are themselves astigmatic, quadrupole lenses enable better beam matching than conventional axially symmetrical lenses. There are also some applications of astigmatic quadrupole lenses in probe-forming systems when an elliptical or linear beam spot is needed rather than a round one (**Baranova and Read 1998**). Probe-forming quadrupole lens provides the following advantages; first, it permits variable spot-shaping by changing the lens excitation; second, the demagnification can be increased without increasing the working distance (**Okayama 1989**).

Electrostatic quadrupole lenses, although effective in focusing ions of high mass, have chromatic aberration coefficients which can be considerable. Quadrupole lenses are also commonly used for focusing an electron or ion beam in high energy devices. An example of such device is the ion implanter (**Martin 1991**).

Electrostatic quadrupole lenses are often preferable to magnetic ones for focusing beams of moderate energy. They are also preferable for dealing

with ion beams since the focal length of an electrostatic lens does not depend on the charged particles mass as it does for a magnetic lens. However, quadrupole lens systems are more sensitive to mechanical defects than round ones (**Baranova and Read 2001**).

An electrostatic quadrupole lens has a four-fold symmetry with respect to the optical axis. Its adjacent electrodes are at 45° with each other. Their construction is not of the conventional round lenses for they are sensitive to mechanical tolerances. The detailed description of their potential arrangement is shown in figure 1.1b, where e_1 and e_1° are at a potential $+U_1$ and the other pair of electrodes e_2 and e_2° are set at a potential $-U_1$. The planes that do not intersect the electrodes are defined by zOX and zOY and the other planes, which intersect the electrodes, are defined by zOx and zOy . The z -axis is normal to the plane of the paper at O . The aperture of the lens is defined by the radius c of a circular channel, which is tangential to the four electrodes.

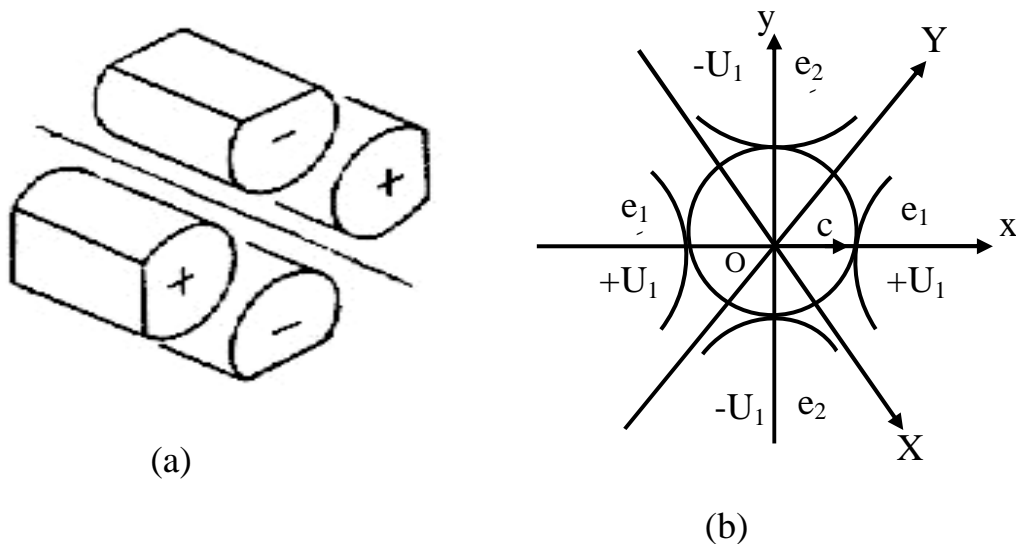
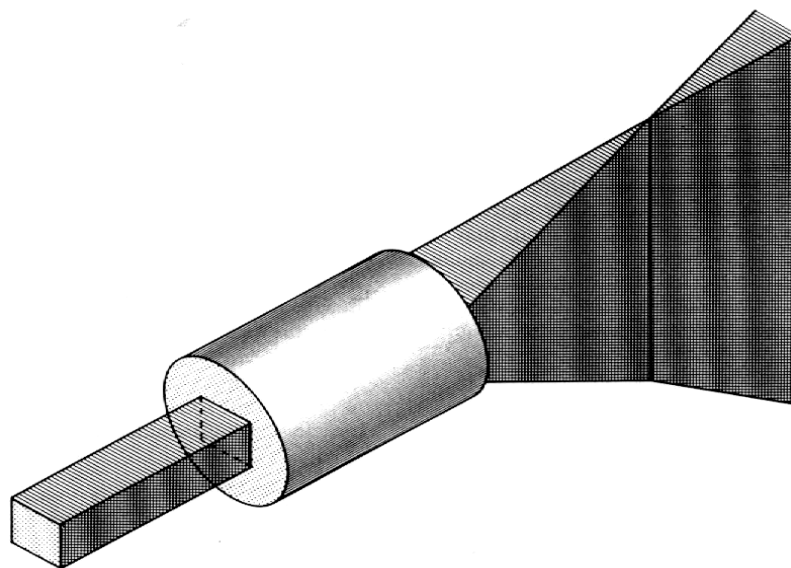


Figure 1.1. A transverse cross-section of an electrostatic quadrupole lens (Grivet 1972).

If a positively-charged particle is incident parallel to the axis in the plane zOx , it will experience a repulsion due to the electrode e_1 (or e_1°), but will not be affected by the presence e_2 and e_2° as a results of the symmetry. The particle will remain in the plane zOx , and will converge toward the axis. In the plane zOy , the trajectory will also be planar, but the particle will be attracted by e_2 (or e_2°) and will diverge away from the axis. Particles, which are incident at the lens, other than in the planes zOx and zOy , will follow skew trajectories, approaching the optical axis Oz in the Ox direction, but moving away from Oz in the Oy direction. Therefore, in one direction there is the effect of convergence and in the other of divergence as shown in figure 1.2. A quadrupole lens is described as converging if particles moving in $x-z$ plane are deflected toward the axis and diverging if the particles moving in the $y-z$ plane are deflected away from the axis (**Grime and Watt 1988**).



*Figure 1.2. The action of a single quadrupole lens on a charged-particles beam; convergence in the horizontal plane and divergence in the vertical plane form a line image (**Grime and Watt 1988**).*

Studies on quadrupole lenses concentrated on their application as corrector units for reducing the spherical aberration (**Hawkes 1970**). However, there are some difficulties in such application since there are a number of variables in any quadrupole system. Nevertheless, the rewards to be gained from a successful quadrupole system are very great, and it seems unlikely that they can be achieved by any other round lenses with less difficulty.

1.3 Three-Element Quadrupole Lens System

A quadrupole doublet is employed in electron-optical devices of moderate accelerating voltage when astigmatic focusing is required. Although the triplet follows the doublet in order of increasing complexity, it is not an inviting combination from the optical point of view. In general, regularity will be achieved by adjusting the three excitations and the two separations once the design of the individual components has been decided (in particular, their effective lengths). The symmetric triplet does, however, offer convenient means of converting a virtual image into a real one with unit magnification. Blewett in 1958 has tabulated few values of the parameters of symmetric triplets for which the imagery is stigmatic. Most published information is in graphical form; however, in 1961 Enge has plotted families of curves illustrating the behavior of a symmetric triplet producing pseudo-stigmatic imagery (**Hawkes 1970**).

Consider figure 1.3a. The length of the central quadrupole is L_2 and the outer components are of lengths L_1 and L_3 . It is seen that the object and image distances (u and v respectively) are the same in both planes. The present work has been focused on symmetric triplets, which means that voltages applied to the first and third quadrupoles are the same. This

reduction of the number of variable parameters makes the tuning of the triplet much easier than doublet while at the same time the triplet remains flexible enough to satisfy various requirements in the first order focusing properties. Voltages are applied to the triplet in such a way that in both x - z and y - z planes converging and diverging lenses alternate. The y - z plane has been taken to be the DCD (diverging-converging-diverging) plane and x - z plane to be the CDC (converging-diverging-converging) plane (**Baranova and Read 1998**).

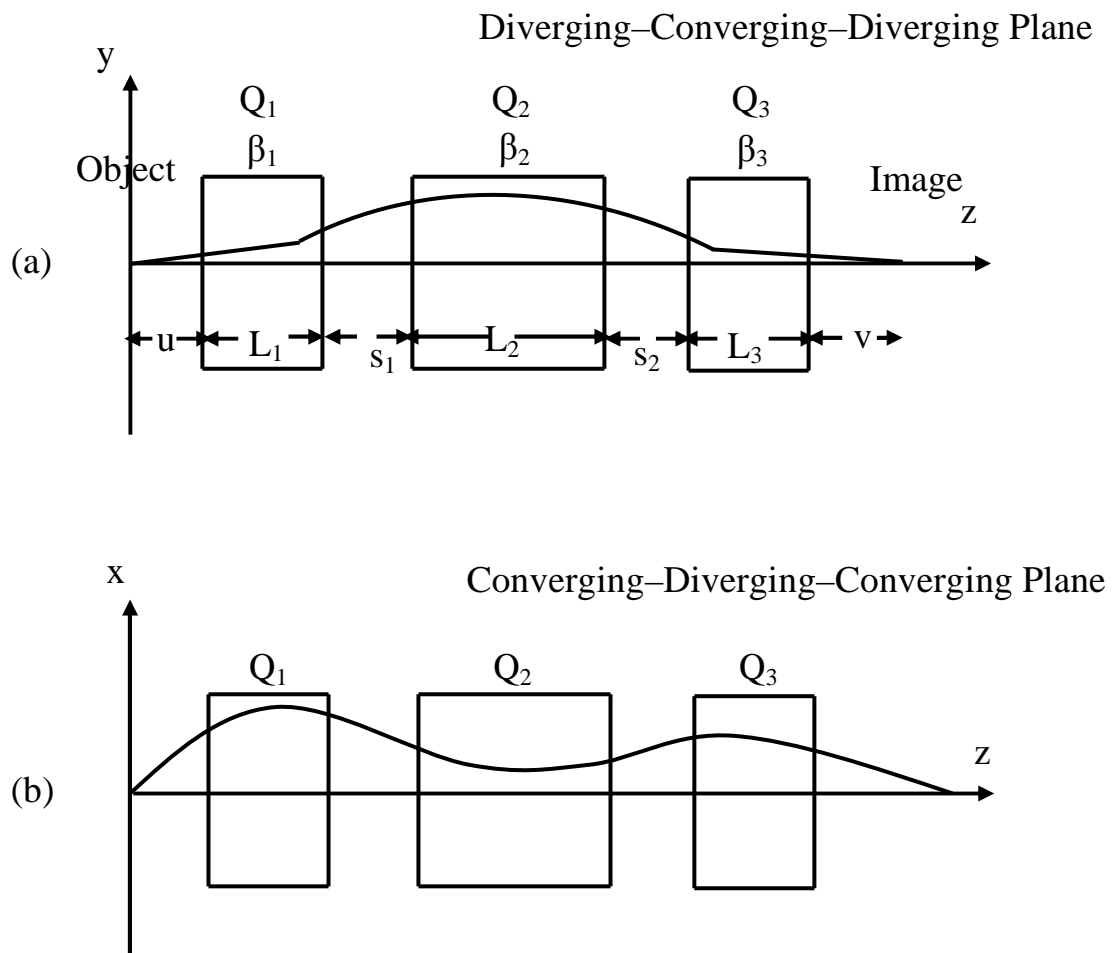


Figure 1.3. Particle trajectories in the two planes of three-element quadrupole lens system (**Engel 1961**).

For the complete three–element lens system, the notations used are as follows: (a) the lens excitation parameter is denoted by β (which will be described in Chapter Two), (b) the field–free distance between the quadrupole lenses is denoted by s i.e. the distance between the first quadrupole lens Q_1 and second quadrupole lens Q_2 is s_1 , and that between second quadrupole lens Q_2 and third quadrupole lens Q_3 is s_2 as shown in figure 1.3a, and (c) the object and image distance u and v respectively.

In stigmatic modes the beam crossover in the x – z plane and y – z plane coincide. In this case the linear magnifications of a doublet are generally quite different in the x and y directions, which might be a limitation for some applications. The triplet allows the magnification ratio to be varied without changing the image position and it can be made equal to unity if necessary (**Baranova and Read 1999**).

1.4 Aim of the Project

A simple quadrupole lens forms a real image in its converging plane and a virtual image in its diverging plane. Since, in practice, a focusing system requires in general a real image in both planes, hence a quadrupole triplet lens has been considered to achieve such requirement. A system consisting of three quadrupole lenses at opposite polarity and separated by drift space is to be investigated in detail. The optical properties of the triplet and the beam trajectory along the fields are to be considered. The present work is mostly restricted to the symmetric triplet for its advantage of remaining flexible enough to satisfy various requirements in the first order focusing properties. The rectangular field model has been taken into consideration to represent the potential distribution of an electrostatic quadrupole triplet

lens. This model has been described in Chapter Two; its distribution resembles the actual field of hyperbolic quadrupoles more accurately. It is aimed in the present work at determining the properties of such lens. The first order optical properties of this model will be computed by solving the trajectory equation of the charged-particles beam traversing each field distribution, taking into account the convergence and divergence planes. The effect of the lens excitation, image and object distance, lens length, and the separation between the lenses on the spherical aberration coefficients will be investigated in detail.

2. PROPERTIES OF ELECTROSTATIC QUADRUPOLE LENSES

2.1 Field Models for Electrostatic Quadrupole Lenses

The field distribution of a quadrupole lens may be represented by various models shown in figure 2.1. These potential distribution models are actually proposed for the hyperbolic cross-section of the quadrupole lens electrodes (**Hawkes 1965/1966**). According to Hawkes the function $f(z)$ of the field distribution can be obtained either by measurement or by computation, and it may transpire that some mathematically convenient model represents $f(z)$ sufficiently. For example, for long narrow quadrupole lenses, the rectangular model figure 2.1a is often a close enough approximation.

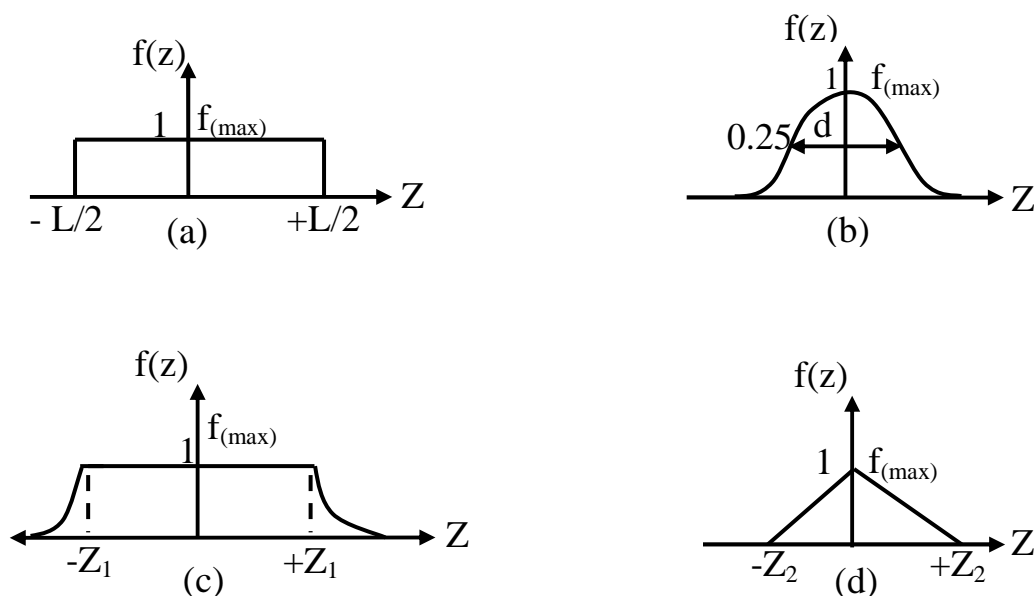


Figure 2.1. Field distribution of a quadrupole lens (**Hawkes 1965/1966**).

(a) Rectangular model

(b) Bell-shaped model

(c) Modified bell-shaped model

(d) Triangular model.

The function $f(z)$ for a rectangular field model of long quadrupole is represented in the following form:

$$f(z) = (f(z))_{\max} = 1 \quad \text{when } -L/2 \leq z \leq L/2 \quad \dots(2.1)$$

At points when $|z| > L/2$ the function $f(z) = 0$. This model is also known as the square-top field distribution. In practice, the length L is the “effective length” which has been found experimentally to be given by (**Hawkes 1970**):

$$L = \ell + 1.1c \quad \dots (2.2)$$

where ℓ is the electrode length and c is the bore radius which is assumed to be very small. According to Hawkes (1970) the coefficient 1.1 of c was measured experimentally by Septier in 1958; however, it has been proposed theoretically by Reisman in 1957. Therefore, the effective length L could be equal to the electrode length ℓ by neglecting the second term of equation (2.2) i.e. $L \approx \ell$. In the present work the rectangular field model has been taken into account since the accuracy and simplicity of this model make it a basic tool.

For short quadrupole lens, Glaser's bell-shaped field model shown in figure 2.1b is found to be more suitable and is represented by the following function (**Hawkes 1970**):

$$f(z) = (f(z))_{\max} / [1 + (z/d)^2]^2 = 1 / [1 + (z/d)^2]^2 \quad \dots (2.3)$$

The excitation parameter β is expressed in mm^{-1} . For a short quadrupole lens the square of the excitation parameter β^2 is given by:

$$\beta^2 = (V / c^2 U_o (1 + \varepsilon U_o)) (1 - (c^2 / 3d^2)) \quad \dots (2.4)$$

where

V = accelerating voltage which must be corrected relativistically at high values of V [i.e. $V_r = V (1 + 10^{-6} V)$].

U_o = the accelerating voltage (volt).

ε = relativistic modification factor: $\varepsilon = e / 2 m_o w^2 \approx 10^{-6} \text{ V}^{-1}$ or MV^{-1} .

e = electron charge ($1.6 \times 10^{-19} \text{ C}$).

m_o = electron rest mass ($9.1 \times 10^{-31} \text{ kg}$).

w = speed of light in a vacuum ($\approx 3 \times 10^8 \text{ m/sec}$).

c = the bore radius (mm).

d = the axial extension of the field between the two points where $f(z) = (f(z))_{\text{max}}/4$; at $z = 0$, $(f(z))_{\text{max}}$ equals to unity.

For a short lens, $c \approx d$; the value of d is determined by the shape of the electrodes (**Hawkes 1970**).

The modified bell-shaped field model shown in figure 2.1c represents the intermediate case between the rectangular and the bell-shaped model such that the field distribution may be represented by the following function:

$$f(z) = 1 / [1 + ((z - z_1)/d)^2]^2 \quad \text{when } z > z_1 \quad \dots (2.5)$$

$$f(z) = 1 / [1 + ((z + z_1)/d)^2]^2 \quad \text{when } z < -z_1 \quad \dots(2.6)$$

The function $f(z)$ has a rectangular section of constant maximum value $(f(z))_{\max}=1$ in the region $-z_1 \leq z \leq z_1$ such that beyond these boundaries it terminates in the form of a half bell-shaped field represented by equations (2.5) and (2.6).

The triangular field distribution model shown in figure 2.1d is another model proposed by **Hawkes (1965/1966)**; it is given by:

$$f(z) = \Phi z + z_2 \quad \text{when } -z_2 \leq z \leq 0 \quad \dots (2.7a)$$

$$f(z) = -\Phi z + z_2 \quad \text{when } 0 \leq z \leq z_2 \quad \dots (2.7b)$$

$$f(z) = (f(z))_{\max} = 1 \quad \text{at } z = 0 \quad \dots (2.7c)$$

where Φ is the slope of the two steep sides of the triangle.

2.2 Quadrupole Lens Potential Distributions

The potential of an electrostatic quadrupole system with two planes of symmetry in cylindrical coordinates has the following representation (**Okayama and Kawakatsu 1978**):

$$U(r, \theta, z) = [r^2 \cos 2\theta (D_2(z) - 1/12 D''_2(z) r^2 + 1/384 D''''_2(z) r^4 - \dots)] + [r^6 \cos 6\theta (D_6(z) - 1/28 D''_6(z) r^2 + \dots)] + [r^{10} \cos 10\theta (D_{10}(z) - 1/44 D''_{10}(z) r^2 + \dots)] + [r^{14} \cos 14\theta (D_{14}(z) - 1/60 D''_{14}(z) r^2 + \dots)] + \dots \quad \dots (2.8)$$

where

$$D_2(z) = U_1 f_2(z)/c^2$$

$$D_6(z) = U_1 f_6(z)/c^6$$

$$D_{10}(z) = U_1 f_{10}(z)/c^{10}$$

$$D_{14}(z) = U_1 f_{14}(z)/c^{14}$$

U_1 denotes the numerical value of the electrostatic potential supplied to each of the four electrodes, c denotes the aperture radius of the quadrupole lens, $f_2(z)$, $f_6(z)$, $f_{10}(z)$, and $f_{14}(z)$ are the characteristic functions representing the potential distribution, and the primes denote the derivatives with respect to z . The first term in equation (2.8) refers to an ideal quadrupole field that has been formed by four hyperbolic electrodes. If the cross-section of the electrode is considered different from the ideal hyperbolic shape, the effect of $\cos 6\theta$ and other higher terms appears. The expression of potential distribution in equation (2.8) in cylindrical coordinates can be expressed in Cartesian coordinates as shown below.

$r = (x^2 + y^2)^{1/2}$, then one can simply write

$$r^{2n} = (x^2 + y^2)^n \quad \dots (2.9)$$

By using the following expressions (**Szilagyi 1988**):

$$r^2 \cos(2\theta) = (x^2 - y^2) \quad \dots (2.10)$$

$$r^6 \cos(6\theta) = x^6 - y^6 - 3(x^4 y^2 - x^2 y^4) \quad \dots (2.11)$$

$$r^{10} \cos(10\theta) = x^{10} - y^{10} - 45(x^8 y^2 - x^2 y^8) + 210(x^6 y^4 - x^4 y^6) \quad \dots (2.12)$$

with the relationship given by equation (2.9) and substituting in equation (2.8) one can get the general expression for the potential distribution in Cartesian coordinates (**Baartman 1995**):

$f(z) = 0$ outside (i.e. $-L/2 > z > L/2$). Equations (2.14) and (2.15) give the values of x and y . If, for example, the origin of the Oz axis is taken in the entry plane of the lens then:

$$x = x_o \cos (\beta z) + x_o' (1/\beta) \sin (\beta z) \quad \dots (2.17)$$

$$x' = -x_o \beta \sin (\beta z) + x_o' \cos (\beta z) \quad \dots (2.18)$$

$$y = y_o \cosh (\beta z) + y_o' (1/\beta) \sinh (\beta z) \quad \dots (2.19)$$

$$y' = y_o \beta \sinh (\beta z) + y_o' \cosh (\beta z) \quad \dots (2.20)$$

where x_o and y_o are the initial displacements from the optical axis in the x - z and y - z plane respectively, and x_o' and y_o' are the initial gradients of the beam in the corresponding planes.

Equations (2.14) and (2.15) can equally be integrated for other forms of the function $f(z)$, but the calculations become more complicated. The approximation of the rectangular model gives results, which are satisfactory to within few per cent; in domain of quadrupole lenses, the accuracy and simplicity of this model make it a basic tool (**Grivet 1972**). Thus the rectangular field model has been taken into account in the present investigation to represent the potential distribution of the quadrupole lenses under consideration.

The general solution of the second-order linear homogeneous differential equations (2.14) and (2.15) can always be written in the following matrix form respectively.

$$\begin{pmatrix} x(z) \\ x'(z) \end{pmatrix} = T_c \begin{pmatrix} x_o(z) \\ x_o'(z) \end{pmatrix} \quad \dots (2.21)$$

$$\begin{pmatrix} y(z) \\ y'(z) \end{pmatrix} \quad \begin{pmatrix} y_o(z) \\ y_o'(z) \end{pmatrix}$$

$$= T_D \quad \dots (2.22)$$

The parameters T_C and T_D are the transfer matrices in the convergence plane xOz and the divergence plane yOz respectively which are given by **Larson 1981** and **Szylagyi 1988**:

$$T_C = \begin{pmatrix} \cos \beta L & 1/\beta \sin \beta L \\ -\beta \sin \beta L & \cos \beta L \end{pmatrix} \quad \dots (2.23)$$

$$T_D = \begin{pmatrix} \cosh \beta L & 1/\beta \sinh \beta L \\ \beta \sinh \beta L & \cosh \beta L \end{pmatrix} \quad \dots (2.24)$$

As already noted, the single quadrupole lens always diverges in one plane and converges in the other. However, two singlet lenses can be placed sequentially along the optical axis to form a doublet lens structure. If the electrodes polarities are opposite in the two lenses then convergence in one plane is followed by divergence i.e. CD, and divergence in the orthogonal plane is followed by convergence i.e. DC. The action of the doublet on an initially parallel beam is shown in figure 2.2 from which it can be seen that the beam is brought to a focus in the axis at a different position in the two planes. This situation is called astigmatic. By using a doublet in which the components are of unequal strength, it is possible to make the foci, f_x and f_y coincident. However, the magnification in the two planes will be unequal. The action, therefore, is not truly stigmatic and the term pseudo-stigmatic has been used to describe the situation. True stigmatism can only be achieved with two or more doublets or with one or

more triplets. The astigmatism of a doublet is not necessarily a disadvantage (**Banford 1966**). For instance, the focusing properties of spectrometers in general differ in the two orthogonal planes of deflection and must therefore be combined with astigmatic lenses (e.g. a quadrupole lens) in order to get a stigmatic beam image at the exit. Furthermore, quadrupole lenses may be used to vary the beam dimensions independently in the two perpendicular directions.

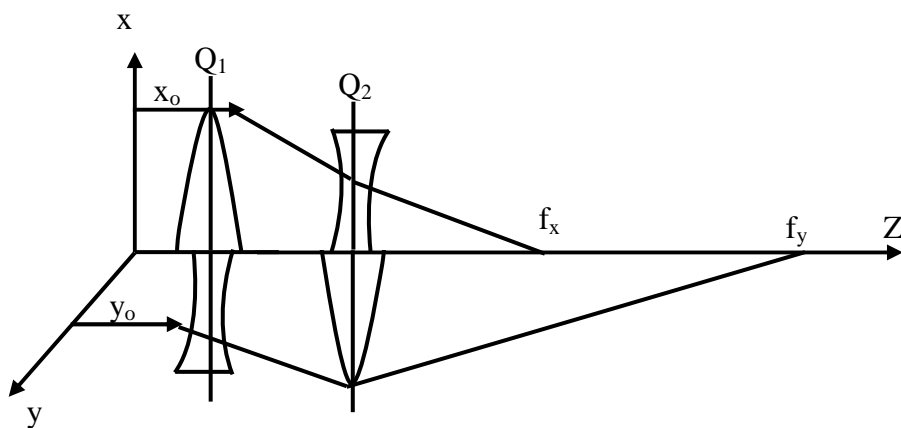


Figure 2.2. Beam trajectory in quadrupole doublet (Banford 1966).

The next degree of sophistication is a system of three quadrupoles rotated by 90° with respect to each neighbor about the optical axis z . Such a system is called a quadrupole triplet. In the rectangular model there are three rectangles of alternating polarity separated from each other by two drift spaces. If the two outer quadrupoles are identical with each other and they are equally separated from the central one by drift spaces of length s each, the $f(z)$ function is symmetric with respect to the mid-plane of the central quadrupole. Then one would have a symmetric triplet as shown in figure 1.3. If the individual elements of the symmetric triplet are thin lenses, its transfer matrix can be simply as follows:

$$T_{\text{triplet}} = \begin{pmatrix} 1 & 0 \\ \pm 1/F_{\text{out}} & 1 \end{pmatrix} \begin{pmatrix} 1 & s \\ 0 & 1 \end{pmatrix} \begin{pmatrix} 1 & 0 \\ \pm 1/F_{\text{cent}} & 1 \end{pmatrix} \begin{pmatrix} 1 & s \\ 0 & 1 \end{pmatrix} \begin{pmatrix} 1 & 0 \\ \pm 1/F_{\text{out}} & 1 \end{pmatrix}$$

where F_{out} and F_{cent} are the focal lengths of the outer and central lenses, respectively. The upper signs correspond to the plane where the central lens is focusing (**Szilagyi 1988**).

Matrices for quadrupole triplet are given as follows (**Regenstreif 1967** and **Larson 1981**):

$$T_{\text{CDC}} = \begin{pmatrix} \cos \beta_3 L_3 & 1/\beta_3 \sin \beta_3 L_3 \\ -\beta_3 \sin \beta_3 L_3 & \cos \beta_3 L_3 \end{pmatrix} \begin{pmatrix} 1 & s_2 \\ 0 & 1 \end{pmatrix} \begin{pmatrix} \cosh \beta_2 L_2 & 1/\beta_2 \sinh \beta_2 L_2 \\ \beta_2 \sinh \beta_2 L_2 & \cosh \beta_2 L_2 \end{pmatrix} \begin{pmatrix} 1 & s_1 \\ 0 & 1 \end{pmatrix} \\ \begin{pmatrix} \cos \beta_1 L_1 & 1/\beta_1 \sin \beta_1 L_1 \\ -\beta_1 \sin \beta_1 L_1 & \cos \beta_1 L_1 \end{pmatrix} \dots (2.25)$$

$$T_{\text{DCD}} = \begin{pmatrix} \cosh \beta_3 L_3 & 1/\beta_3 \sinh \beta_3 L_3 \\ \beta_3 \sinh \beta_3 L_3 & \cosh \beta_3 L_3 \end{pmatrix} \begin{pmatrix} 1 & s_2 \\ 0 & 1 \end{pmatrix} \begin{pmatrix} \cos \beta_2 L_2 & 1/\beta_2 \sin \beta_2 L_2 \\ -\beta_2 \sin \beta_2 L_2 & \cos \beta_2 L_2 \end{pmatrix} \begin{pmatrix} 1 & s_1 \\ 0 & 1 \end{pmatrix} \\ \begin{pmatrix} \cosh \beta_1 L_1 & 1/\beta_1 \sinh \beta_1 L_1 \\ \beta_1 \sinh \beta_1 L_1 & \cosh \beta_1 L_1 \end{pmatrix} \dots (2.26)$$

where s_1 and s_2 represent the separations (usually small) between lenses; subscript “1” refers to the first lens, “2” to the second lens, and “3” to the

third one. By carrying out the calculations, the various matrix elements can be found as follows:

$$\begin{aligned}
 a_{11CDC} = & \cos \theta_1 \cos \theta_3 \cosh \theta_2 + s_2 \beta_2 \cos \theta_1 \cos \theta_3 \sinh \theta_2 + (\beta_2 / \beta_3) \cos \theta_1 \\
 & \sin \theta_3 \sinh \theta_2 - s_1 \beta_1 \sin \theta_1 \cos \theta_3 \cosh \theta_2 - s_1 s_2 \beta_1 \beta_2 \sin \theta_1 \cos \theta_3 \sinh \theta_2 - \\
 & s_1 (\beta_1 \beta_2 / \beta_3) \sin \theta_1 \sin \theta_3 \sinh \theta_2 - (\beta_1 / \beta_2) \sin \theta_1 \cos \theta_3 \sinh \theta_2 - s_2 \beta_1 \sin \theta_1 \\
 & \cos \theta_3 \cosh \theta_2 - (\beta_1 / \beta_3) \sin \theta_1 \sin \theta_3 \cosh \theta_2 \quad \dots(2.27a)
 \end{aligned}$$

$$\begin{aligned}
 a_{12CDC} = & (1 / \beta_1) \sin \theta_1 \cos \theta_3 \cosh \theta_2 + s_2 (\beta_2 / \beta_1) \sin \theta_1 \cos \theta_3 \sinh \theta_2 + (\beta_2 / \\
 & \beta_1 \beta_3) \sin \theta_1 \sin \theta_3 \sinh \theta_2 + s_1 \cos \theta_1 \cos \theta_3 \cosh \theta_2 + s_1 s_2 \beta_2 \cos \theta_1 \cos \theta_3 \\
 & \sinh \theta_2 + s_1 (\beta_2 / \beta_3) \cos \theta_1 \sin \theta_3 \sinh \theta_2 + (1 / \beta_2) \cos \theta_1 \cos \theta_3 \sinh \theta_2 + s_2 \\
 & \cos \theta_1 \cos \theta_3 \cosh \theta_2 + (1 / \beta_3) \cos \theta_1 \sin \theta_3 \cosh \theta_2 \quad \dots(2.27b)
 \end{aligned}$$

$$\begin{aligned}
 a_{21CDC} = & -\beta_3 \cos \theta_1 \sin \theta_3 \cosh \theta_2 - s_2 \beta_2 \beta_3 \cos \theta_1 \sin \theta_3 \sinh \theta_2 + \beta_2 \cos \theta_1 \\
 & \cos \theta_3 \sinh \theta_2 + s_1 \beta_1 \beta_3 \sin \theta_1 \sin \theta_3 \cosh \theta_2 + s_1 s_2 \beta_1 \beta_2 \beta_3 \sin \theta_1 \sin \theta_3 \\
 & \sinh \theta_2 - s_1 \beta_1 \beta_2 \sin \theta_1 \cos \theta_3 \sinh \theta_2 + (\beta_1 \beta_3 / \beta_2) \sin \theta_1 \sin \theta_3 \sinh \theta_2 + s_2 \\
 & \beta_1 \beta_3 \sin \theta_1 \sin \theta_3 \cosh \theta_2 - \beta_1 \sin \theta_1 \cos \theta_3 \cosh \theta_2 \quad \dots (2.27c)
 \end{aligned}$$

$$\begin{aligned}
 a_{22CDC} = & -(\beta_3 / \beta_1) \sin \theta_1 \sin \theta_3 \cosh \theta_2 - s_2 (\beta_2 \beta_3 / \beta_1) \sin \theta_1 \sin \theta_3 \sinh \theta_2 + \\
 & (\beta_2 / \beta_1) \sin \theta_1 \cos \theta_3 \sinh \theta_2 - s_1 \beta_3 \cos \theta_1 \sin \theta_3 \cosh \theta_2 - s_1 s_2 \beta_2 \beta_3 \cos \theta_1 \\
 & \sin \theta_3 \sinh \theta_2 + s_1 \beta_2 \cos \theta_1 \cos \theta_3 \sinh \theta_2 - (\beta_3 / \beta_2) \cos \theta_1 \sin \theta_3 \sinh \theta_2 - s_2 \\
 & \beta_3 \sin \theta_3 \cos \theta_1 \cosh \theta_2 + \cos \theta_1 \cos \theta_3 \cosh \theta_2 \quad \dots(2.27d)
 \end{aligned}$$

$$\begin{aligned}
 a_{11DCD} = & \cos \theta_2 \cosh \theta_3 \cosh \theta_1 - s_2 \beta_2 \sin \theta_2 \cosh \theta_3 \cosh \theta_1 - (\beta_2 / \beta_3) \sin \theta_2 \\
 & \sinh \theta_3 \cosh \theta_1 + s_1 \beta_1 \cos \theta_2 \cosh \theta_3 \sinh \theta_1 - s_1 s_2 \beta_1 \beta_2 \sin \theta_2 \cosh \theta_3 \\
 & \sinh \theta_1 - s_1 (\beta_1 \beta_2 / \beta_3) \sin \theta_2 \sinh \theta_1 \sinh \theta_3 + (\beta_1 / \beta_2) \sin \theta_2 \cosh \theta_3 \sinh \theta_1 + s_2 \\
 & \beta_1 \cos \theta_2 \cosh \theta_3 \sinh \theta_1 + (\beta_1 / \beta_3) \cos \theta_2 \sinh \theta_1 \sinh \theta_3 \quad \dots(2.28a)
 \end{aligned}$$

$$a_{12DCD} = (1/\beta_1) \sinh \theta_1 \cos \theta_2 \cosh \theta_3 - s_2 (\beta_2/\beta_1) \sinh \theta_1 \sin \theta_2 \cosh \theta_3 - (\beta_2/\beta_1 \beta_3) \sin \theta_2 \sinh \theta_1 \sinh \theta_3 + s_1 \cos \theta_2 \cosh \theta_1 \cosh \theta_3 - s_1 s_2 \beta_2 \sin \theta_2 \cosh \theta_3 \cosh \theta_1 - s_1 (\beta_2/\beta_3) \cosh \theta_1 \sin \theta_2 \sinh \theta_3 + (1/\beta_2) \sin \theta_2 \cosh \theta_3 \cosh \theta_1 + s_2 \cos \theta_2 \cosh \theta_1 \cosh \theta_3 + (1/\beta_3) \sinh \theta_3 \cos \theta_2 \cosh \theta_1 \quad \dots (2.28b)$$

$$a_{21DCD} = \beta_3 \sinh \theta_3 \cos \theta_2 \cosh \theta_1 - s_2 \beta_2 \beta_3 \sin \theta_2 \sinh \theta_3 \cosh \theta_1 - \beta_2 \cosh \theta_1 \cosh \theta_3 \sin \theta_2 + s_1 \beta_1 \beta_3 \sinh \theta_3 \cos \theta_2 \sinh \theta_1 - s_1 s_2 \beta_1 \beta_2 \beta_3 \sin \theta_2 \sinh \theta_1 \sinh \theta_3 - s_1 \beta_1 \beta_2 \sinh \theta_1 \cosh \theta_3 \sin \theta_2 + (\beta_1 \beta_3/\beta_2) \sin \theta_2 \sinh \theta_1 \sinh \theta_3 + s_2 \beta_1 \beta_3 \cos \theta_2 \sinh \theta_1 \sinh \theta_3 + \beta_1 \sinh \theta_1 \cos \theta_2 \cosh \theta_3 \quad \dots (2.28c)$$

$$a_{22DCD} = (\beta_3/\beta_1) \sinh \theta_1 \sinh \theta_3 \cos \theta_2 - s_2 (\beta_2 \beta_3/\beta_1) \sinh \theta_1 \sin \theta_2 \sinh \theta_3 - (\beta_2/\beta_1) \sinh \theta_1 \cosh \theta_3 \sin \theta_2 + s_1 \beta_3 \sinh \theta_3 \cos \theta_2 \cosh \theta_1 - s_1 s_2 \beta_2 \beta_3 \cosh \theta_1 \sin \theta_2 \sinh \theta_3 - s_1 \beta_2 \cosh \theta_1 \cosh \theta_3 \sin \theta_2 + (\beta_3/\beta_2) \sin \theta_2 \cosh \theta_1 \sinh \theta_3 + s_2 \beta_3 \cosh \theta_1 \cos \theta_2 \sinh \theta_3 + \cos \theta_2 \cosh \theta_3 \cosh \theta_1 \quad \dots (2.28d)$$

where $\theta_1 = \beta_1 L_1$, $\theta_2 = \beta_2 L_2$, $\theta_3 = \beta_3 L_3$.

From these matrices the basic properties of the symmetric triplet can be derived. It turns out that the symmetric triplet (figure 2.3) composed of three thin lenses usually can still be considered a thin lens because its principal planes are close to the mid-plane. The most important property of the symmetric triplet is that it can provide stigmatic imaging (**Szilagyi 1988**).

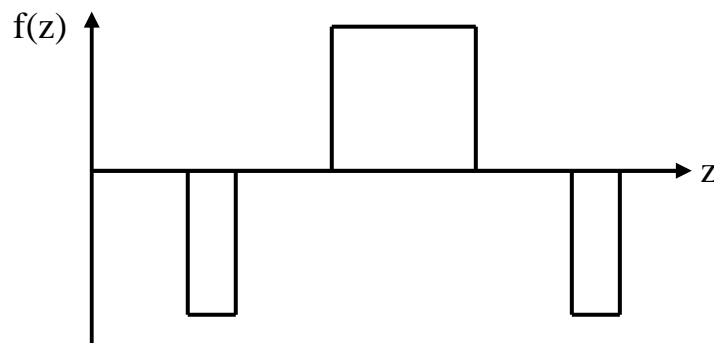


Figure 2.3. Symmetric triplet (Szilagyı 1988).

Although the doublet achieves a significant improvement with respect to a single quadrupole, and although its construction is inherently simpler than that of a three-lens system, the latter system is more favorable in many cases. The chief disadvantage of the doublet lens is the fact that the variation of a parameter in one of the basic planes may entail an important variation of the parameters in the other plane. If one tries, for example, to adjust the position of the principal plane in the CD direction, the position of the principal plane in the DC direction will equally vary. Supposing that the doublet can be assimilated to a thin lens, the position of this lens may then be quite different in the two perpendicular planes as the variation of the excitation will modify not only the focusing strength of the lens but also its position in space.

In a symmetrical triplet, the principle planes are symmetrical with respect to the median plane of the lens and this applies equally well to the CDC as to the DCD direction and is, to a large extent, independent of the excitation. If a symmetric triplet can be considered as a thin lens, the position of this equivalent lens is almost fixed in space and independent of excitation (**Regenstreif 1967**).

2.3.2 The cardinal elements

All first-order optical properties of a quadrupole lens can be derived from the matrices given in equations (2.25) and (2.26). If these matrices are represented by (**Regenstreif 1967**)

$$T_{CDC} = \begin{pmatrix} a_{11CDC} & a_{12CDC} \\ a_{21CDC} & a_{22CDC} \end{pmatrix} \quad \dots (2.29a)$$

Then the following first-order optical properties can be determined (see figure 2.4).

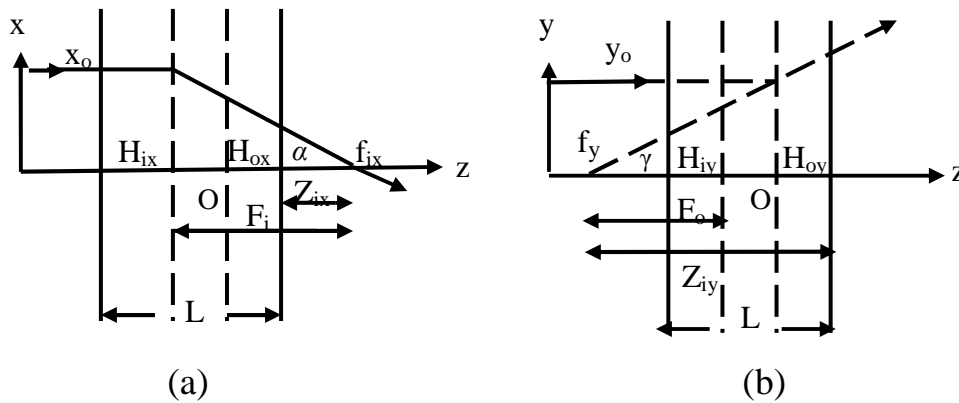
$$T_{DCD} = \begin{pmatrix} a_{11DCD} & a_{12DCD} \\ a_{21DCD} & a_{22DCD} \end{pmatrix} \quad \dots (2.29b)$$


Figure 2.4. The cardinal elements of a quadrupole lens, (a) in the convergence plane, (b) in the divergence plane (Grivet 1972).

(a) focal planes:

An incoming ray parallel to the optical axis will, after passing through the lens system, intersect the axis at a point whose distance Z_i from the exit plane is given by (Grivet 1972):

$$Z_{iCDC} = - a_{11CDC}/a_{21CDC} \quad \dots (2.30a)$$

$$Z_{iDCD} = - a_{11DCD}/a_{21DCD} \quad \dots (2.30b)$$

where the subscript “i” refers to image, and “CDC” and “DCD” refer to the convergence–divergence–convergence and divergence–convergence–

divergence planes respectively. Similarly, a ray emerging parallel to the optical axis, originates from a point at a distance Z_o from the entry plane given by:

$$Z_{oCDC} = -a_{22CDC}/a_{21CDC} \quad \dots (2.31a)$$

$$Z_{oDCD} = -a_{22DCD}/a_{21DCD} \quad \dots (2.31b)$$

where the subscript “o” refers to the object.

(b) principal planes:

These planes are conjugate and defined by (**Grivet 1972**):

$$H_{iCDC} = (1 - a_{11CDC})/a_{21CDC} \quad \dots (2.32a)$$

$$H_{iDCD} = (1 - a_{11DCD})/a_{21DCD} \quad \dots (2.32b)$$

Similarly,

$$H_{oCDC} = (1 - a_{22CDC})/a_{21CDC} \quad \dots (2.33a)$$

$$H_{oDCD} = (1 - a_{22DCD})/a_{21DCD} \quad \dots (2.33b)$$

(c) focal lengths:

The focal length is defined as the distance between the focal point f and the corresponding principal plane. Therefore, the image- and object-side focal lengths F_i and F_o respectively are given by:

$$F_{iCDC} = F_{oCDC} = -1/a_{21CDC} \quad \dots (2.34a)$$

Similarly,

$$F_{iDCD} = F_{oDCD} = -1/a_{21DCD} \quad \dots (2.34b)$$

(d) magnification:

The magnification M can be given as:

$$M_{CDC} = 1/ (a_{21CDC} u+ a_{11CDC}) \quad \dots (2.35a)$$

$$M_{DCD} = 1/ (a_{21DCD} u+ a_{11DCD}) \quad \dots (2.35b)$$

where u is the object distance.

2.4 Lens Aberrations Parameters

In an ideal optical system, all rays of light from a point in the object plane would converge to the same point in the image plane, forming a clear image. The influences which cause different rays to converge to different points are called aberrations. Thus aberration can be defined as the defect that the image suffers from, when it is formed by an optical device (single or system of lenses). The aberration is a subject of great importance, since it causes limitation to the performance of various electron optical elements and systems (Nave 2001).

Error may occur from different velocities that the charged particles may have in the accelerated beam since they leave the source with different initial velocities (energy spread). The result is that different particles (ions or electrons) are focused at different points even if the paraxial

approximation is exactly valid. The reason of this effect is that the imaging field less influences the particles with high initial energy than lower-energy particles. This effect is called chromatic aberration because it is equivalent to the fact in light optics that the index of refraction for photons of different frequencies (colors) is different (**Szilagyi 1988**). In the present work, energy spread of charged particles traversing the optical system under consideration is assumed absent; hence computations on chromatic aberration will not be carried out.

Aberration is not the only defect that the image suffers from. Other type of defects are due to the fabrication of lenses such as mechanical imperfection and misalignment. The electrostatic repulsion forces between particles of the same charge causes a deviation in charged particles path. It is another defects, known as the space charge effect, and it is a case of charged-particle optics alone that cannot be found in light optics (**Szilagyi 1988**). However, in the present work attention is paid only on the spherical aberration of electrostatic quadrupole lenses due to its significant effect in various ion and electron optical systems. Mechanical defects and space charge effects are assumed absent in the devices under consideration.

2.5 Spherical Aberration

Optical systems for focusing charged particles by means of magnetic or electrostatic lenses have their performance limited by spherical aberration of the lenses. It is also called aperture aberration. In 1936, Scherzer showed that the coefficient of spherical aberration of round lenses has the same sign and one, therefore, presumes that it cannot be made zero. Scherzer's conclusions are based upon the symmetry of the lenses and

therefore one might hope to avoid the problem by using systems of lenses, which are not cylindrically symmetric. In 1947, he proposed a scheme, which uses what are now called multiple lenses (**Crewe et al 1981**).

The aberrations of a quadrupole lens may be parasitic or intrinsic. Parasitic aberrations arise from mechanical misalignment of the lens electrodes. Intrinsic aberration, on the other hand, exists even in perfectly aligned quadrupole lenses. The most significant intrinsic aberration in a lens system, which focuses a beam with large divergence, is spherical aberration (**Jamieson and Legge 1987**).

In a quadrupole lens, the spherical aberration in the Gaussian image plane can be expressed as (**Okayama 1989; Okayama and Kawakatsu 1983**):

$$\Delta x (z_i) = (C_{30} \alpha^3 + C_{12} \alpha \gamma^2) \quad \dots(2.36)$$

$$\Delta y (z_i) = (D_{21} \alpha^2 \gamma + D_{03} \gamma^3) \quad \dots (2.37)$$

where α and γ are the image side semi-aperture angles in the x-z and y-z plane respectively, the coefficients C characterize the aberration in the convergence plane, and D in the divergence plane. The coefficient C_{30} determines the aberration of the width of the real image in the plane $y = 0$, and D_{03} is that for the imaginary image in the plane $x = 0$. The analytic formulas for the relative spherical aberration coefficients, where the field distribution along the electrostatic quadrupole lens axis is approximated by a rectangular model, are given by **Fishkova et al (1968)**:

$$C_{30}/L = 1/16\{ \eta^2 - (1 - 6\mu^2 + \mu^4) (\sin 4\theta/4\theta) + (u/L) \xi (1 - \cos 4\theta) + 1/3(2 - 2n + 3n^2) [3\eta^2 - 4(1 - \mu^4) (\sin 2\theta/2\theta) + (1 - 6\mu^2 + \mu^4) (\sin 4\theta/4\theta) + 4(u/L) \eta (1 - \cos 2\theta) - (u/L) \xi (1 - \cos 4\theta)] \} \quad \dots(2.38)$$

$$C_{12}/L = 1/16 \{ 6\eta\xi + 8(u/L) - [2\xi^2 + (5\xi\eta - 4\mu^2) \cosh 2\theta] (\sin 2\theta/2\theta) + [2\eta^2 - (\xi\eta + 20\mu^2) \cos 2\theta] (\sinh 2\theta/2\theta) - 2u/L (\xi \cos 2\theta - \eta \cosh 2\theta) + u/L (\eta - 5\xi) \sin 2\theta \sinh 2\theta - u/L (5\eta + \xi) \cos 2\theta \cosh 2\theta + (2 + 2n - n^2) \{-2\eta\xi - 2u/L + [2\xi^2 - (\eta\xi - 4\mu^2) \cosh 2\theta] (\sin 2\theta/2\theta) + [2\eta^2 - (\eta\xi + 4\mu^2) \cos 2\theta] (\sinh 2\theta/2\theta) + 2u/L (\xi \cos 2\theta + \eta \cosh 2\theta) + u/L(\eta - \xi) \sin 2\theta \sinh 2\theta - u/L(\eta + \xi) \cos 2\theta \cosh 2\theta \} \} \quad \dots(2.39)$$

where $\theta = \beta L$, $\mu = \beta u$, $\eta = 1 + \mu^2$, and $\xi = 1 - \mu^2$, $n = -1$ for electrostatic quadrupole lenses (**Fishkova et al 1968**).

The coefficients D_{03} and D_{21} are derived from equations (2.38) and (2.39) by replacing β by $i\beta$. In addition the trigonometry functions are transformed into hyperbolic functions and vice versa. The subscript CDC refers to the xOz plane in which the first and third lens converges and the second lens diverges; the subscript DCD refers to the yOz plane, perpendicular to the xOz plane, in which the lens performance is the reverse. The spherical aberration coefficients, P_{CDC} , P_{DCD} , S_{CDC} , and S_{DCD} of the triplet lens are determined from (a) the spherical aberration coefficients P_{CD} , P_{DC} , S_{CD} , and S_{DC} of the doublet lens and the spherical aberration coefficients $C_{30}(3)$, $D_{30}(3)$, $C_{12}(3)$, and $D_{21}(3)$ of the third lens in the triplet, and (b) the magnification M_{CD} and M_{DC} of the doublet lens.

$$P_{CDC} = P_{CD} + C_{30}(3) / (M_{CD})^4 \quad \dots (2.40a)$$

$$P_{DCD} = P_{DC} + D_{03}(3) / (M_{DC})^4 \quad \dots (2.40b)$$

$$S_{CDC} = S_{CD} + C_{12}(3) / ((M_{CD})^2 (M_{DC})^2) \quad \dots (2.40c)$$

$$S_{DCD} = S_{DC} + D_{21}(3) / ((M_{CD})^2 (M_{DC})^2) \quad \dots (2.40d)$$

The spherical aberrations ΔCDC and ΔDCD of a quadrupole triplet lens in the plane of the Gaussian image are given by the following formulas:

$$\Delta CDC = (P_{CDC} \alpha^3 + S_{CDC} \alpha \gamma^2) \quad \dots(2.41)$$

$$\Delta DCD = (P_{DCD} \alpha^2 \gamma + S_{DCD} \gamma^3) \quad \dots(2.42)$$

2.6 Computer Programs

Complete statements of the following computer programs are listed in Appendices A.

2.6.1 Computer program for computing the trajectory and the first-order optical properties of a quadrupole triplet lens

A computer program written in Fortran 77 language has been used for computing the trajectory of charged particles traversing the field of a quadrupole triplet lens in both the CDC-plane and DCD-plane, by using the transfer matrices given in equations (2.27) and (2.28) where the axial potential field has been approximated to have a rectangular distribution. The first order optical properties such as the focal length, focal plane, principal plane, and magnification have been computed with the aid of equations (2.30) to (2.35) in the planes of convergence and divergence.

2.6.2 Program for computing the spherical aberration coefficients of a quadrupole triplet lens

A computer program written in Fortran 77 language has been used to compute the spherical aberration coefficients P_{CDC} , P_{DCD} , S_{CDC} , and S_{DCD} for a quadrupole triplet lens using equation (2.40) and by computing the spherical aberration coefficients C_{30} , C_{12} , D_{03} , and D_{21} for each of the three single quadrupole lenses forming the triplet lens.

3. RESULTS AND DISCUSSION

3.1 The Quadrupole Triplet Lens and Its Field

Figure 3.1 depicts a diagram of the electrostatic quadrupole triplet lens under consideration. It consists of three coaxial quadrupole lenses Q_1 , Q_2 , and Q_3 . The present investigation takes into consideration that the field distribution of each lens is of a rectangular shape of length L_1 , L_2 , and L_3 respectively as shown in figure 3.2. In fact it is assumed that the effective length of each field is equal to the length of the corresponding quadrupole lens. The axial distance s_1 separates the lenses Q_1 and Q_2 and s_2 separates Q_2 and Q_3 . This quadrupole triplet lens takes into account the focusing of an accelerated charged-particles beam of positive ions traveling from the left to the right-hand-side. Thus the object is assumed to be situated on the left-hand-side at an axial distance u from the starting point of the field of lens Q_1 and the image position is on the right-hand-side at a distance v from the end point of the field of lens Q_3 . Since the positive potential ($+U$) is applied on the x -axis electrodes of lenses Q_1 and Q_3 , then the positively charged particles will be repelled along the x -axis and hence will be directed towards the z -axis. The positively charged particles will be attracted by the negative potential ($-U$) along the y -axis of Q_1 and Q_3 . Therefore, in lenses Q_1 and Q_3 the convergence process takes place in the x -axis and the divergence process takes place in the y -axis; whereas in lens Q_2 the convergence and divergence processes take place in the y - and x -axis respectively. In the present work the polarities of the electrodes of each lens in the x and y axes shown in figure 3.1 are taken into account. Hence, the positively charged particles traverse the three electrostatic fields of the quadrupole triplet lens in two planes, namely the

x-z plane where the convergence-divergence-convergence (CDC) process takes place and the y-z plane where the divergence-convergence-divergence (DCD) process takes place.

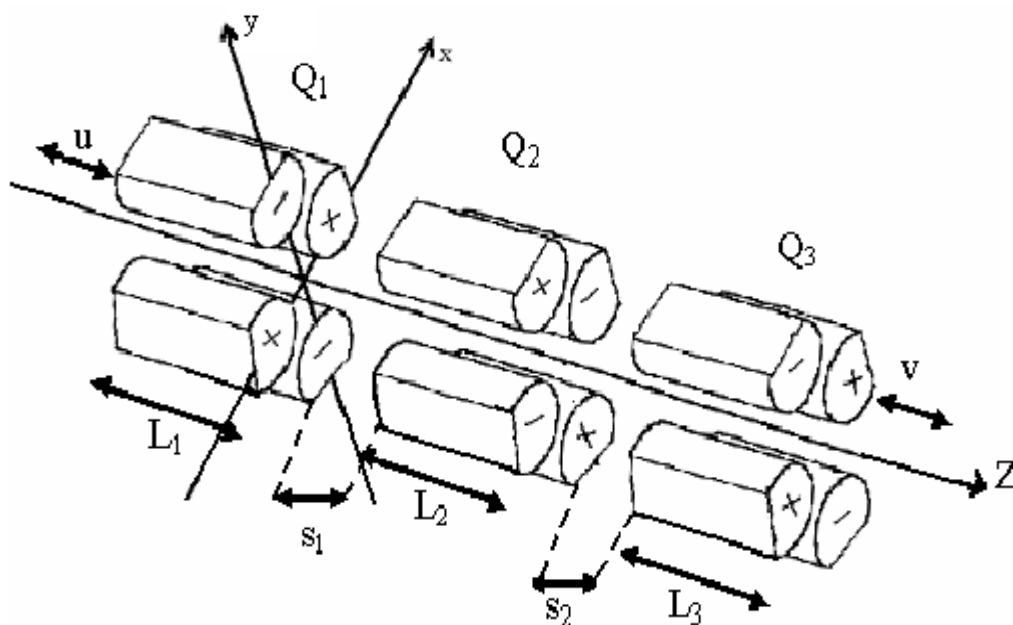


Figure 3.1 Diagram of an electrostatic quadrupole triplet lens.

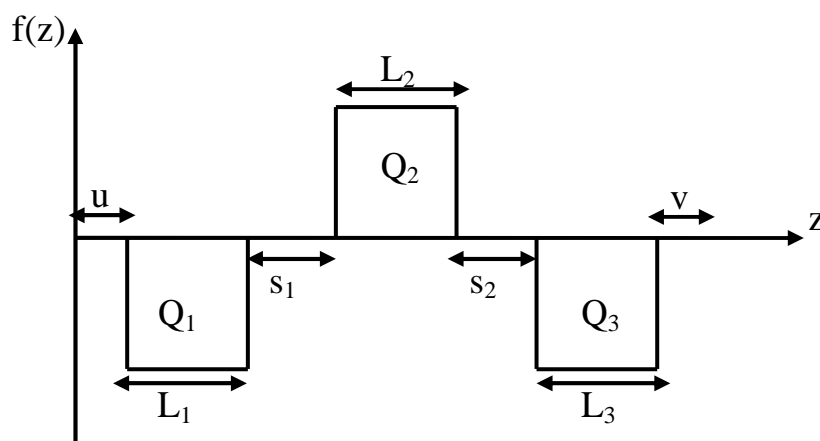


Figure 3.2 Field distribution of an electrostatic quadrupole triplet lens (rectangular model).

The trajectory of the accelerated charged particles along the optical axis is affected by the geometrical parameters L_1 , L_2 , L_3 , s_1 , s_2 , u , and v . In order to reduce the large number of variables, some of the computations have been carried out under the conditions where $u=v$, $s_1=s_2$, $L_1=L_2=L_3$, and the excitations of the lenses are made equal, i.e. $\beta_1=\beta_2=\beta_3$. However, most of the computations take into account different values for the L 's, s 's, β 's, and u and v so that a complete picture of the charged-particles path along the whole length of the quadrupole triplet lens can be visualized.

3.2 Beam Trajectory and Focal Properties of Triplet Lens

The trajectory of the positively charged-particles beam traversing the electrostatic quadrupole triplet lens under consideration has been computed in both $x-z$ and $y-z$ planes under various conditions taking into account the polarity of each electrode shown in figure 3.1. At a distance u from the first lens Q_1 the incoming beam is not necessarily parallel to the optical axis z . With the aid of this trajectory the following focal properties have been computed: the spherical aberration coefficient P , the spherical aberration coefficient S , the focal length F , the focal plane Z , the magnification in each plane, and the total magnification $M (= M_{CDC} \times M_{DCD})$. The computed focal properties have been tabulated for each set of geometrical and operational parameters.

Considering the focus that is situated on the optical axis z , the action of the triplet lens on a beam is similar to that of the doublet lens shown in figure 2.2 where it is seen that the beam is brought to a focus in the z -axis at a different position in the $x-z$ and $y-z$ planes. This situation, which is called astigmatic, is not necessarily a disadvantage since it may be

exploited for correction in ion–optical instruments in order to obtain a stigmatic beam image at the exit.

3.2.1 Three lenses of equal length

The quadrupole triplet lens has been investigated for the case where its three lenses are of equal length. By keeping the following parameters equal (a) the lenses lengths L_1 , L_2 , and L_3 , (b) the lenses separations s_1 and s_2 , and (c) the object and image distances u and v , the best focusing (i.e. a crossover) that could be achieved in the x – z and y – z planes has been taken into account. The beam trajectory is sensitive to the above mentioned parameters in addition to the excitation parameters β_1 , β_2 , and β_3 of the three lenses.

Figure 3.3 shows the beam trajectory in both CDC (x – z) and DCD (y – z) planes at various excitation parameters. The most favourable focusing is achieved when the excitation $\beta_1 = \beta_3 = 0.0268 \text{ mm}^{-1}$ and $u = v = 20 \text{ mm}$. The effect of β_2 on the trajectories in both planes is shown in figure 3.3. The trajectory is terminated at $z = 87 \text{ mm}$ i.e. at a distance of 20 mm from the field of lens Q_3 as one would expect since it represents the image distance v . The figure shows how the beam enters the field of lens Q_1 at $z = 20 \text{ mm}$. Under the conditions of figure 3.3, the CDC and DCD focal parameters have been computed.

Table 3.1 shows the computed focal parameters of the quadrupole triplet lens under various excitation parameters when $L_1 = L_2 = L_3 = L$, $s_1 = s_2 = s$, and $u = v = 20 \text{ mm}$. Under the conditions listed in the first column of table 3.1, figure 3.4 shows an enlarged diagram of the trajectory where the paraxial beam enters the lens at $z = 20 \text{ mm}$ and focusing is achieved in the

x - z and y - z planes though not on the same point of the z -axis. The negative sign of the focal length in the CDC plane indicates that the quadrupole triplet lens is a diverging one in this case. However, a converging triplet lens is found in the DCD plane where the focal length is positive. Figure 3.4 shows that in the x - z plane the beam inflection occurs at $x = 0.13$ mm where $z = 40$ mm (i.e. within the field-free region s_1 between lenses Q_1 and Q_2) whereas in the y - z plane it occurs at $y = 0.09$ mm where $z = 30.6$ mm, which is also within the distance s_1 . The crossover in the y - z plane occurs at $z = 49.4$ mm (i.e. within the distance s_2 which is a field-free region) whereas that in x - z plane occurs at $z = 78.9$ mm which is positioned outside the field of the third quadrupole lens Q_3 on the image side.

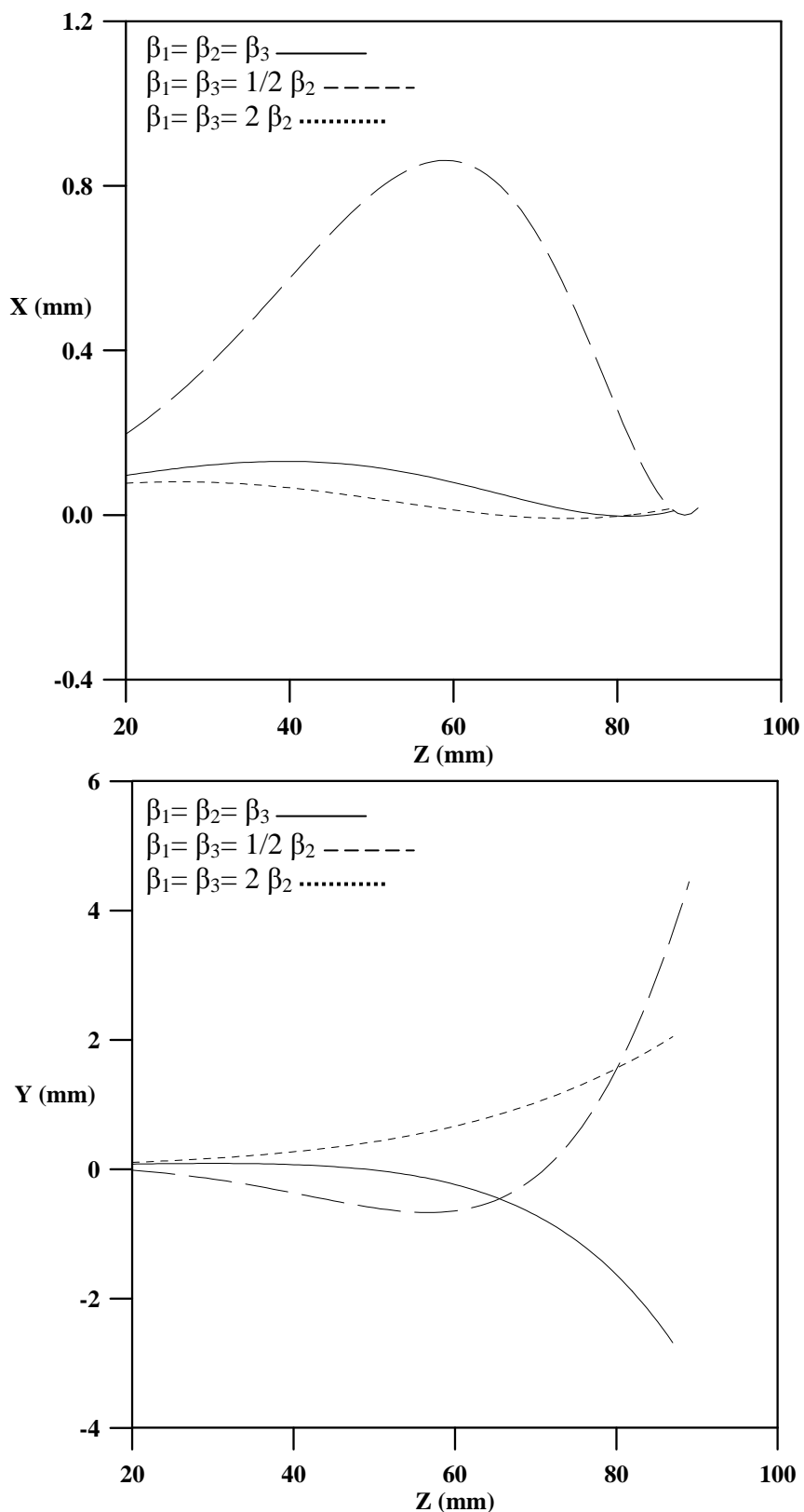


Figure 3.3. Beam trajectory in quadrupole triplet lens at various excitation parameters in both CDC ($x-z$) and DCD ($y-z$) planes for $L_1 = L_2 = L_3 = L$, $s_1 = s_2 = s$, $u = v = 20$ mm, and $\beta_1 = \beta_3 = 0.0268$ mm⁻¹.

Table 3.1

Focal parameters of the quadrupole triplet lens under the following conditions:
 $L_1 = L_2 = L_3 = L$, $s_1 = s_2 = s$, and $u = v = 20$ mm.

$\beta_1 = \beta_2 = \beta_3 = 0.0268 \text{ mm}^{-1}$ $L = 5 \text{ mm}, s = 16 \text{ mm}$	$\beta_1 = \beta_3 = 1/2 \beta_2$ $\beta_1 = \beta_3 = 0.0268 \text{ mm}^{-1}$ $\beta_2 = 0.0536 \text{ mm}^{-1}$ $L = 11 \text{ mm}, s = 18 \text{ mm}$	$\beta_1 = \beta_3 = 2 \beta_2$ $\beta_1 = \beta_3 = 0.0268 \text{ mm}^{-1}$ $\beta_2 = 0.0134 \text{ mm}^{-1}$ $L = 5 \text{ mm}, s = 16 \text{ mm}$
$P_{\text{CDC}} = -4.06 \text{ mm}$	$P_{\text{CDC}} = -7.05 \text{ mm}$	$P_{\text{CDC}} = -3.90 \text{ mm}$
$P_{\text{DCD}} = -8.88 \text{ mm}$	$P_{\text{DCD}} = -22.37 \text{ mm}$	$P_{\text{DCD}} = -2.09 \text{ mm}$
$S_{\text{CDC}} = 36.96 \text{ mm}$	$S_{\text{CDC}} = 979.67 \text{ mm}$	$S_{\text{CDC}} = 34.00 \text{ mm}$
$S_{\text{DCD}} = 25.76 \text{ mm}$	$S_{\text{DCD}} = 168.12 \text{ mm}$	$S_{\text{DCD}} = 24.84 \text{ mm}$
$F_{\text{CDC}} = -2.44 \text{ mm}$	$F_{\text{CDC}} = -0.008 \text{ mm}$	$F_{\text{CDC}} = -7.78 \text{ mm}$
$F_{\text{DCD}} = 0.51 \text{ mm}$	$F_{\text{DCD}} = -0.01 \text{ mm}$	$F_{\text{DCD}} = -0.71 \text{ mm}$
$ P_{\text{CDC}}/F_{\text{CDC}} = 1.66$	$ P_{\text{CDC}}/F_{\text{CDC}} = 881.25$	$ P_{\text{CDC}}/F_{\text{CDC}} = 0.50$
$ P_{\text{DCD}}/F_{\text{DCD}} = 17.41$	$ P_{\text{DCD}}/F_{\text{DCD}} = 2237.00$	$ P_{\text{DCD}}/F_{\text{DCD}} = 2.94$
$ S_{\text{CDC}}/F_{\text{CDC}} = 15.15$	$ S_{\text{CDC}}/F_{\text{CDC}} = 122458.75$	$ S_{\text{CDC}}/F_{\text{CDC}} = 4.37$
$ S_{\text{DCD}}/F_{\text{DCD}} = 50.51$	$ S_{\text{DCD}}/F_{\text{DCD}} = 16812.00$	$ S_{\text{DCD}}/F_{\text{DCD}} = 34.99$
$Z_{\text{iCDC}} = -55.61 \text{ mm}$	$Z_{\text{iCDC}} = -81.03 \text{ mm}$	$Z_{\text{iCDC}} = -35.79 \text{ mm}$
$Z_{\text{iDCD}} = -37.13 \text{ mm}$	$Z_{\text{iDCD}} = -37.31 \text{ mm}$	$Z_{\text{iDCD}} = -38.22 \text{ mm}$
$M_{\text{CDC}} = 1.09$	$M_{\text{CDC}} = 0.84$	$M_{\text{CDC}} = 1.16$
$M_{\text{DCD}} = 0.93$	$M_{\text{DCD}} = 2.93$	$M_{\text{DCD}} = 0.87$
$M = 1.02$	$M = 2.46$	$M = 1.01$

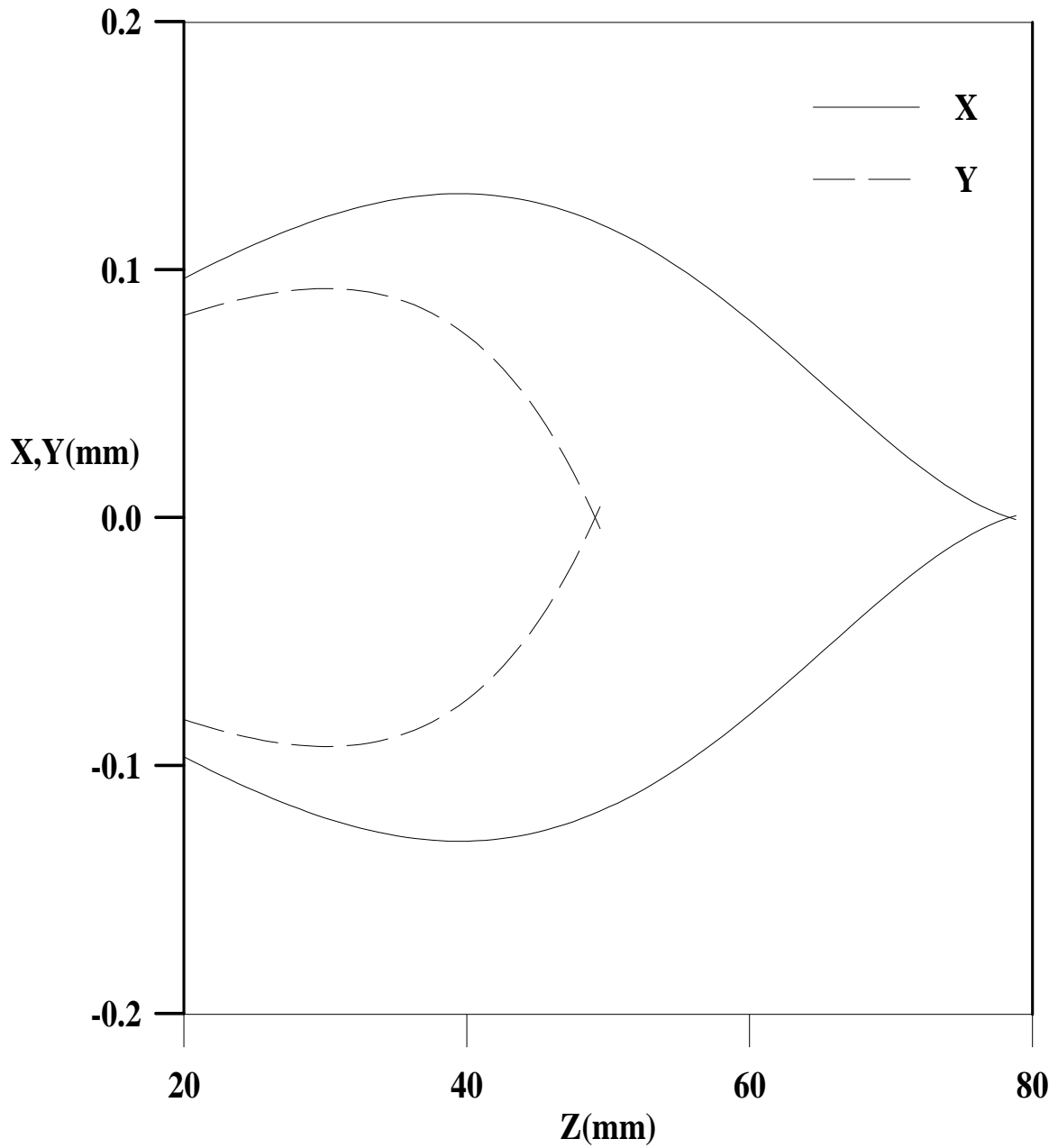


Figure 3.4. An enlarged diagram of the beam trajectory in both CDC ($x-z$) and DCD ($y-z$) planes under the following conditions: $\beta_1 = \beta_2 = \beta_3 = 0.0268 \text{ mm}^{-1}$, $L_1 = L_2 = L_3 = 5 \text{ mm}$, $s_1 = s_2 = 16 \text{ mm}$, and $u = v = 20 \text{ mm}$.

A trajectory diagram similar to that of figure 3.4 is drawn in figure 3.5 under the conditions shown in the second column of table 3.1. In this case where $\beta_1 = \beta_3 = 0.5$, $\beta_2 = 0.0268 \text{ mm}^{-1}$ and $u = v = 20 \text{ mm}$, focusing in CDC and DCD planes could only be achieved if L is made equal to 11 mm instead of 5 mm and s is increased to 18 mm. The conditions of the second column gave rise to the lowest focal length. It is seen that the focal length has a negative sign in both CDC and DCD planes which indicates that the triplet lens acts as a diverging one. Figure 3.5 shows that the inflection points of the beam trajectory in the $x-z$ and $y-z$ planes are found within the field-free distance s_2 separating lenses Q_2 and Q_3 . For minimum focal length, a crossover in the $y-z$ plane always occurs before that in the $x-z$ plane under the above conditions. Although the focal lengths F_{CDC} and F_{DCD} are at their lowest values the spherical aberration coefficients, however, are at their highest values which are undesirable from the optical point of view.

The computed results listed in the third column of table 3.1 suggest that as far as the spherical aberration coefficients P and S are concerned it is more favourable to have the excitations $\beta_1 = \beta_3 = 2 \beta_2$ since these coefficients are at their lowest values in both CDC and DCD planes when $\beta_1 = 0.0268 \text{ mm}^{-1}$, $L = 5 \text{ mm}$, $s = 16 \text{ mm}$, and $u = v = 20 \text{ mm}$. Furthermore, this case introduces the lowest relative spherical aberration coefficients P/F and S/F at the corresponding planes. For example, the values of $(P/F)_{\text{CDC}} = 0.5$, $(P/F)_{\text{DCD}} = 2.94$, $(S/F)_{\text{CDC}} = 4.37$, and $(S/F)_{\text{DCD}} = 34.99$ are very small for an electrostatic lens of this shape compared to those published by Baranova and Read (1999) for a conventional quadrupole triplet. Their lens and that of the present work both have unit magnification although the excitation parameters of their lens are much higher. It is seen that the values of P/F and S/F in the CDC plane are far

below those in the DCD plane; therefore, one may exploit this advantage of the quadrupole triplet lens when operated in ion-optical instruments under the conditions listed in the third column of table 3.1.

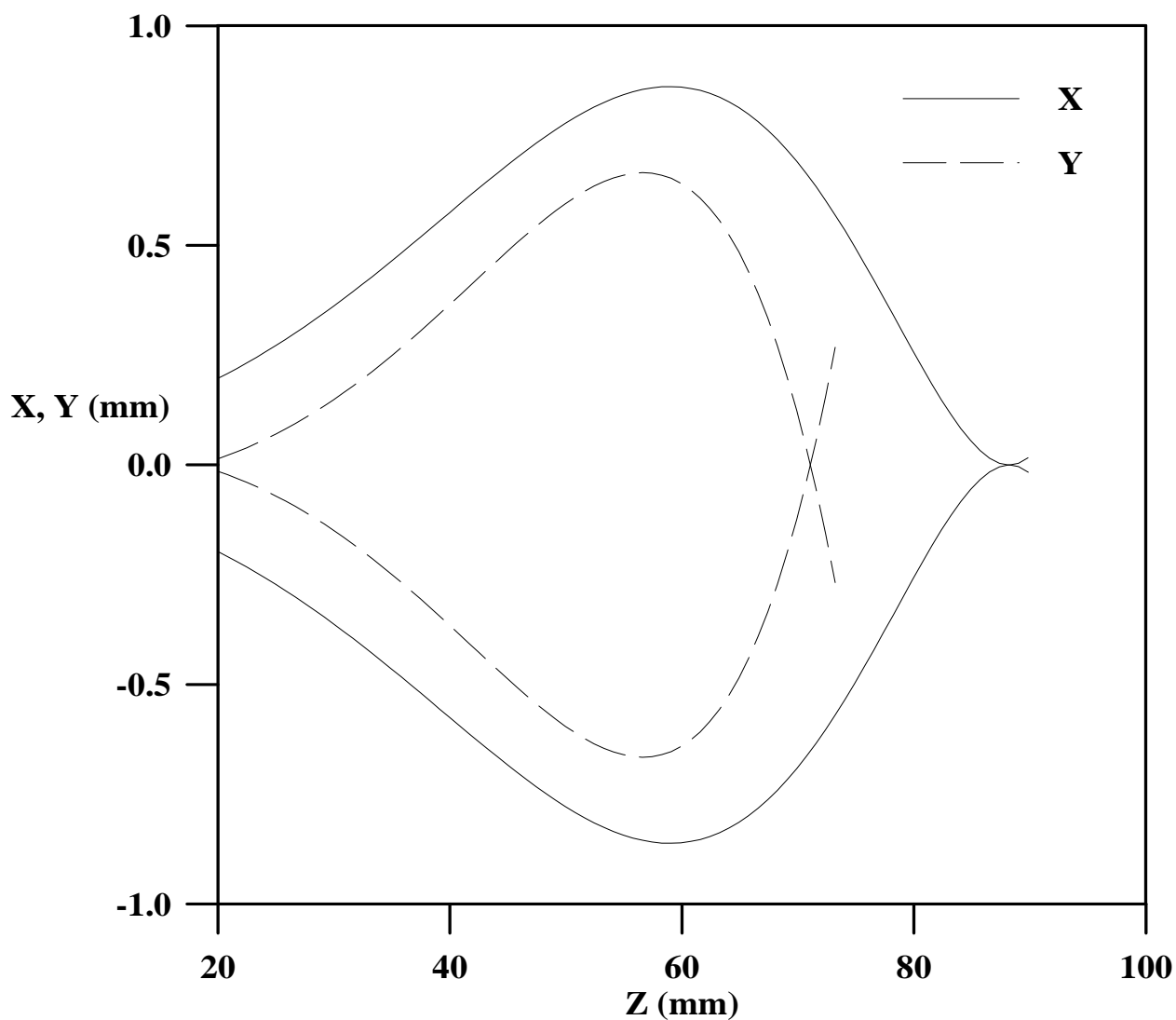


Figure 3.5. An enlarged trajectory diagram of the beam traversing the quadrupole triplet lens in both CDC ($x-z$) and DCD ($y-z$) planes for the case of lowest focal length under the following conditions: $L_1 = L_2 = L_3 = 11$ mm, $s_1 = s_2 = 18$ mm, $u = v = 20$ mm, $\beta_1 = \beta_3 = 1/2 \beta_2 = 0.0268$ mm⁻¹, and $\beta_2 = 0.0536$ mm⁻¹.

The beam trajectory that gave rise to the lowest spherical aberration coefficients is shown in figure 3.6 for the x–z and y–z planes. In the x–z plane the inflection point of the beam is situated at $x = 0.08$ mm and $z = 26.9$ mm (i.e. within the field-free region s_1 separating the lenses Q_1 and Q_2). The beam crossover is positioned at $z = 65.7$ mm i.e. within the field of lens Q_3 . However, in the y–z plane it is seen that the beam diverges away from the optical axis as it traverses the whole length of the triplet lens, i.e. there is no crossover in the y–z plane.

Concerning the position of the focal plane Z_i , table 3.1 indicates that in the DCD plane it is very little affected by the variations imposed on the excitation parameter β_2 of lens Q_2 . Furthermore, it is not much too far from that in the CDC plane when $\beta_1 = \beta_3 = 2 \beta_2$ where the lowest spherical aberration coefficients are obtained. It is seen that in the CDC plane the position of the focal plane is highly affected by the excitation parameters.

Table 3.1 shows the weak influence of the focusing planes and the excitation parameters on the image magnification. Depending on these factors the image is either little magnified or demagnified. However, highest magnification M is found when the focal length has its lowest value as indicated in the second column of table 3.1. This result is expected from the optics point of view.

It is seen that when best focusing is taken into consideration, one may either achieve lowest focal lengths or lowest spherical aberration coefficients when the excitation parameter of lens Q_2 is different from that applied on lenses Q_1 and Q_3 . Thus, one may conclude that as far as the lowest focal lengths and the lowest spherical aberration coefficients in both CDC and DCD planes are concerned a quadrupole triplet lens of equal

excitation parameters has no optical advantages under these two cases. However, since the spherical aberration coefficients P_{CDC} and P_{DCD} are both negative, the triplet lens may be employed for correcting this spherical aberration of other rotationally symmetric lenses that have the corresponding spherical aberration coefficients positive.

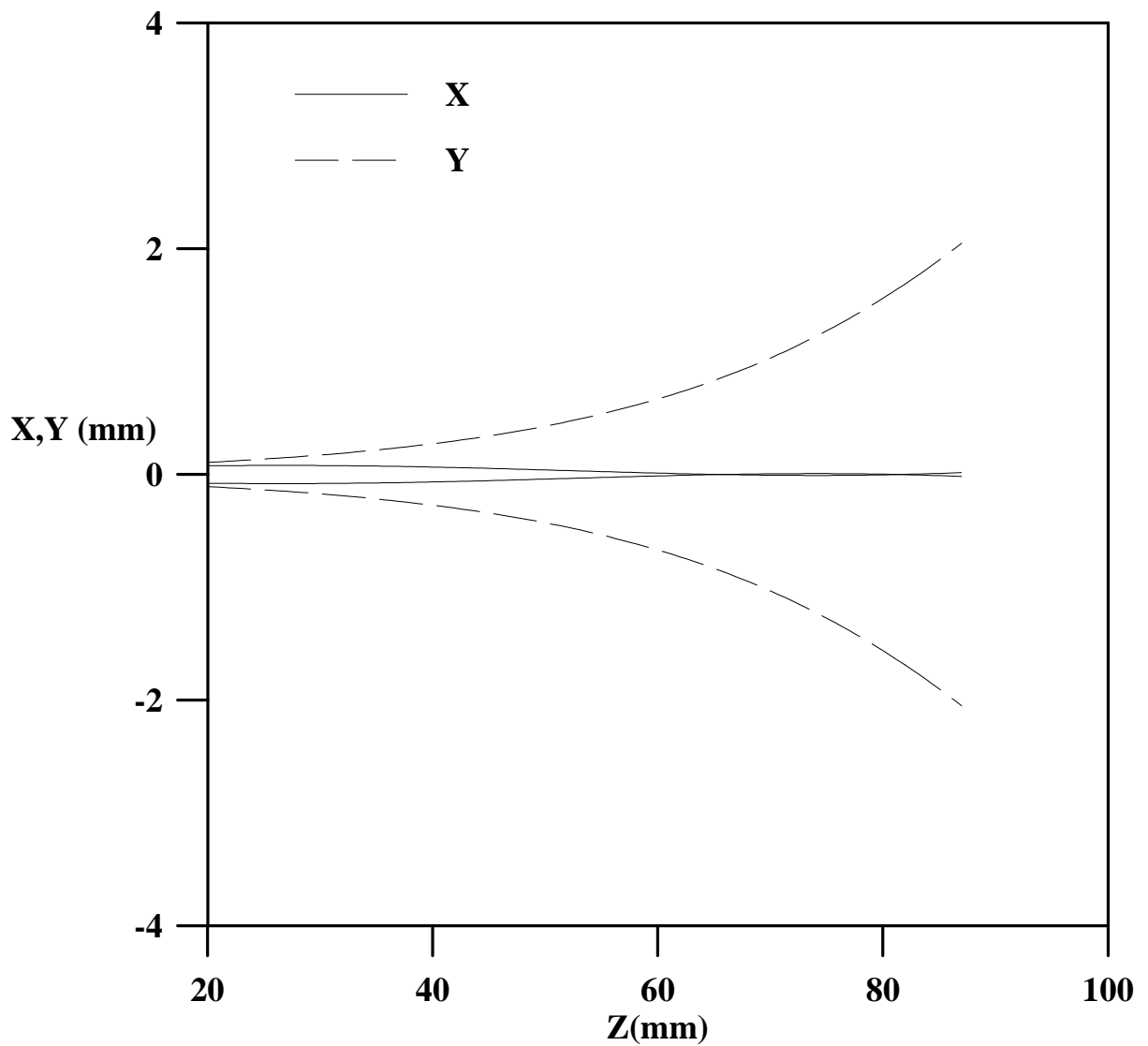


Figure 3.6. The beam trajectory in $x-z$ and $y-z$ planes that produced the lowest spherical aberration coefficients under the following conditions: $\beta_1 = \beta_3 = 2 \beta_2 = 0.0268 \text{ mm}^{-1}$, $\beta_2 = 0.0134 \text{ mm}^{-1}$, $L_1 = L_2 = L_3 = 5 \text{ mm}$, $s_1 = s_2 = 16 \text{ mm}$, and $u = v = 20 \text{ mm}$.

3.2.2 Three lenses of equal excitation

The effect of varying the length L_2 of lens Q_2 on the beam trajectory and hence on the focal properties of the quadrupole triplet lens has been investigated under equal and constant excitation parameters ($\beta_1 = \beta_2 = \beta_3 = 0.0268 \text{ mm}^{-1}$) and by keeping $L_1 = L_3 = 5 \text{ mm}$, $s_1 = s_2 = 16 \text{ mm}$, and $u = v = 20 \text{ mm}$. Figure 3.7 shows the beam trajectory in the $x-z$ and $y-z$ planes at various values of L_2 . It is seen that the length L_2 has no influence on the beam trajectory in the CDC and DCD planes. The paraxial beam enters the lens at a distance $u = 20 \text{ mm}$ from lens Q_1 and the trajectory is terminated at a distance $v = 20 \text{ mm}$ from the lens Q_3 . The focal properties of the triplet lens under the above mentioned conditions are listed in table 3.2 for the CDC and DCD planes. Table 3.2 indicates that the values of the spherical aberration coefficients P_{CDC} and S_{DCD} and the focal length F_{CDC} are little affected by variations of L_2 . In the CDC plane and regardless of the value of L_2 the triplet lens acts as a diverging one since its focal length is negative. However, in the DCD plane the lens is a converging one since its focal length is positive.

The computed results listed in the first column of table 3.2 are the same as those listed in the corresponding column of table 3.1. The second column of table 3.2 shows that by making L_2 equal to double the length of L_1 (or L_3) the lens will give rise to the lowest focal lengths in both planes. However, in this case the lens has an undesirable spherical aberration coefficients P and S and the corresponding relative aberration coefficients P/F and S/F since their values are high in both CDC and DCD planes.

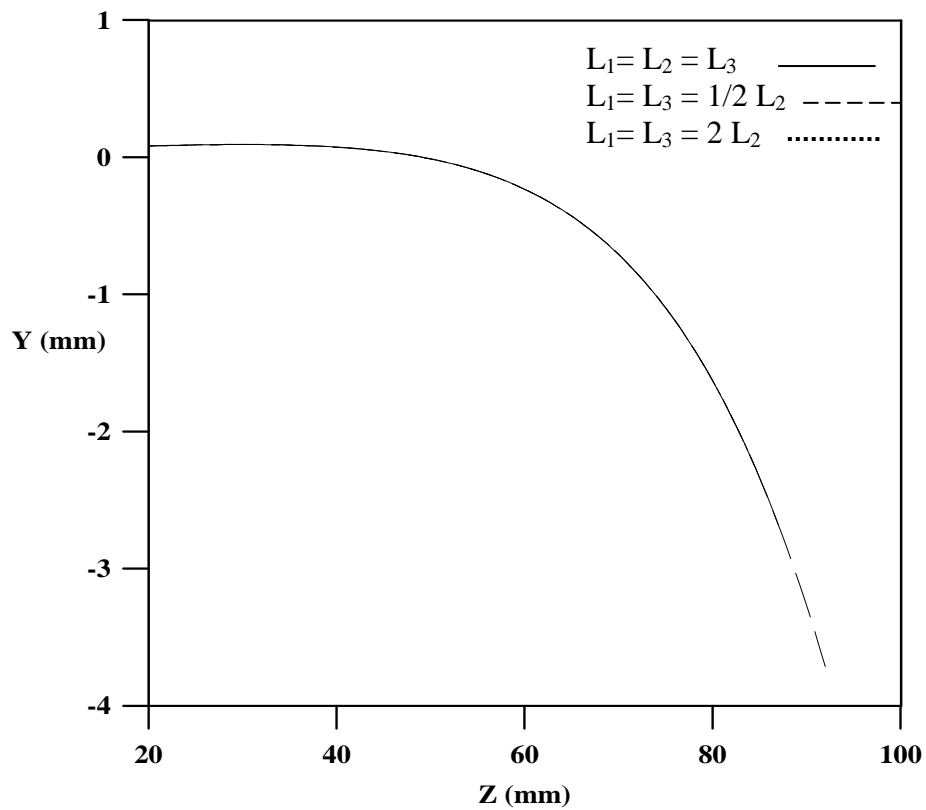
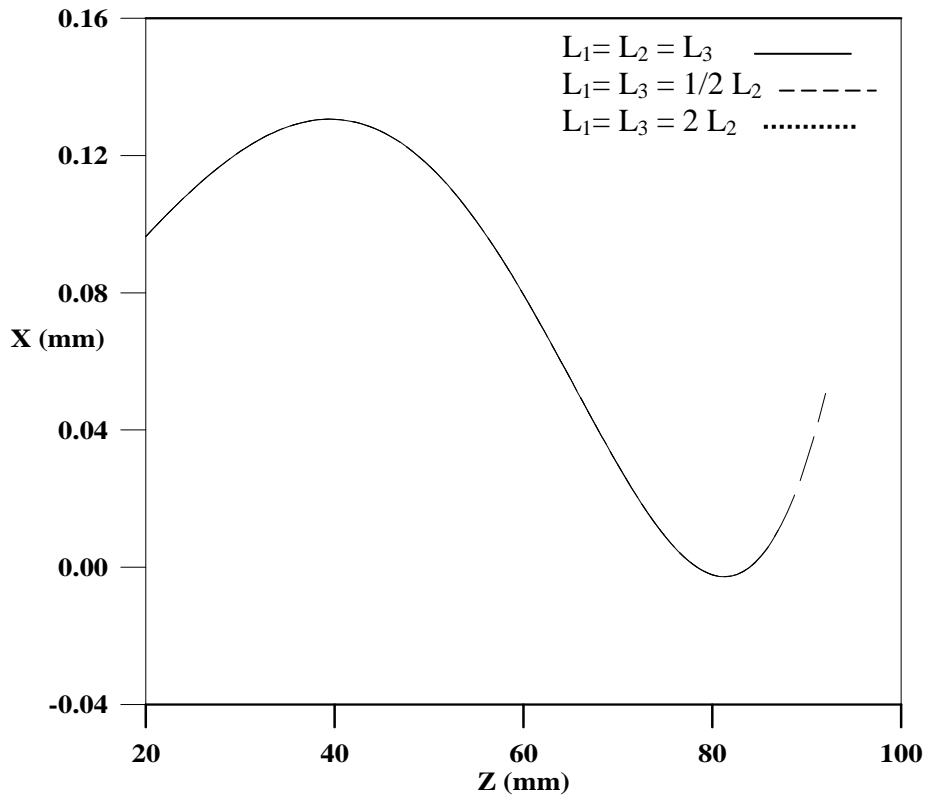


Figure 3.7. Beam trajectory in quadrupole triplet lens at various lengths of the lenses in both CDC ($x-z$) and DCD ($y-z$) planes for $\beta_1 = \beta_2 = \beta_3 = 0.0268 \text{ mm}^{-1}$, $L_1 = L_3 = 5 \text{ mm}$, $s_1 = s_2 = 16 \text{ mm}$, and $u = v = 20 \text{ mm}$.

Table 3.2

Focal parameters of the quadrupole triplet lens under the following conditions:
 $\beta_1 = \beta_2 = \beta_3 = 0.0268 \text{ mm}^{-1}$, $s_1 = s_2 = 16 \text{ mm}$, and $u = v = 20 \text{ mm}$.

$L_1 = L_2 = L_3 = 5 \text{ mm}$	$L_1 = L_3 = 1/2 L_2 = 5 \text{ mm},$ $L_2 = 10 \text{ mm}$	$L_1 = L_3 = 2 L_2 = 5 \text{ mm},$ $L_2 = 2.5 \text{ mm}$
$P_{\text{CDC}} = -4.06 \text{ mm}$	$P_{\text{CDC}} = -4.55 \text{ mm}$	$P_{\text{CDC}} = -3.94 \text{ mm}$
$P_{\text{DCD}} = -8.88 \text{ mm}$	$P_{\text{DCD}} = -10.13 \text{ mm}$	$P_{\text{DCD}} = -5.28 \text{ mm}$
$S_{\text{CDC}} = 36.96 \text{ mm}$	$S_{\text{CDC}} = 60.25 \text{ mm}$	$S_{\text{CDC}} = 26.28 \text{ mm}$
$S_{\text{DCD}} = 25.76 \text{ mm}$	$S_{\text{DCD}} = 27.96 \text{ mm}$	$S_{\text{DCD}} = 25.03 \text{ mm}$
$F_{\text{CDC}} = -2.44 \text{ mm}$	$F_{\text{CDC}} = -2.26 \text{ mm}$	$F_{\text{CDC}} = -2.57 \text{ mm}$
$F_{\text{DCD}} = 0.51 \text{ mm}$	$F_{\text{DCD}} = 0.37 \text{ mm}$	$F_{\text{DCD}} = 0.61 \text{ mm}$
$/P_{\text{CDC}}/ F_{\text{CDC}}/ = 1.66$	$/P_{\text{CDC}}/ F_{\text{CDC}}/ = 2.01$	$/P_{\text{CDC}}/ F_{\text{CDC}}/ = 1.53$
$/P_{\text{DCD}}/ F_{\text{DCD}}/ = 17.41$	$/P_{\text{DCD}}/ F_{\text{DCD}}/ = 27.38$	$/P_{\text{DCD}}/ F_{\text{DCD}}/ = 8.66$
$/S_{\text{CDC}}/ F_{\text{CDC}}/ = 15.15$	$/S_{\text{CDC}}/ F_{\text{CDC}}/ = 26.66$	$/S_{\text{CDC}}/ F_{\text{CDC}}/ = 10.23$
$/S_{\text{DCD}}/ F_{\text{DCD}}/ = 50.51$	$/S_{\text{DCD}}/ F_{\text{DCD}}/ = 75.57$	$/S_{\text{DCD}}/ F_{\text{DCD}}/ = 41.03$
$Z_{\text{iCDC}} = -55.61 \text{ mm}$	$Z_{\text{iCDC}} = -63.27 \text{ mm}$	$Z_{\text{iCDC}} = -51.89 \text{ mm}$
$Z_{\text{iDCD}} = -37.13 \text{ mm}$	$Z_{\text{iDCD}} = -37.23 \text{ mm}$	$Z_{\text{iDCD}} = -37.06 \text{ mm}$
$M_{\text{CDC}} = 1.09$	$M_{\text{CDC}} = 1.00$	$M_{\text{CDC}} = 1.14$
$M_{\text{DCD}} = 0.93$	$M_{\text{DCD}} = 1.04$	$M_{\text{DCD}} = 0.89$
$M = 1.02$	$M = 1.04$	$M = 1.01$

The enlarged beam trajectory under the conditions listed in the second column of table 3.2 is shown in figure 3.8 where the lowest focal lengths are achieved. In the x-z plane the beam deviates towards the z-axis at $x = 0.13$ mm and $z = 40.187$ mm i.e. within the field-free region s_1 and very close to lens Q_2 . The beam intersects the z-axis at $z = 78.54$ mm which is a field-free region and away from lens Q_3 . In the y-z plane the beam deviates towards the z-axis in the field-free region between Q_1 and Q_2 at $z = 30.77$ mm and intersects the z-axis at $z = 49.6$ mm i.e. within the field of lens Q_2 .

The position of the focal plane Z_i in the DCD plane is not affected by varying the length L_2 of lens Q_2 as shown in table 3.2. This case is also found in table 3.1 at various values of β_2 . Thus, one may conclude that $Z_{iDCD} \square - 37$ mm is independent of the length and excitation parameter of lens Q_2 . However, the effect of L_2 on the position of the focal plane appears in the CDC plane where its lowest value is found when the spherical aberration coefficients P and S are at their lowest values.

Table 3.2 shows that the total magnification $M (= M_{CDC} \times M_{DCD})$ is not affected by the variations of L_2 . In general, M is about unity irrespective of the value of L_2 under the conditions given in table 3.2.

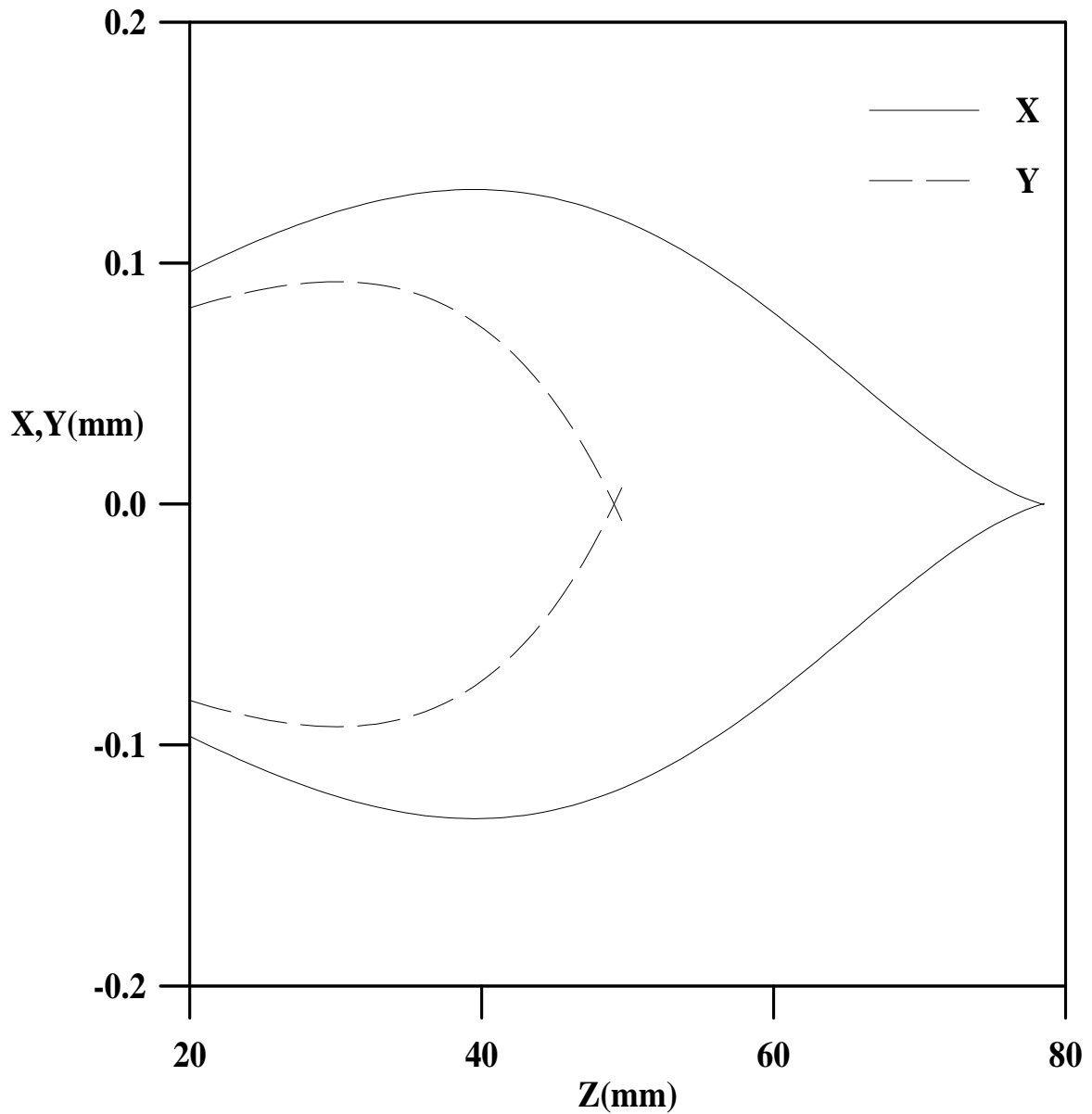


Figure 3.8. An enlarged trajectory diagram of the beam traversing the quadrupole triplet lens in both CDC ($x-z$) and DCD ($y-z$) planes under the following conditions where the lowest focal lengths are achieved:

$$L_1 = L_3 = 1/2 L_2 = 5 \text{ mm}, L_2 = 10 \text{ mm}, s_1 = s_2 = 16 \text{ mm}, u = v = 20 \text{ mm}, \text{ and } \beta_1 = \beta_2 = \beta_3 = 0.0268 \text{ mm}^{-1}.$$

The third column of table 3.2 indicates that the lowest spherical aberration coefficients P and S and the corresponding relative aberration coefficients P/F and S/F can be achieved in both CDC and DCD planes if the length L_2 of lens Q_2 is reduced. It is seen that in this case the coefficients P and S are little affected by the trajectory plane. The values of P/F and S/F are not better than those listed in the third column of table 3.1. Therefore, as far as the spherical aberration coefficients are concerned, no advantage is gained under these conditions in comparison with the conditions imposed in table 3.1. An enlarged diagram of the beam trajectory for this case is shown in figure 3.9. In the x - z plane the beam deviates towards the z -axis at $x = 0.13$ mm and $z = 39.89$ mm i.e. in the field-free region s_1 and very close to lens Q_2 ; it then intersects the z -axis in the field-free region at $z = 78.47$ mm. In the y - z plane the beam deviates towards the z -axis at $y = 0.09$ mm and $z = 30.85$ mm i.e. within s_1 that separates lenses Q_1 and Q_2 and it then intersects the z -axis at $z = 49.54$ mm i.e. within s_2 that separates lenses Q_2 and Q_3 .

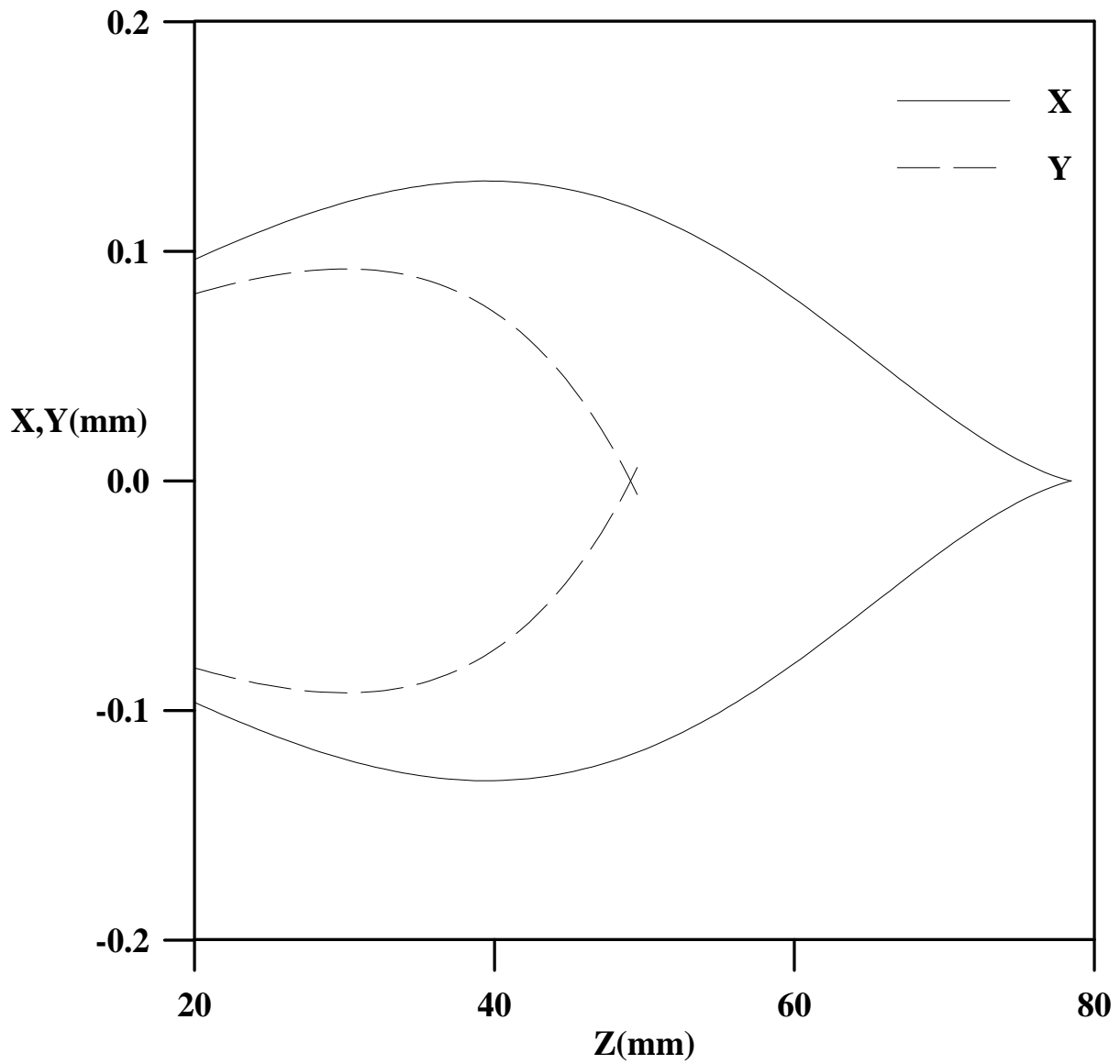


Figure 3.9. An enlarged trajectory diagram of the beam traversing the quadrupole triplet lens in both CDC ($x-z$) and DCD ($y-z$) planes under the following conditions where the lowest spherical aberration coefficients are achieved:
 $L_1 = L_3 = 2 L_2 = 5$ mm, $L_2 = 2.5$ mm, $s_1 = s_2 = 16$ mm,
 $u = v = 20$ mm, and $\beta_1 = \beta_2 = \beta_3 = 0.0268$ mm⁻¹.

3.2.3 Effect of object and image distance

The effect of object and image distance u and v respectively on the optical properties of the electrostatic quadrupole triplet lens under various conditions has been investigated in both CDC and DCD planes. Figures 3.10a and b show the beam trajectory along the z -axis at constant u and constant v respectively. In each figure it is seen that the trajectory is not affected by variations of either v or u in both x - z and y - z planes. With the aid of these trajectories, the optical properties have been computed for three values of v and three values of u as shown in tables 3.3a and b. The results of the first column of tables 3.3a and b are the same as those listed in the first column of tables 3.1 and 3.2.

Considering the sign of the focal length F , it is seen from tables 3.3 a and b that the triplet lens is a diverging one in the CDC plane and a converging one in the DCD plane irrespective of the values of the object or image distance. Furthermore, table 3.3a indicates that F_{CDC} is very little affected by variations in v when focusing in the z -axis is achieved.

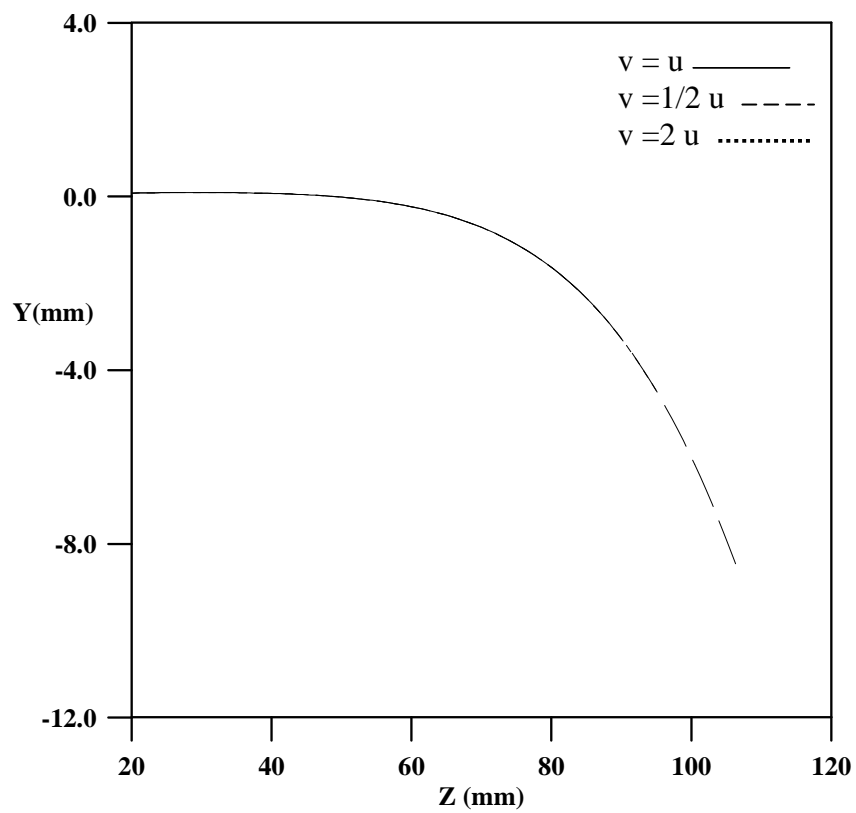
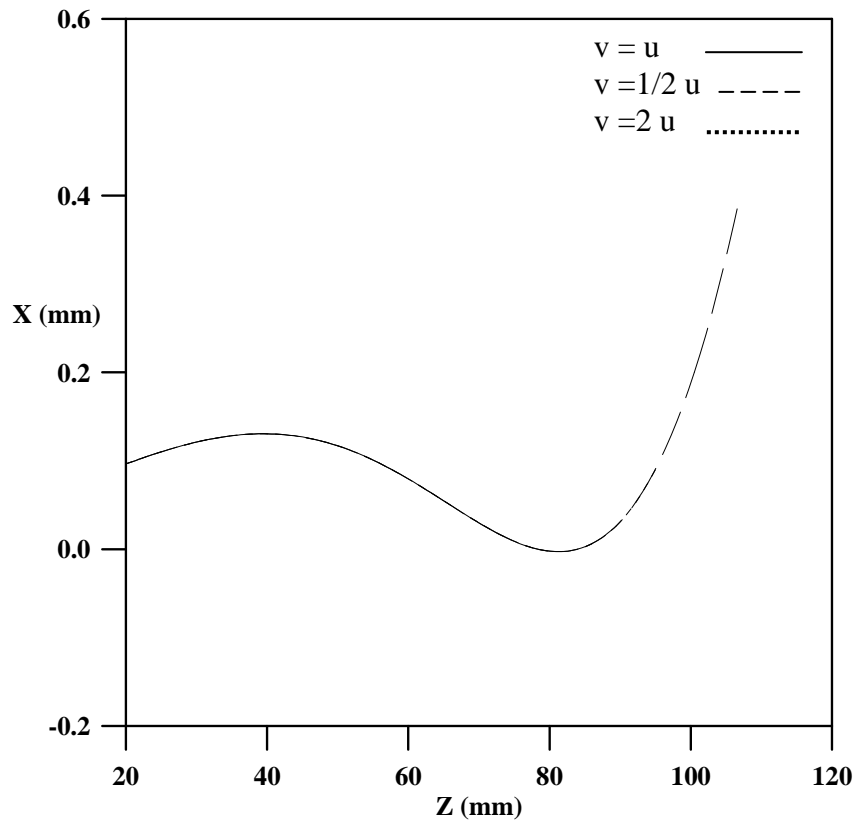


Figure 3.10a. Beam trajectory in the quadrupole triplet lens at various values of v ($u = 20$ mm) in both CDC ($x-z$) and DCD ($y-z$) planes at $\beta_1 = \beta_2 = \beta_3 = 0.0268 \text{ mm}^{-1}$, $L_1 = L_2 = L_3 = L$, and $s_1 = s_2 = 16$ mm.

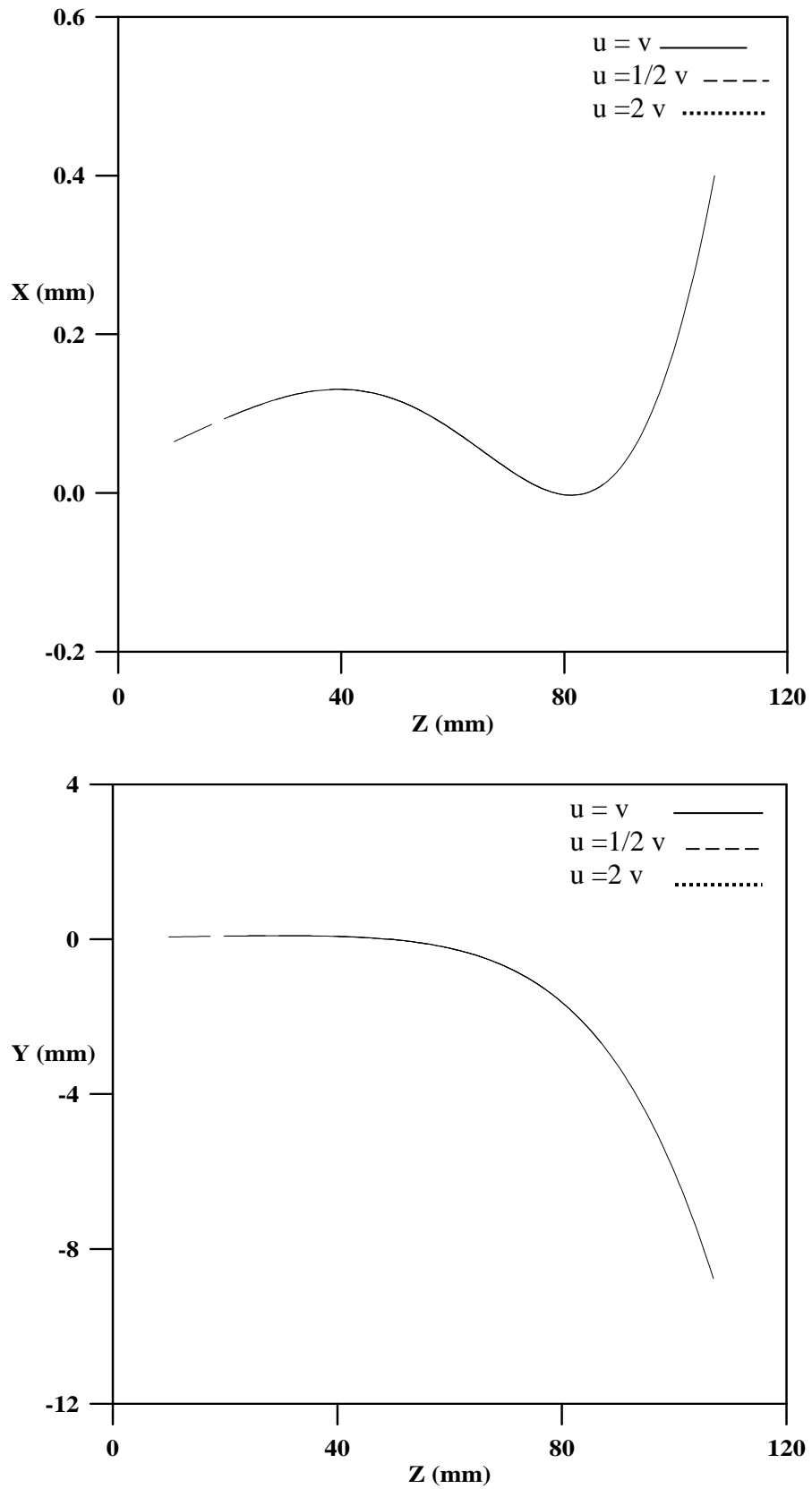


Figure 3.10b. Beam trajectory in the quadrupole triplet lens at various values of u ($v = 20 \text{ mm}$) in both CDC ($x-z$) and DCD ($y-z$) planes at $\beta_1 = \beta_2 = \beta_3 = 0.0268 \text{ mm}^{-1}$, $L_1 = L_2 = L_3 = 5 \text{ mm}$, and $s_1 = s_2 = 16 \text{ mm}$.

Table 3.3a

Focal parameters of the quadrupole triplet lens under the following conditions:
 $\beta_1 = \beta_2 = \beta_3 = 0.0268 \text{ mm}^{-1}$, $L_1 = L_2 = L_3 = L$, $s_1 = s_2 = 16 \text{ mm}$, and $u = 20 \text{ mm}$.

$u = v = 20 \text{ mm}$ $L = 5 \text{ mm}$	$u = 1/2 v = 20 \text{ mm}$ $v = 40 \text{ mm}$ $L = 5 \text{ mm}$	$u = 2 v = 20 \text{ mm}$ $v = 10 \text{ mm}$ $L = 11 \text{ mm}$
$P_{\text{CDC}} = -4.06 \text{ mm}$	$P_{\text{CDC}} = -4.06 \text{ mm}$	$P_{\text{CDC}} = -2.83 \text{ mm}$
$P_{\text{DCD}} = -8.88 \text{ mm}$	$P_{\text{DCD}} = -8.88 \text{ mm}$	$P_{\text{DCD}} = -5.78 \text{ mm}$
$S_{\text{CDC}} = 36.96 \text{ mm}$	$S_{\text{CDC}} = 36.96 \text{ mm}$	$S_{\text{CDC}} = 71.57 \text{ mm}$
$S_{\text{DCD}} = 25.76 \text{ mm}$	$S_{\text{DCD}} = 25.76 \text{ mm}$	$S_{\text{DCD}} = 43.63 \text{ mm}$
$F_{\text{CDC}} = -2.44 \text{ mm}$	$F_{\text{CDC}} = -2.33 \text{ mm}$	$F_{\text{CDC}} = -2.26 \text{ mm}$
$F_{\text{DCD}} = 0.51 \text{ mm}$	$F_{\text{DCD}} = 0.16 \text{ mm}$	$F_{\text{DCD}} = 0.18 \text{ mm}$
$ P_{\text{CDC}}/F_{\text{CDC}} = 1.66$	$ P_{\text{CDC}}/F_{\text{CDC}} = 1.74$	$ P_{\text{CDC}}/F_{\text{CDC}} = 1.25$
$ P_{\text{DCD}}/F_{\text{DCD}} = 17.41$	$ P_{\text{DCD}}/F_{\text{DCD}} = 55.50$	$ P_{\text{DCD}}/F_{\text{DCD}} = 32.11$
$ S_{\text{CDC}}/F_{\text{CDC}} = 15.15$	$ S_{\text{CDC}}/F_{\text{CDC}} = 15.86$	$ S_{\text{CDC}}/F_{\text{CDC}} = 31.67$
$ S_{\text{DCD}}/F_{\text{DCD}} = 50.51$	$ S_{\text{DCD}}/F_{\text{DCD}} = 161.00$	$ S_{\text{DCD}}/F_{\text{DCD}} = 242.39$
$Z_{\text{iCDC}} = -55.61 \text{ mm}$	$Z_{\text{iCDC}} = -82.25 \text{ mm}$	$Z_{\text{iCDC}} = -81.06 \text{ mm}$
$Z_{\text{iDCD}} = -37.13 \text{ mm}$	$Z_{\text{iDCD}} = -37.34 \text{ mm}$	$Z_{\text{iDCD}} = -129.45 \text{ mm}$
$M_{\text{CDC}} = 1.09$	$M_{\text{CDC}} = 1.09$	$M_{\text{CDC}} = 1.29$
$M_{\text{DCD}} = 0.93$	$M_{\text{DCD}} = 0.93$	$M_{\text{DCD}} = 0.86$
$M = 1.02$	$M = 1.02$	$M = 1.11$

Table 3.3b

Focal parameters of the quadrupole triplet lens under the following conditions: $\beta_1 = \beta_2 = \beta_3 = 0.0268 \text{ mm}^{-1}$, $L_1 = L_2 = L_3 = 5 \text{ mm}$, $s_1 = s_2 = 16 \text{ mm}$, and $v = 20 \text{ mm}$.

$u = v = 20 \text{ mm}$	$u = 1/2 v = 10 \text{ mm}$ $v = 20 \text{ mm}$	$u = 2 v = 40 \text{ mm}$ $v = 20 \text{ mm}$
$P_{\text{CDC}} = -4.06 \text{ mm}$	$P_{\text{CDC}} = 2.17 \text{ mm}$	$P_{\text{CDC}} = -29.61 \text{ mm}$
$P_{\text{DCD}} = -8.88 \text{ mm}$	$P_{\text{DCD}} = 5.07 \text{ mm}$	$P_{\text{DCD}} = -78.23 \text{ mm}$
$S_{\text{CDC}} = 36.96 \text{ mm}$	$S_{\text{CDC}} = 35.52 \text{ mm}$	$S_{\text{CDC}} = 38.97 \text{ mm}$
$S_{\text{DCD}} = 25.76 \text{ mm}$	$S_{\text{DCD}} = 21.43 \text{ mm}$	$S_{\text{DCD}} = 33.78 \text{ mm}$
$F_{\text{CDC}} = -2.44 \text{ mm}$	$F_{\text{CDC}} = -3.16 \text{ mm}$	$F_{\text{CDC}} = -2.33 \text{ mm}$
$F_{\text{DCD}} = 0.51 \text{ mm}$	$F_{\text{DCD}} = 1.04 \text{ mm}$	$F_{\text{DCD}} = 0.16 \text{ mm}$
$ P_{\text{CDC}}/F_{\text{CDC}} = 1.66$	$ P_{\text{CDC}}/F_{\text{CDC}} = 0.69$	$ P_{\text{CDC}}/F_{\text{CDC}} = 12.71$
$ P_{\text{DCD}}/F_{\text{DCD}} = 17.41$	$ P_{\text{DCD}}/F_{\text{DCD}} = 4.875$	$ P_{\text{DCD}}/F_{\text{DCD}} = 488.94$
$ S_{\text{CDC}}/F_{\text{CDC}} = 15.15$	$ S_{\text{CDC}}/F_{\text{CDC}} = 11.24$	$ S_{\text{CDC}}/F_{\text{CDC}} = 16.73$
$ S_{\text{DCD}}/F_{\text{DCD}} = 50.51$	$ S_{\text{DCD}}/F_{\text{DCD}} = 20.61$	$ S_{\text{DCD}}/F_{\text{DCD}} = 211.13$
$Z_{\text{iCDC}} = -55.61 \text{ mm}$	$Z_{\text{iCDC}} = -41.29 \text{ mm}$	$Z_{\text{iCDC}} = -82.25 \text{ mm}$
$Z_{\text{iDCD}} = -37.13 \text{ mm}$	$Z_{\text{iDCD}} = -36.70 \text{ mm}$	$Z_{\text{iDCD}} = -37.34 \text{ mm}$
$M_{\text{CDC}} = 1.09$	$M_{\text{CDC}} = 1.05$	$M_{\text{CDC}} = 1.21$
$M_{\text{DCD}} = 0.93$	$M_{\text{DCD}} = 0.96$	$M_{\text{DCD}} = 0.89$
$M = 1.02$	$M = 1.008$	$M = 1.08$

According to the conditions in the second and third columns of tables 3.3a and b, the beam trajectory and the focusing in the $x-z$ and $y-z$ planes are shown in figures 3.11a and b and 3.12a and b respectively. Figure 3.11a shows that the crossover in the $x-z$ plane is found at $z = 78.6$ mm; a point on the image side in the field-free region at a distance of 11.6 mm from lens Q_3 . The crossover in the $y-z$ plane is situated at $z = 49.27$ mm which is within the field-free region s_2 separating lenses Q_2 and Q_3 . In figure 3.11b where v is constant and $u = 10$ mm the crossover in $x-z$ plane is found at $z = 77$ mm and that in the $y-z$ plane at $z = 49.45$ mm; both crossovers are situated within the above mentioned field-free regions for the corresponding planes. In order to achieve the focusing in the $x-z$ and $y-z$ planes shown in figure 3.12a the length of the three lenses has been increased to 11 mm as indicated in the third column of table 3.3a. In this case the crossover in the $x-z$ plane is situated at $z = 78.9$ mm which is within the field of Q_3 and that in $y-z$ plane is at $z = 49.44$ mm which is within the field of lens Q_2 . The enlarged trajectory diagram according to the conditions of the third column of table 3.3b is shown in figure 3.12b where the crossovers in the $x-z$ and $y-z$ planes are situated at $z = 78.8$ mm and $z = 49.4$ mm respectively. The positions of these two crossovers are within the field-free regions s_2 and s_1 .

The conditions shown in the first and second columns of table 3.3a have no effect on the spherical aberration coefficients P and S in the CDC and DCD planes. However, the conditions imposed in the third column of table 3.3a to achieve focusing in $x-z$ and $y-z$ planes gave rise to lower P_{CDC} and P_{DCD} but higher S_{CDC} and S_{DCD} than the corresponding coefficients shown in the other two columns. In table 3.3b, the spherical aberration coefficients P and S and the relative coefficients P/F and S/F of the second column are lower than those of the other two columns. Therefore, it may

be deduced that the results of tables 3.3a and b are not conclusive and from the optical point of view, there is no advantage to be gained by varying the object or image distance if the lenses have equal excitation parameters.

It is seen that the object and image distance have nearly no effect on the total magnification. As indicated in tables 3.3a and b the total magnification M remains nearly unchanged at a value of about unity at various positions of object and image.

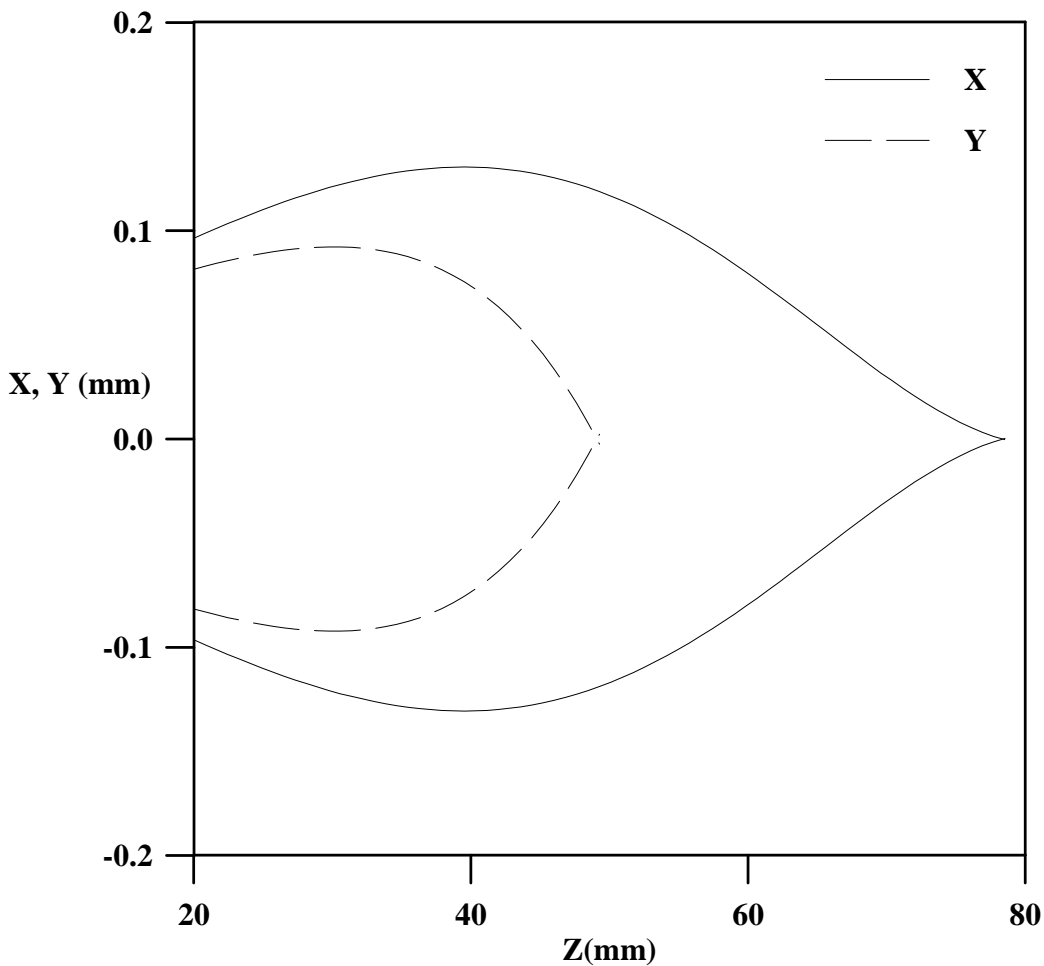


Figure 3.11a. An enlarged trajectory diagram of the beam traversing the quadrupole triplet lens in both CDC (x-z) and DCD (y-z) planes under the following conditions:

$L_1 = L_2 = L_3 = 5 \text{ mm}$, $s_1 = s_2 = 16 \text{ mm}$, $u = 1/2 v = 20 \text{ mm}$,
 $v = 40 \text{ mm}$, and $\beta_1 = \beta_2 = \beta_3 = 0.0268 \text{ mm}^{-1}$.

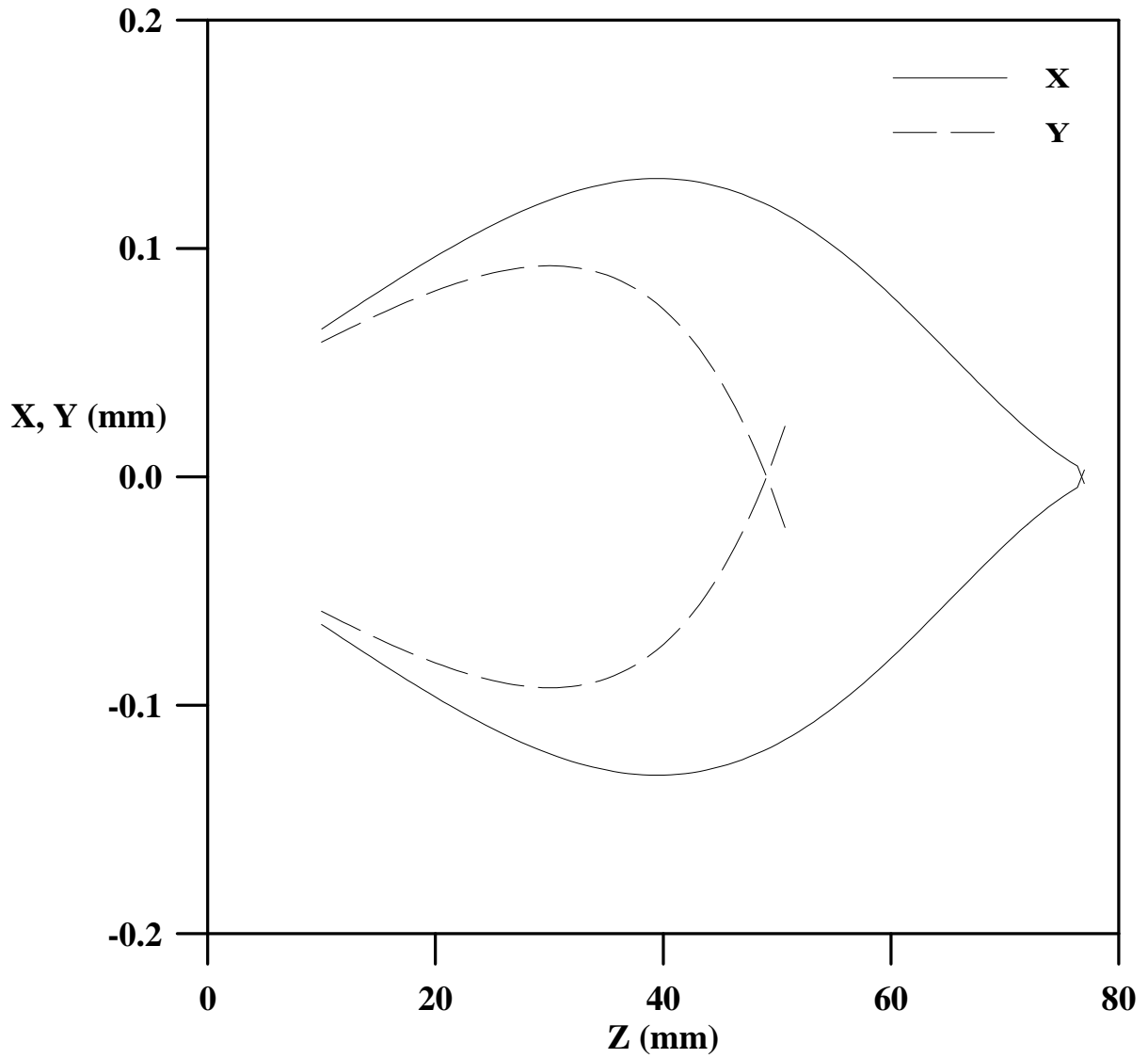


Figure 3.11b. An enlarged trajectory diagram of the beam traversing the quadrupole triplet lens in both CDC ($x-z$) and DCD ($y-z$) planes under the following conditions:

$L_1 = L_2 = L_3 = 5 \text{ mm}$, $s_1 = s_2 = 16 \text{ mm}$, $u = 1/2 v = 10 \text{ mm}$,
 $v = 20 \text{ mm}$, and $\beta_1 = \beta_2 = \beta_3 = 0.0268 \text{ mm}^{-1}$.

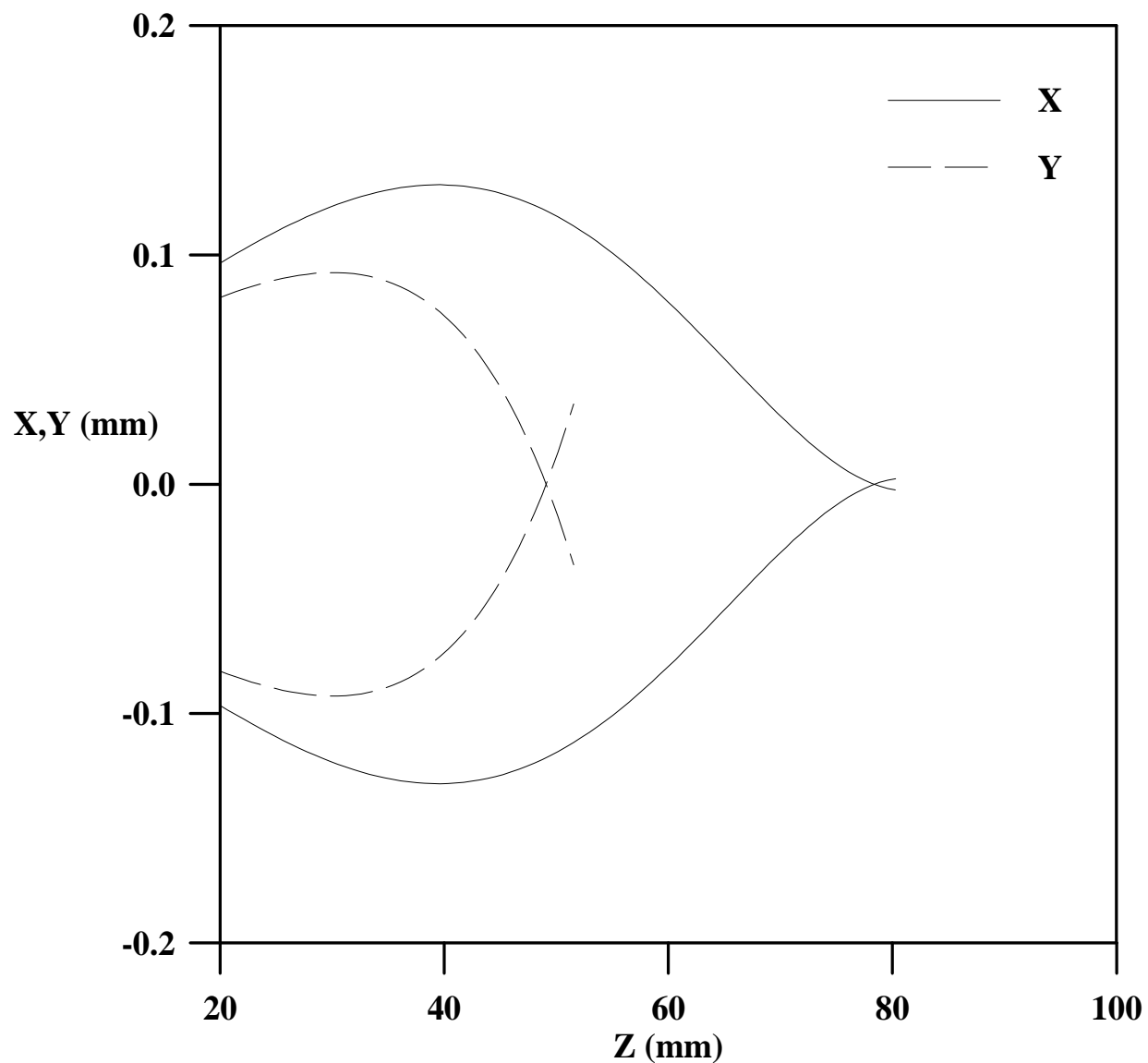


Figure 3.12a. An enlarged trajectory diagram of the beam traversing the quadrupole triplet lens in both CDC ($x-z$) and DCD ($y-z$) planes under the following conditions:
 $L_1 = L_2 = L_3 = 11$ mm, $s_1 = s_2 = 16$ mm, $u = 2$ $v = 20$ mm,
 $v = 10$ mm, and $\beta_1 = \beta_2 = \beta_3 = 0.0268$ mm⁻¹.

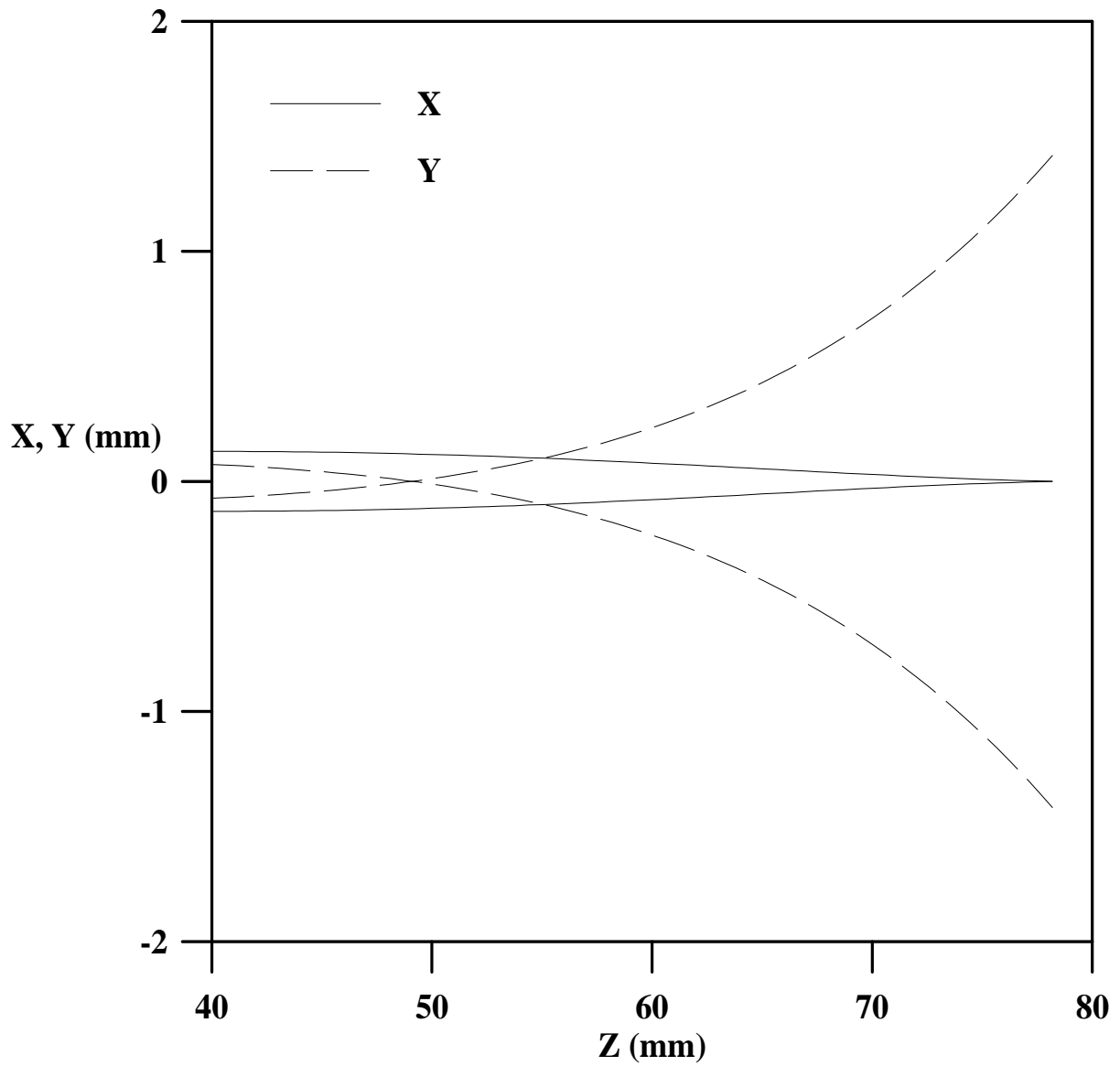


Figure 3.12b. An enlarged trajectory diagram of the beam traversing the quadrupole triplet lens in both CDC (x-z) and DCD (y-z) planes under the following conditions:

$L_1 = L_2 = L_3 = 5 \text{ mm}$, $s_1 = s_2 = 16 \text{ mm}$, $u = 2 \text{ v} = 40 \text{ mm}$, $v = 20 \text{ mm}$, and $\beta_1 = \beta_2 = \beta_3 = 0.0268 \text{ mm}^{-1}$.

3.2.4 Effect of the distances separating the lenses

Computations have been carried out to investigate the effect of the lenses separation distances s_1 and s_2 on the optical properties of the quadrupole triplet lens under the conditions $\beta_1 = \beta_2 = \beta_3 = 0.0268 \text{ mm}^{-1}$, $L_1 = L_2 = L_3 = 5 \text{ mm}$, and $u = v = 20 \text{ mm}$. The beam trajectories under the above mentioned conditions in the $x-z$ and $y-z$ planes are shown in figure 3.13 at various values of s_2 and keeping s_1 at constant value of 16 mm. The regions of widths s_1 and s_2 are field-free and thus they have weak influence on the beam trajectory as shown in figure 3.13. With the aid of the beam trajectory the focal parameters have been computed and listed in table 3.4 at various values of s_2 .

In the CDC and DCD planes the spherical aberration coefficient P is negative and remains unchanged by changing s_2 . The spherical aberration coefficient S is positive and remains constant. However, the values of S are higher than those of P . The negative and positive signs of P and S respectively may be employed in the process of correcting an equivalent spherical aberration present in an ion-optical instrument.

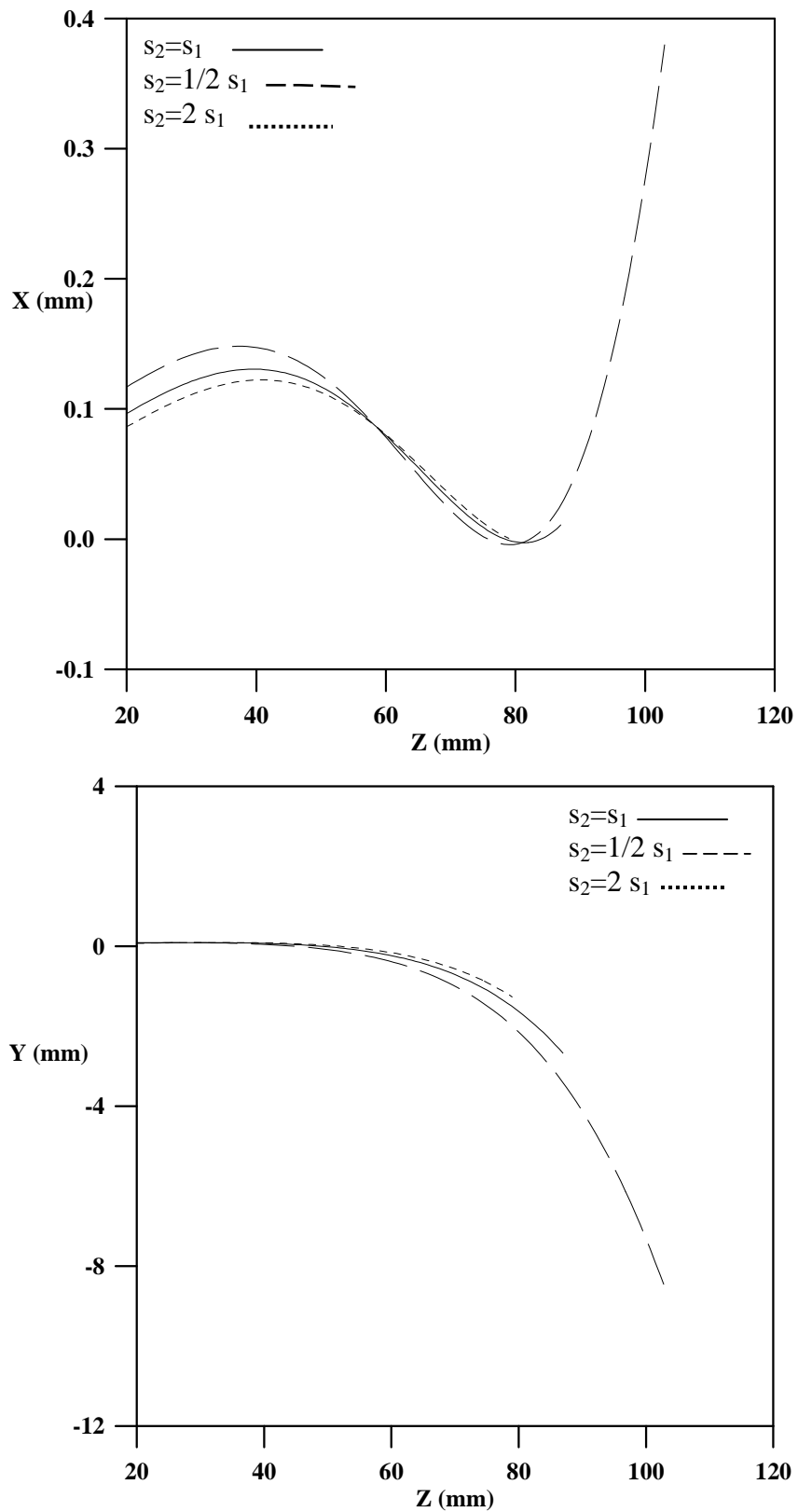


Figure 3.13. Beam trajectory in the quadrupole triplet lens at various values of s_2 ($s_1 = 16$ mm) in both CDC ($x-z$) and DCD ($y-z$) planes at $\beta_1 = \beta_2 = \beta_3 = 0.0268$ mm⁻¹, $L_1 = L_2 = L_3 = 5$ mm, and $u = v = 20$ mm.

Table 3.4

Focal parameters of the quadrupole triplet lens under the following conditions:
 $\beta_1 = \beta_2 = \beta_3 = 0.0268 \text{ mm}^{-1}$, $L_1 = L_2 = L_3 = 5 \text{ mm}$, $u = v = 20 \text{ mm}$.

$s_1 = s_2 = 16 \text{ mm}$	$s_1 = 1/2 \ s_2 = 16 \text{ mm}$ $s_2 = 32 \text{ mm}$	$s_1 = 2 \ s_2 = 16 \text{ mm}$ $s_2 = 8 \text{ mm}$
$P_{\text{CDC}} = -4.06 \text{ mm}$	$P_{\text{CDC}} = -4.06 \text{ mm}$	$P_{\text{CDC}} = -4.06 \text{ mm}$
$P_{\text{DCD}} = -8.88 \text{ mm}$	$P_{\text{DCD}} = -8.88 \text{ mm}$	$P_{\text{DCD}} = -8.88 \text{ mm}$
$S_{\text{CDC}} = 36.96 \text{ mm}$	$S_{\text{CDC}} = 36.96 \text{ mm}$	$S_{\text{CDC}} = 36.96 \text{ mm}$
$S_{\text{DCD}} = 25.76 \text{ mm}$	$S_{\text{DCD}} = 25.76 \text{ mm}$	$S_{\text{DCD}} = 25.76 \text{ mm}$
$F_{\text{CDC}} = -2.44 \text{ mm}$	$F_{\text{CDC}} = -2.00 \text{ mm}$	$F_{\text{CDC}} = -3.31 \text{ mm}$
$F_{\text{DCD}} = 0.51 \text{ mm}$	$F_{\text{DCD}} = 0.16 \text{ mm}$	$F_{\text{DCD}} = 1.06 \text{ mm}$
$ P_{\text{CDC}}/F_{\text{CDC}} = 1.66$	$ P_{\text{CDC}}/F_{\text{CDC}} = 2.03$	$ P_{\text{CDC}}/F_{\text{CDC}} = 1.23$
$ P_{\text{DCD}}/F_{\text{DCD}} = 17.41$	$ P_{\text{DCD}}/F_{\text{DCD}} = 55.50$	$ P_{\text{DCD}}/F_{\text{DCD}} = 8.38$
$ S_{\text{CDC}}/F_{\text{CDC}} = 15.15$	$ S_{\text{CDC}}/F_{\text{CDC}} = 18.48$	$ S_{\text{CDC}}/F_{\text{CDC}} = 11.17$
$ S_{\text{DCD}}/F_{\text{DCD}} = 50.51$	$ S_{\text{DCD}}/F_{\text{DCD}} = 161.00$	$ S_{\text{DCD}}/F_{\text{DCD}} = 24.30$
$Z_{\text{iCDC}} = -55.61 \text{ mm}$	$Z_{\text{iCDC}} = -80.49 \text{ mm}$	$Z_{\text{iCDC}} = -46.55 \text{ mm}$
$Z_{\text{iDCD}} = -37.13 \text{ mm}$	$Z_{\text{iDCD}} = -37.38 \text{ mm}$	$Z_{\text{iDCD}} = -36.54 \text{ mm}$
$M_{\text{CDC}} = 1.09$	$M_{\text{CDC}} = 1.09$	$M_{\text{CDC}} = 1.09$
$M_{\text{DCD}} = 0.93$	$M_{\text{DCD}} = 0.93$	$M_{\text{DCD}} = 0.93$
$M = 1.02$	$M = 1.02$	$M = 1.02$

The sign of the focal length F indicates for a diverging and converging lens in the CDC and DCD planes respectively. The conditions of the second column of table 3.4 gave rise to the lowest possible focal lengths when focusing is achieved in the x - z and y - z planes shown in figure 3.14. The crossover in the x - z plane is situated at $z = 75.85$ mm i.e. within the field-free region of width s_2 . In the y - z plane the crossover is found at $z = 45.6$ mm where the field of lens Q_2 exists. In the DCD plane the position of the focal plane Z_i remains unchanged by changing s_2 as indicated in table 3.4. The value of s_2 affects Z_i in the CDC plane.

The lowest possible relative spherical aberration coefficients P/F and S/F in both CDC and DCD planes are found under the conditions listed in the third column of table 3.4. However, their values are high when compared with those in the third column of table 3.1. A diagram of the beam focusing for this case is shown in figure 3.15. In x - z plane the beam intersects the optical axis at $z = 79$ mm where $v = 20$ mm whereas in the y - z plane the point of intersection is at $z = 52$ mm i.e. within s_2 .

Table 3.4 shows that s_2 has no effect on the magnification in both CDC and DCD planes. As a result the total magnification M remains constant of about unity with the variations of s_2 . Thus, one may conclude that the total magnification of the quadrupole triplet lens under consideration remains constant at a value of about unity under the various conditions that have been imposed on the lens. Therefore, the magnification, in general, does not exceed unity when one takes into account beam focusing in the x - z and y - z planes to achieve lowest focal length or lowest spherical aberration coefficients.

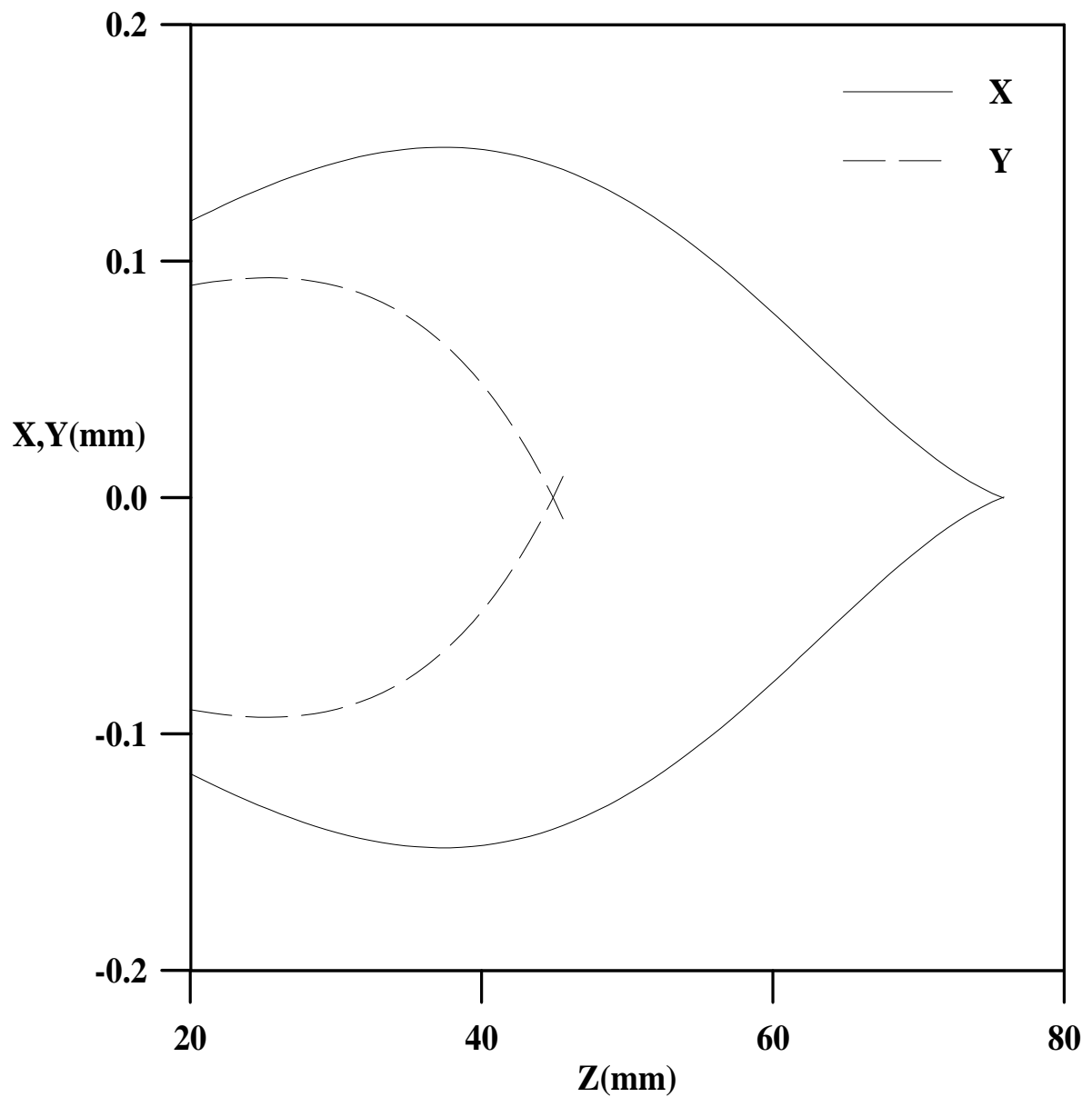


Figure 3.14. An enlarged trajectory diagram of the beam traversing the quadrupole triplet lens in both CDC ($x-z$) and DCD ($y-z$) planes under the following conditions:

$L_1 = L_2 = L_3 = 5$ mm, $u = v = 20$ mm, $s_1 = 1/2$ $s_2 = 16$ mm, $s_2 = 32$ mm, and $\beta_1 = \beta_2 = \beta_3 = 0.0268$ mm^{-1} .

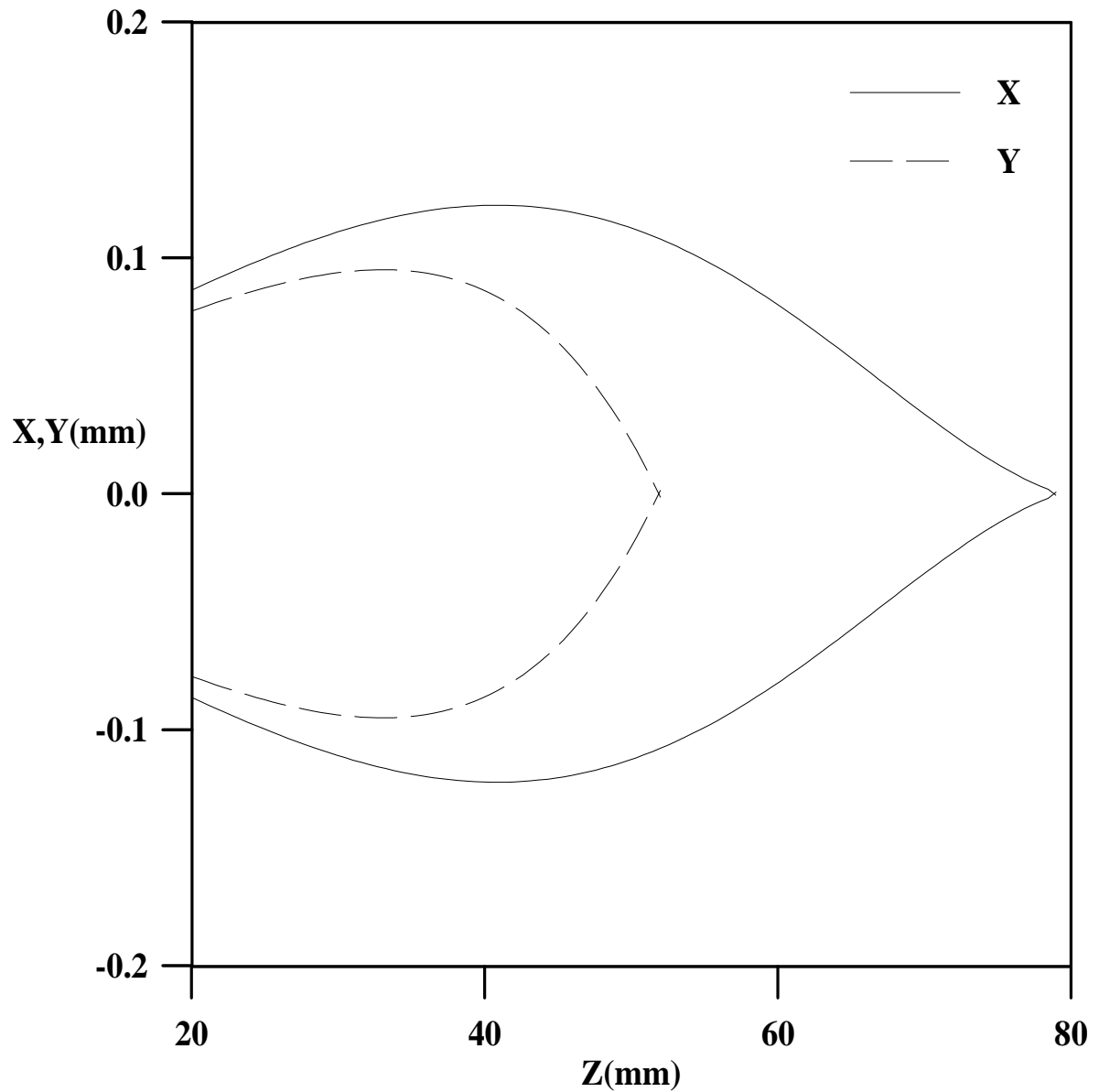


Figure 3.15. An enlarged trajectory diagram of the beam traversing the quadrupole triplet lens in both CDC ($x-z$) and DCD ($y-z$) planes under the following conditions:
 $L_1 = L_2 = L_3 = 5 \text{ mm}$, $u = v = 20 \text{ mm}$, $s_1 = 2 s_2 = 16 \text{ mm}$,
 $s_2 = 8 \text{ mm}$, and $\beta_1 = \beta_2 = \beta_3 = 0.0268 \text{ mm}^{-1}$.

3.3 Special Performances of the Quadrupole Triplet Lens

The main function of quadrupole lenses in a system of accelerated charged particles is to reduce spherical aberrations and if astigmatic properties are needed. The computations of the present work have shown that there are no optical advantages in operating the quadrupole triplet lens to perform lowest focal length since the spherical aberration coefficients P and S and the relative aberration coefficients P/F and S/F will become high and undesirable in both CDC and DCD planes. In another example, the lowest possible focal lengths that could be achieved by the quadrupole triplet lens under consideration have been determined by imposing the conditions shown in table 3.5.

The trajectory of the beam traversing the quadrupole triplet lens under the conditions of table 3.5 is shown in figure 3.16 in two and three dimensions. The triplet lens is a diverging one in both CDC and DCD planes. The focal lengths are extremely small but the resulting spherical aberration coefficients are high particularly S_{CDC} and S_{DCD} . Consequently, the relative spherical aberration coefficients are very high and undesirable. Therefore, one may conclude that operation of the quadrupole lens to perform the lowest focal lengths needs to be avoided.

Performance of the quadrupole triplet lens in order to give rise to the lowest spherical aberration coefficients is found under the conditions shown in table 3.6. In this case the trajectory of the beam traversing the triplet lens is shown in figure 3.17. It is seen that in the y - z plane the beam converges towards the z -axis at $y = 0.002$ mm and $z = 57$ mm which is situated within the field-free region s_2 ; it is then brought into focus at the

Table 3.5

Parameters of the quadrupole triplet lens for lowest focal length under the following conditions:

$$\beta_1 = \beta_3 = 1/2 \beta_2 = 0.0268 \text{ mm}^{-1}, \beta_2 = 0.0536 \text{ mm}^{-1}, L_1 = L_2 = L_3 = 15 \text{ mm}, u = v = 20 \text{ mm}, \text{ and } s_1 = s_2 = 16 \text{ mm}.$$

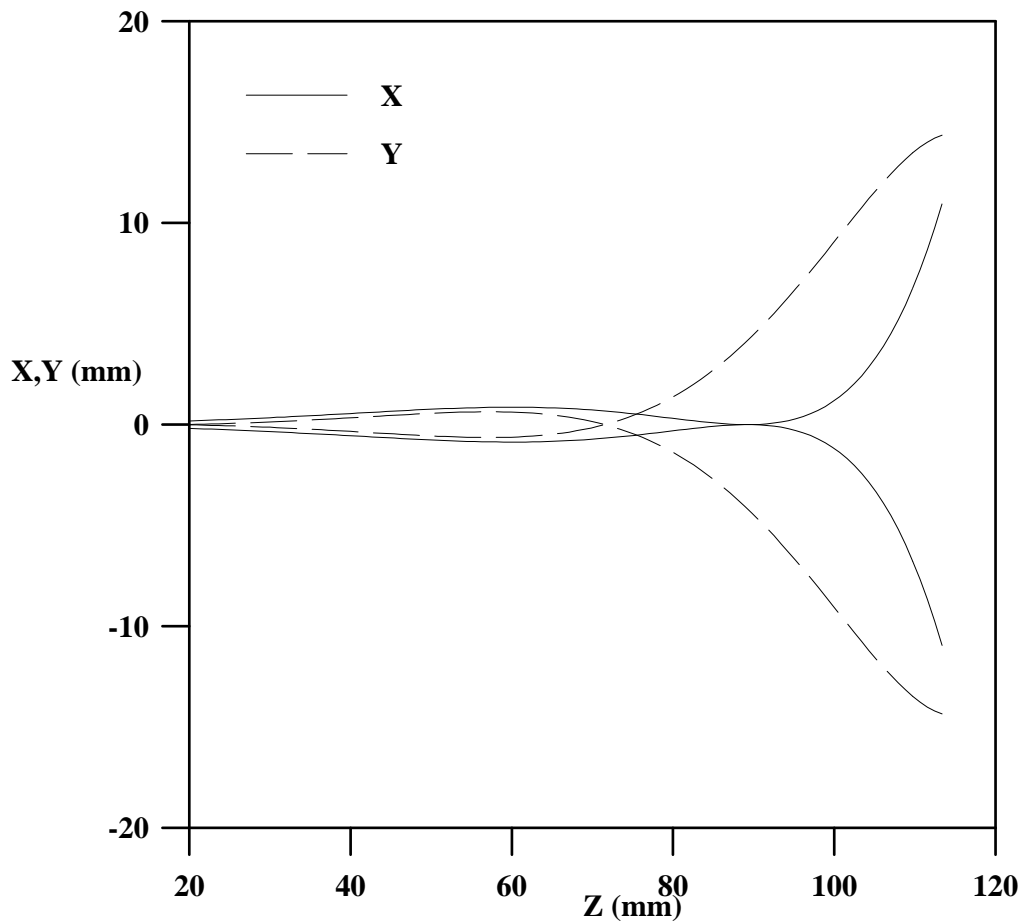
$P_{\text{CDC}} = -11.85 \text{ mm}$	$F_{\text{DCD}} = -0.002 \text{ mm}$
$P_{\text{DCD}} = -3.01 \text{ mm}$	$/P_{\text{CDC}}/ F_{\text{CDC}}/ = 9115.38$
$S_{\text{CDC}} = 11977.94 \text{ mm}$	$/P_{\text{DCD}}/ F_{\text{DCD}}/ = 1770.59$
$S_{\text{DCD}} = 1316.16 \text{ mm}$	$/S_{\text{CDC}}/ F_{\text{CDC}}/ = 9285224.81$
$F_{\text{CDC}} = -0.001 \text{ mm}$	$/S_{\text{DCD}}/ F_{\text{DCD}}/ = 774211.76$

Table 3.6

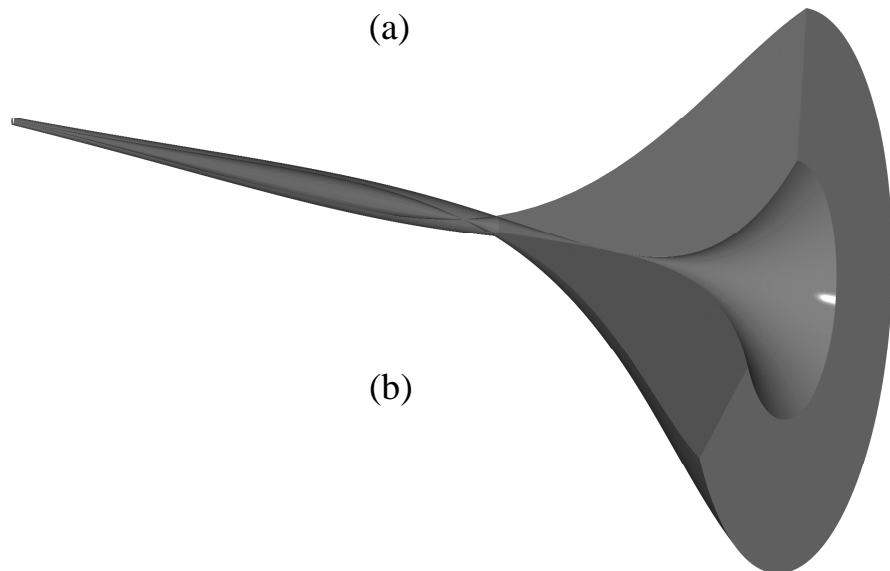
Parameters of the quadrupole triplet lens for lowest spherical aberration coefficients under the following conditions:

$$\beta_1 = \beta_3 = 0.02168 \text{ mm}^{-1}, \beta_2 = 0.01825 \text{ mm}^{-1}, L_1 = L_3 = 1/2 L_2 = 1 \text{ mm}, L_2 = 2 \text{ mm}, u = v = 20 \text{ mm}, \text{ and } s_1 = s_2 = 18 \text{ mm}.$$

$P_{\text{CDC}} = 0.28 \text{ mm}$	$F_{\text{DCD}} = 0.12 \text{ mm}$
$P_{\text{DCD}} = 0.60 \text{ mm}$	$/P_{\text{CDC}}/ F_{\text{CDC}}/ = 0.0096$
$S_{\text{CDC}} = 14.08 \text{ mm}$	$/P_{\text{DCD}}/ F_{\text{DCD}}/ = 5.00$
$S_{\text{DCD}} = 12.55 \text{ mm}$	$/S_{\text{CDC}}/ F_{\text{CDC}}/ = 0.48$
$F_{\text{CDC}} = 29.25 \text{ mm}$	$/S_{\text{DCD}}/ F_{\text{DCD}}/ = 104.58$



(a)

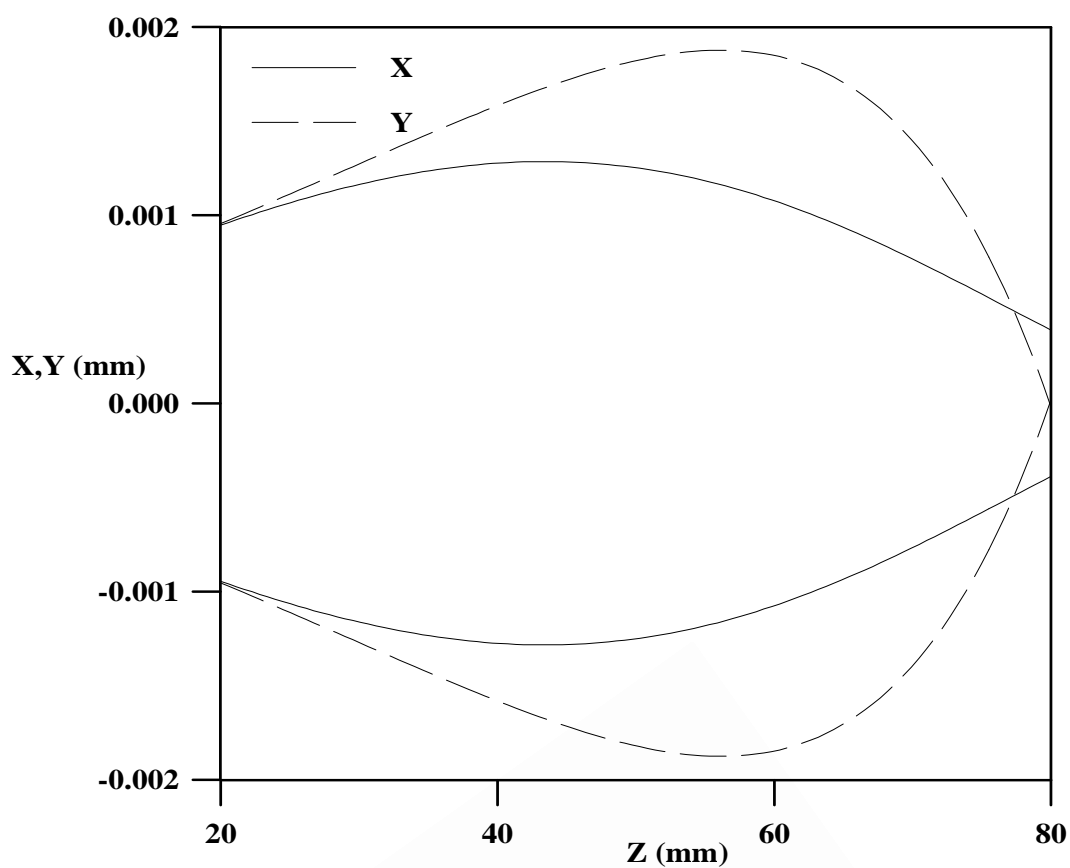


(b)

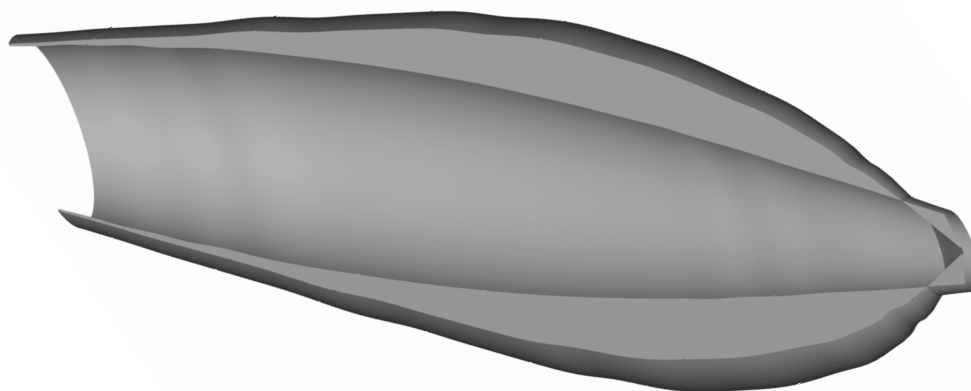
Figure 3.16. (a) Trajectory of the beam traversing the quadrupole triplet lens in the x - z and y - z planes that gave rise to the lowest focal lengths.

(b) The corresponding three-dimensional beam trajectory diagram determined by AutoCAD under the following conditions:

$$L_1 = L_2 = L_3 = 15 \text{ mm}, u = v = 20 \text{ mm}, s_1 = s_2 = 16 \text{ mm}, \\ \beta_1 = \beta_3 = 1/2 \beta_2 = 0.0268 \text{ mm}^{-1}, \text{ and } \beta_2 = 0.0536 \text{ mm}^{-1}.$$



(a)



(b)

Figure 3.17. (a) Trajectory of the beam traversing the quadrupole triplet lens in the x - z and y - z planes that gave rise to the lowest spherical aberration coefficients.

(b) The corresponding three-dimensional beam trajectory diagram determined by AutoCAD under the following conditions:

$L_1 = L_3 = 1/2 L_2 = 1$ mm, $L_2 = 2$ mm, $u = v = 20$ mm, $s_1 = s_2 = 18$ mm, $\beta_1 = \beta_3 = 1/2 \beta_2 = 0.02168$ mm⁻¹, and $\beta_2 = 0.01825$ mm⁻¹.

point where $z = 80$ mm i.e. $v = 20$ mm. In the x - z plane the beam does not intersect the z -axis at $v = 20$ mm. The extremely small value of the radial height of the beam above the z -axis suggests that these rays are paraxial. The computed spherical aberration coefficients listed in table 3.6 indicate that their values are very small; they are the lowest coefficients that have been achieved in the present work under various conditions. However, one should make it clear that from the practical point of view it is extremely difficult to assemble such triplet lens due to the short length of the electrodes where $L_1 = L_3 = 1$ mm and $L_2 = 2$ mm. Thus, a compromise is necessary in order to gain the advantages of the quadrupole triplet lens and make it practically possible to visualize.

3.4 Single Focus Quadrupole Triplet Lens

Application of quadrupole triplet lenses in an ion-optical instrument such as an ion implanter is usually intended to produce a single focus common for the x - z and y - z planes. Computations have been carried out to achieve this special case. In the present work it has been found that a single focus (or stigmatic focusing) can be obtained under the following conditions: $L_1 = L_2 = L_3 = 5$ mm, $\beta_1 = \beta_3 = 0.0268$ mm⁻¹, $\beta_2 = 0.0487$ mm⁻¹, $s_1 = s_2 = 16$ mm and $u = v = 20$ mm. It is seen that the excitation parameter of lens Q_2 is higher than that applied on lenses Q_1 and Q_3 .

Figure 3.18 shows the single focus beam trajectory in two and three dimensions respectively. Figure 3.19 depicts a three-dimensional diagram of the paraxial charged-particles beam traversing the three excited quadrupole lenses that gave rise to a single focus situated in the field-free region outside the field of lens Q_3 under the above mentioned conditions.

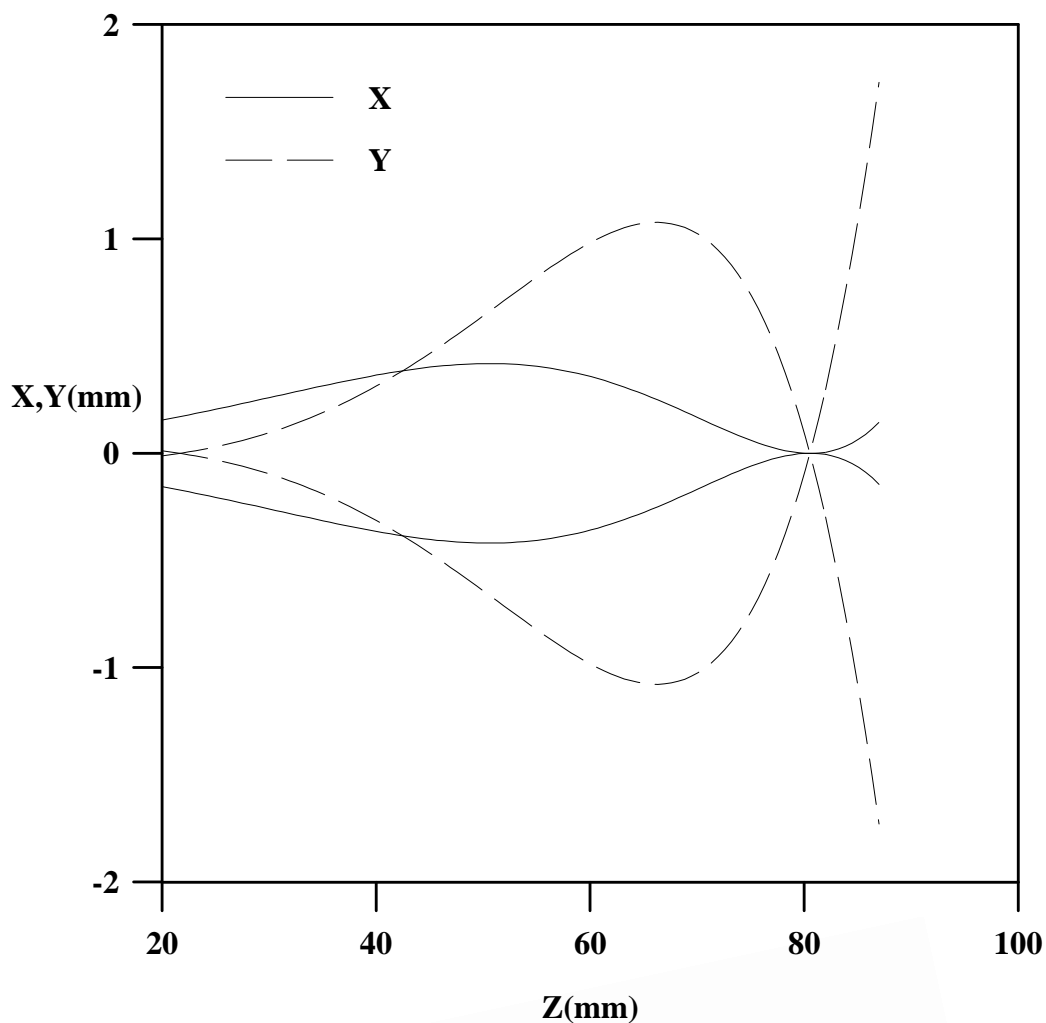
The optical properties of the triplet lens under stigmatic focusing are listed in table 3.7. It is seen that the focal lengths are very small. The aberration coefficients are higher than the corresponding lowest values listed in table 3.6. The values of these aberration coefficients appear to be a good compromise if one aims at achieving a single focus electrostatic quadrupole triplet lens.

Table 3.7

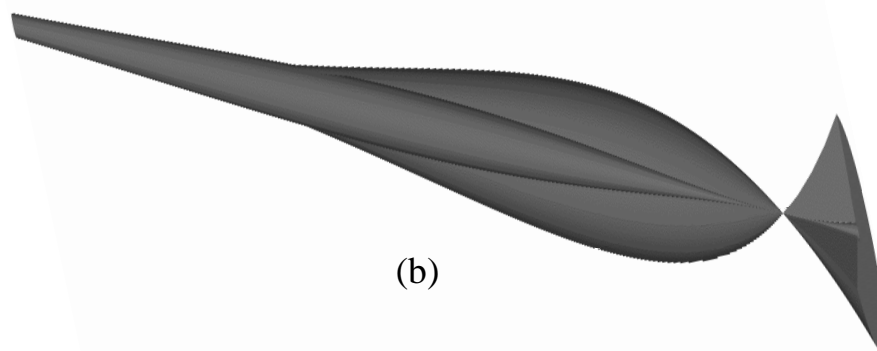
Parameters of the quadrupole triplet lens for stigmatic focusing under the following conditions:

$\beta_1 = \beta_3 = 0.0268 \text{ mm}^{-1}$, $\beta_2 = 0.0487 \text{ mm}^{-1}$, $L_1 = L_2 = L_3 = 5 \text{ mm}$,
 $u = v = 20 \text{ mm}$, and $s_1 = s_2 = 16 \text{ mm}$.

$P_{\text{CDC}} = -4.51 \text{ mm}$	$/P_{\text{CDC}}/ F_{\text{CDC}}/ = 14.88$
$P_{\text{DCD}} = -28.85 \text{ mm}$	$/P_{\text{DCD}}/ F_{\text{DCD}}/ = 31.70$
$S_{\text{CDC}} = 53.97 \text{ mm}$	$/S_{\text{CDC}}/ F_{\text{CDC}}/ = 178.12$
$S_{\text{DCD}} = 31.10 \text{ mm}$	$/S_{\text{DCD}}/ F_{\text{DCD}}/ = 34.06$
$F_{\text{CDC}} = -0.30 \text{ mm}$	$M_{\text{CDC}} = 1.00$
$F_{\text{DCD}} = -0.91 \text{ mm}$	$M_{\text{DCD}} = 1.00$
$Z_{\text{iCDC}} = -76.35 \text{ mm}$	$M = 1.00$
$Z_{\text{iDCD}} = -33.89 \text{ mm}$	



(a)



(b)

Figure 3.18. (a) Beam trajectory in a quadrupole triplet lens for a single focus in both x - z and y - z planes (stigmatic focusing).

(b) The corresponding three-dimensional diagram of the beam trajectory determined by AutoCAD under the following conditions:

$$L_1 = L_2 = L_3 = 5 \text{ mm}, \quad u = v = 20 \text{ mm}, \quad s_1 = s_2 = 16 \text{ mm}, \\ \beta_1 = \beta_3 = 0.0268 \text{ mm}^{-1}, \quad \text{and} \quad \beta_2 = 0.0487 \text{ mm}^{-1}.$$

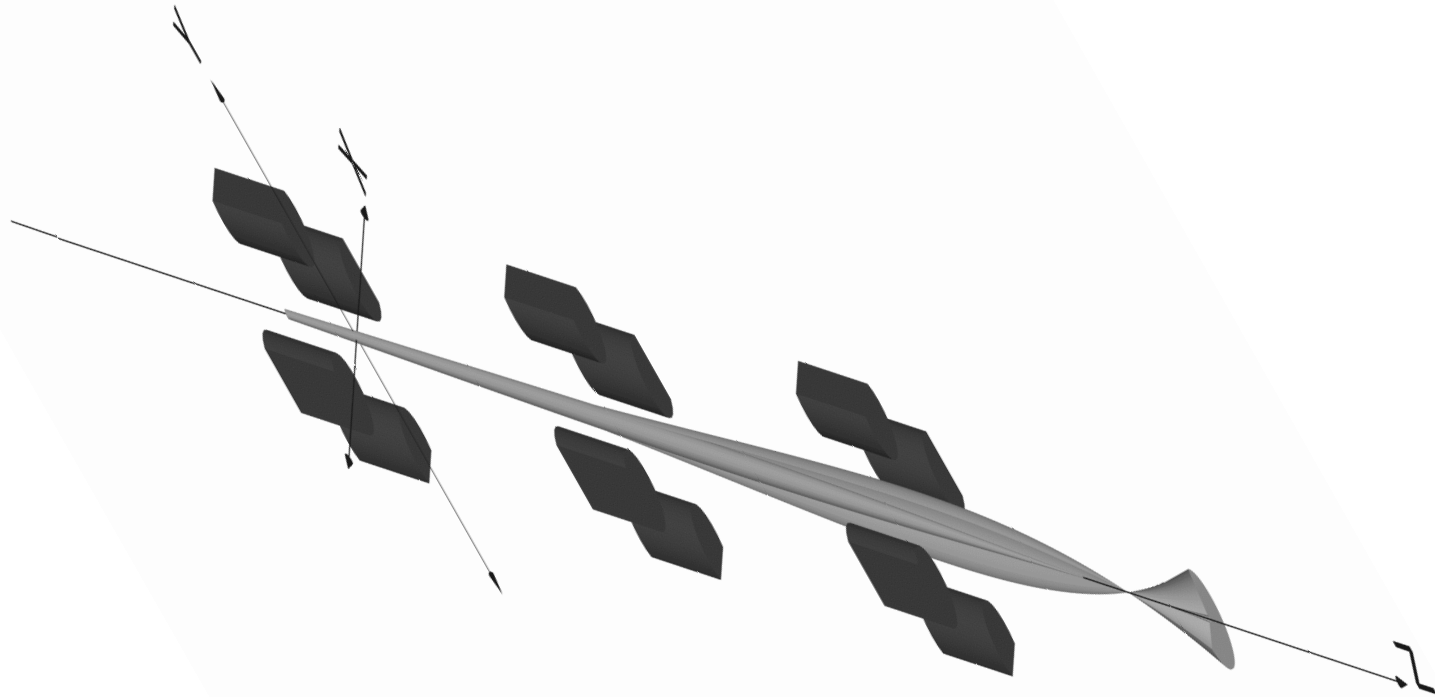


Figure 3.19. A three-dimensional diagram of the electrodes of the electrostatic quadrupole triplet lens with trajectory that gave rise to a common focus in x - z and y - z planes under the following conditions:

$L_1 = L_2 = L_3 = 5 \text{ mm}$, $s_1 = s_2 = 16 \text{ mm}$, $u = v = 20 \text{ mm}$, $\beta_1 = \beta_3 = 0.0268 \text{ mm}^{-1}$, and $\beta_2 = 0.0487 \text{ mm}^{-1}$.

3.5 Antisymmetric Quadrupole Triplet Lens

In the present work the focal properties of the quadrupole triplet lens have been computed under various geometrical and operational conditions. The excitation parameter and the electrodes length of lenses Q_1 and Q_3 were considered either equal to or a fraction of those in lens Q_2 . Under these conditions the triplet lens has about its middle lens some kind of symmetry, which is not always necessary in designing such lenses. A quadrupole triplet lens is considered antisymmetric if three different excitation parameters are applied and if the lengths of the electrodes of the three lenses are not equal. An investigation on antisymmetric quadrupole lens will be a lengthy process since there are so many variables. Thus one example has been considered to illustrate the behaviour of antisymmetric quadrupole lens.

The focal properties of a geometrically symmetric quadrupole triplet lens have been investigated when three different excitation parameters are applied on the lenses. The trajectory of the incoming paraxial charged-particles beam traversing the triplet lens is shown in figure 3.20 under the following conditions: $\beta_1 = 0.0145 \text{ mm}^{-1}$, $\beta_2 = 0.0268 \text{ mm}^{-1}$, $\beta_3 = 0.0268 \text{ mm}^{-1}$, $L_1 = L_2 = L_3 = L = 5 \text{ mm}$, $s_1 = s_2 = s = 16 \text{ mm}$, and $u = v = 20 \text{ mm}$. These values have been chosen in order to achieve focusing along the optical axis z in both the x - z and y - z planes. It is seen that a crossover at $z = 81.36 \text{ mm}$ is found in the x - z plane whereas that in the y - z plane is situated at $z = 46.92 \text{ mm}$. With the aid of this trajectory the focal parameters have been computed and listed in table 3.8. These parameters may be compared with those of the geometrically equivalent triplet lens given in the first column of table 3.1. It is seen that there is an insignificant change in the spherical aberration coefficient S , which

suggests that under the same geometrical conditions, S is little affected by variations in β . However, the spherical aberration coefficients P and S have improved. The relative spherical aberration coefficients P/F and S/F of the antisymmetric triplet lens are better than those of the symmetric as indicated in tables 3.8 and 3.1 respectively. Furthermore, both tables show that the total magnification of unity is not affected by applying three different excitations.

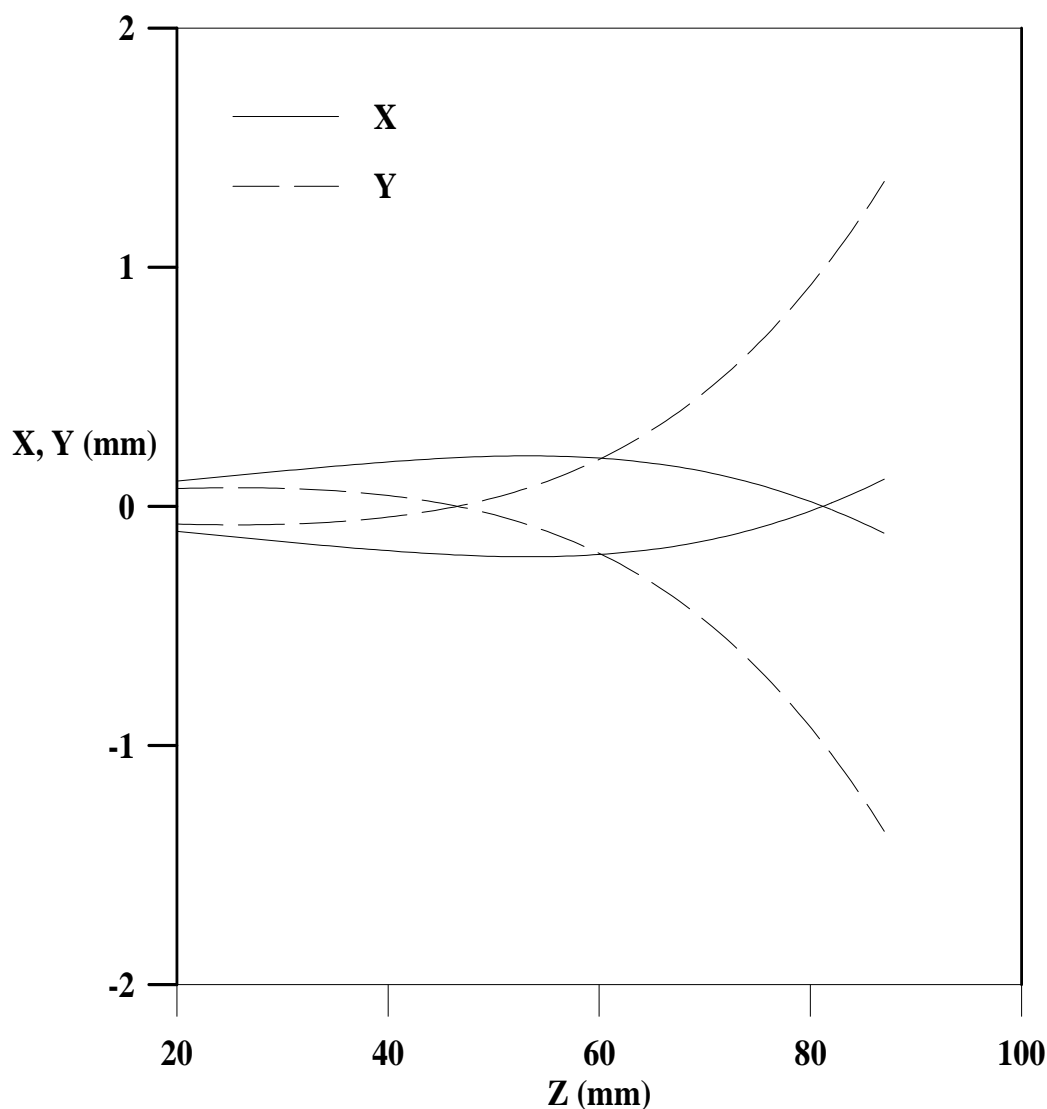


Figure 3.20. A diagram of the beam trajectory in CDC ($x-z$) and DCD ($y-z$) planes for an antisymmetric quadrupole triplet lens under the following conditions: $\beta_1 = 0.0145 \text{ mm}^{-1}$, $\beta_2 = 0.0268 \text{ mm}^{-1}$, $\beta_3 = 0.0268 \text{ mm}^{-1}$, $L_1 = L_2 = L_3 = 5 \text{ mm}$, $s_1 = s_2 = 16 \text{ mm}$, and $u = v = 20 \text{ mm}$.

Thus it appears that an antisymmetric quadrupole triplet lens has the advantage that it may give rise to desirable focal properties. Therefore, such type of lenses would require further investigations in future work.

Table 3.8

Focal parameters of the antisymmetric quadrupole triplet lens under the following conditions:

$$\beta_1 = 0.0145 \text{ mm}^{-1}, \beta_2 = 0.0268 \text{ mm}^{-1}, \beta_3 = 0.0268 \text{ mm}^{-1},$$

$$L_1 = L_2 = L_3 = 5 \text{ mm}, u = v = 20 \text{ mm}, \text{ and } s_1 = s_2 = 16 \text{ mm}.$$

$P_{\text{CDC}} = 1.25 \text{ mm}$	$ P_{\text{CDC}}/ F_{\text{CDC}} = 0.22$
$P_{\text{DCD}} = -7.03 \text{ mm}$	$ P_{\text{DCD}}/ F_{\text{DCD}} = 6.45$
$S_{\text{CDC}} = 14.42 \text{ mm}$	$ S_{\text{CDC}}/ F_{\text{CDC}} = 2.53$
$S_{\text{DCD}} = 20.56 \text{ mm}$	$ S_{\text{DCD}}/ F_{\text{DCD}} = 18.86$
$F_{\text{CDC}} = 5.7 \text{ mm}$	$M_{\text{CDC}} = 1.03$
$F_{\text{DCD}} = 1.09 \text{ mm}$	$M_{\text{DCD}} = 0.98$
$Z_{\text{iCDC}} = -62.79 \text{ mm}$	$M = 1.01$
$Z_{\text{iDCD}} = -37.25 \text{ mm}$	

4. CONCLUSIONS AND RECOMMENDATIONS FOR FUTURE WORK

4.1 Conclusions

It appears that the simple rectangular field model may be used to represent the axial field distribution of each electrostatic quadrupole lens constituting the triplet lens under investigation. The three-element lens system has many variable geometrical and operational parameters; thus a conclusive result is rather difficult. However, from the present investigation one may conclude the following:

(a) It has been found that under various conditions, the total magnification of the quadrupole triplet lens remained nearly unchanged at a value of about unity. This result is not a problem since the main use of quadrupole lenses is aimed at correcting spherical aberration present in the image formed by an ion-optical system without affecting its performance. The present work computations have shown that this aim can be achieved by taking advantage of the two foci that appear along the optical axis in the horizontal and vertical planes of the trajectory of charged particles traversing the three rectangular fields of the electrostatic quadrupole triplet lens.

(b) Taking into account the spherical aberration coefficients, it has been found that there is no advantage to be gained in operating the triplet lens at minimum focal lengths. However, certain geometrical and operational conditions gave rise to a triplet lens of very low spherical aberration. Such lens may be used as a good device for correcting spherical aberration.

(c) Generally, variations in the field-free regions present along the triplet lens optical axis from object to image do not necessarily improve the performance of the lens with regard to spherical aberration coefficients. In fact the main crucial geometrical and operational parameters are the electrodes length and the applied excitations respectively.

(d) The computed results have shown that it is essential to operate the middle quadrupole lens under geometrical and operational conditions that are different from those of the first and third lenses which are usually identical in all aspects. Such triplet lens is considered symmetrical.

(e) A symmetrical triplet lens that has a common focus on the optical axis for the horizontal and vertical planes of the charged-particles beam trajectory has been achieved under certain geometrical and operational conditions. This single focus lens is found to have optically acceptable spherical aberration coefficients at unit magnification.

(f) An antisymmetric quadrupole triplet lens may give rise to desirable focal properties. The choice of the lens geometrical and operational parameters depends on its function in an ion-optical system since no specific conclusion can be drawn for such lens design.

4.2 Recommendations for Future Work

The following topics may be recommended for future work:

- (a) An investigation on the design and properties of an electrostatic quadrupole triplet lens when the effect of the relativistic velocities of the charged particles is taken into account.
- (b) The effect of the charged-particles initial energy when taken into account on the optical properties of electrostatic quadrupole triplet lenses.
- (c) Design considerations of achromatic lens triplet consisting of an electrostatic and magnetic quadrupole lenses.
- (d) An investigation on antisymmetric electrostatic quadrupole triplet lenses under various geometrical and operational conditions.
- (e) Effect of other types of field distribution on the focal properties of electrostatic quadrupole triplet lenses.

Contents

vi

Synopsis iv

List of Symbols viii

1. ELECTROSTATIC QUADRUPOLE LENSES

1.1 Electrostatic Lenses 1

1.2 Quadrupole Lenses 2

1.3 Three–Element Quadrupole Lens System 5

1.4 Aim of the Project 7

2. PROPERTIES OF ELECTROSTATIC QUADRUPOLE LENSES

2.1 Field Models for Electrostatic Quadrupole Lenses 9

2.2 Quadrupole Lens Potential Distributions 12

2.3 First–Order Optical Properties for an Electrostatic
Quadrupole Lens 14

2.3.1 The equation of motion 14

2.3.2 The cardinal elements 21

2.4 Lens Aberrations Parameters 24

2.5 Spherical Aberration 25

2.6 Computer Programs 28

2.6.1 Computer program for computing the trajectory and the
first–order optical properties of a quadrupole triplet
lens 28

2.6.2 Program for computing the spherical aberration coefficients of a quadrupole triplet lens	28
--	----

3. RESULTS AND DISCUSSION

3.1 The Quadrupole Triplet Lens and Its Field	29
3.2 Beam Trajectory and Focal Properties of Triplet Lens	31
3.2.1 Three lenses of equal length	32
3.2.2 Three lenses of equal excitation	41
3.2.3 Effect of object and image distance	48
3.2.4 Effect of the distances separating the lenses	58
3.3 Special Performances of the Quadrupole Triplet Lens	64
3.4 Single Focus Quadrupole Triplet Lens	68
3.5 Antisymmetric Quadrupole Triplet Lens	72

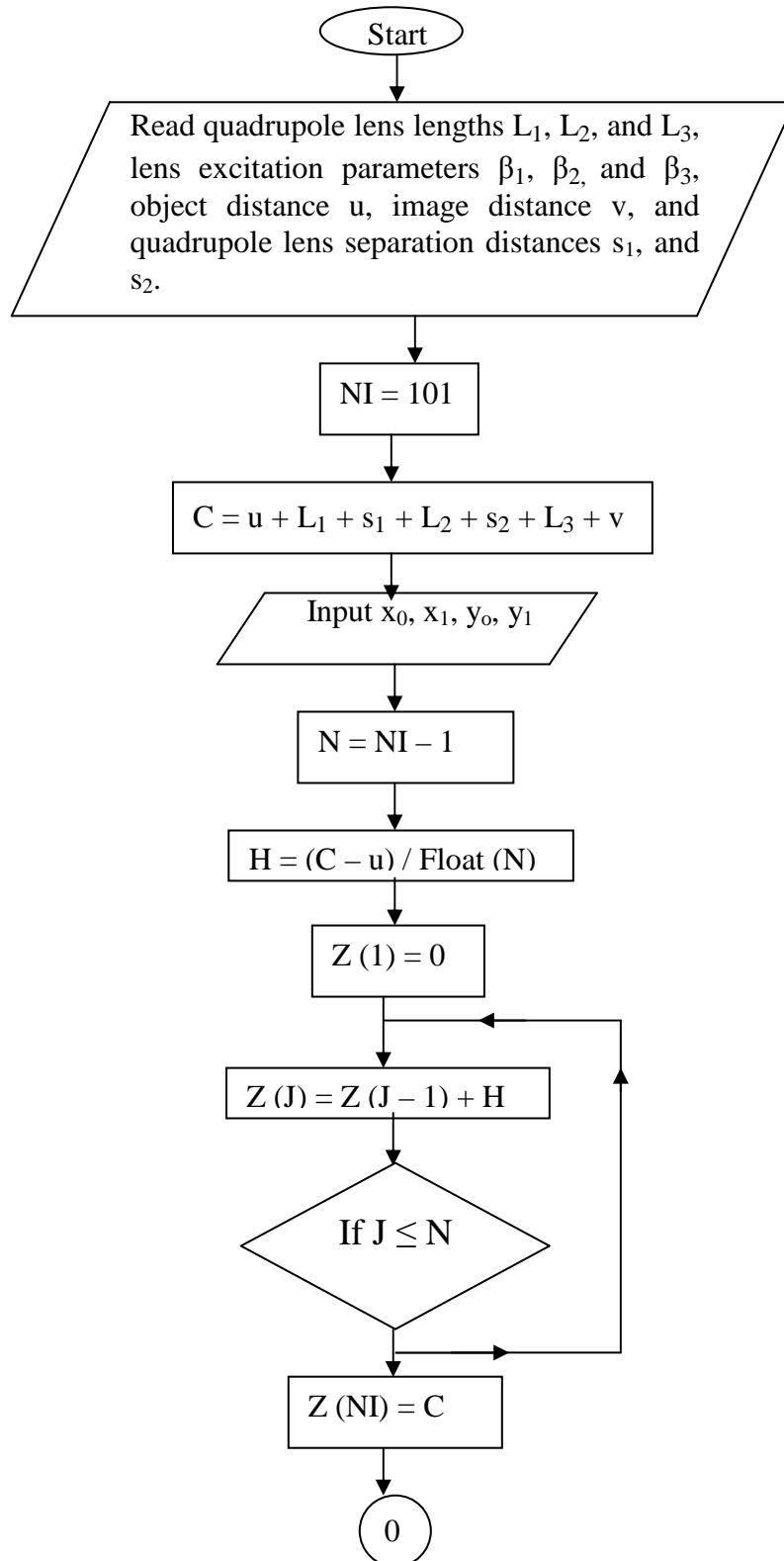
4. CONCLUSIONS AND RECOMMENDATIONS FOR FUTURE WORK

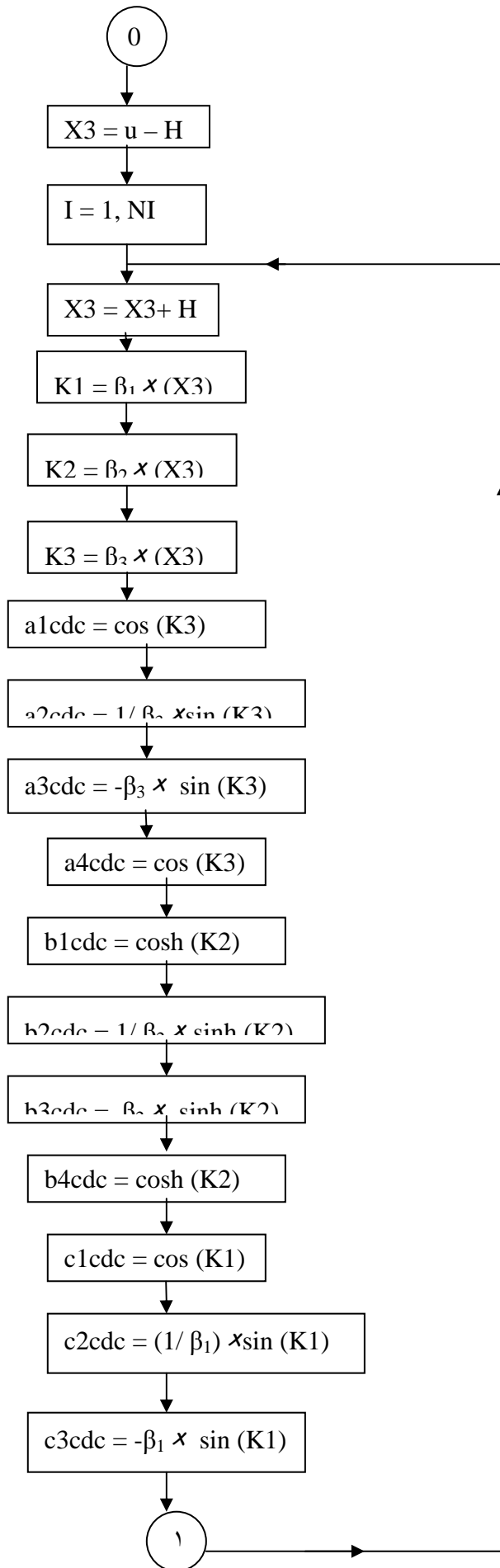
4.1 Conclusions	75
4.2 Recommendations for Future Work	77

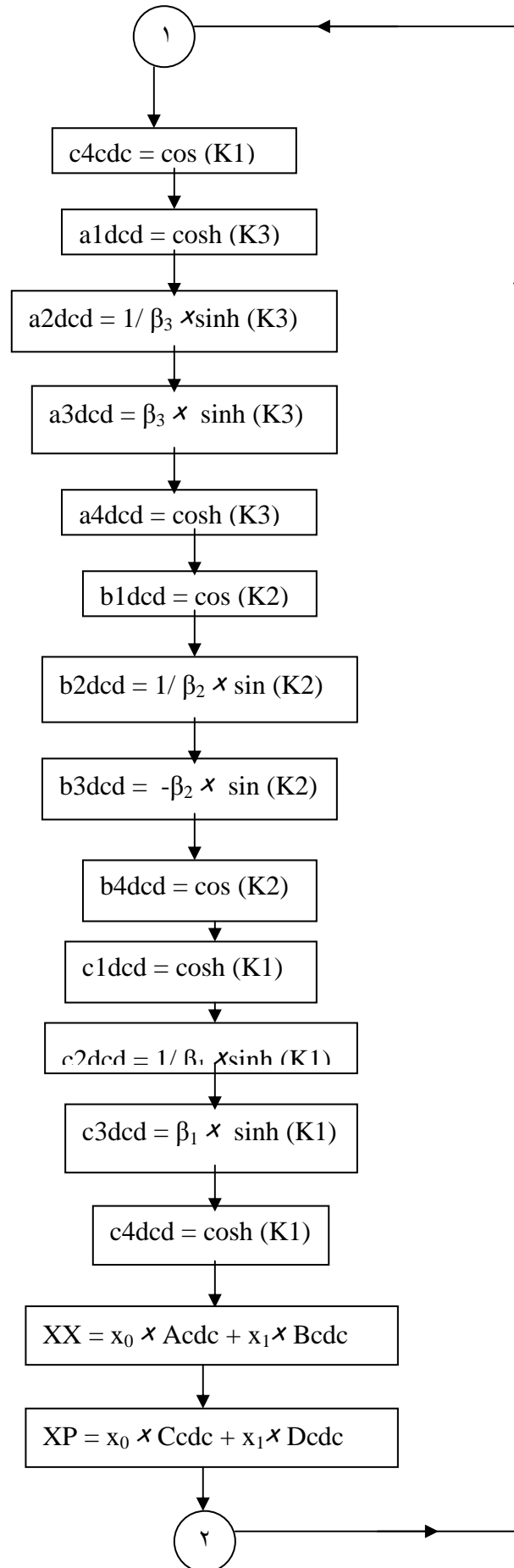
Appendices A

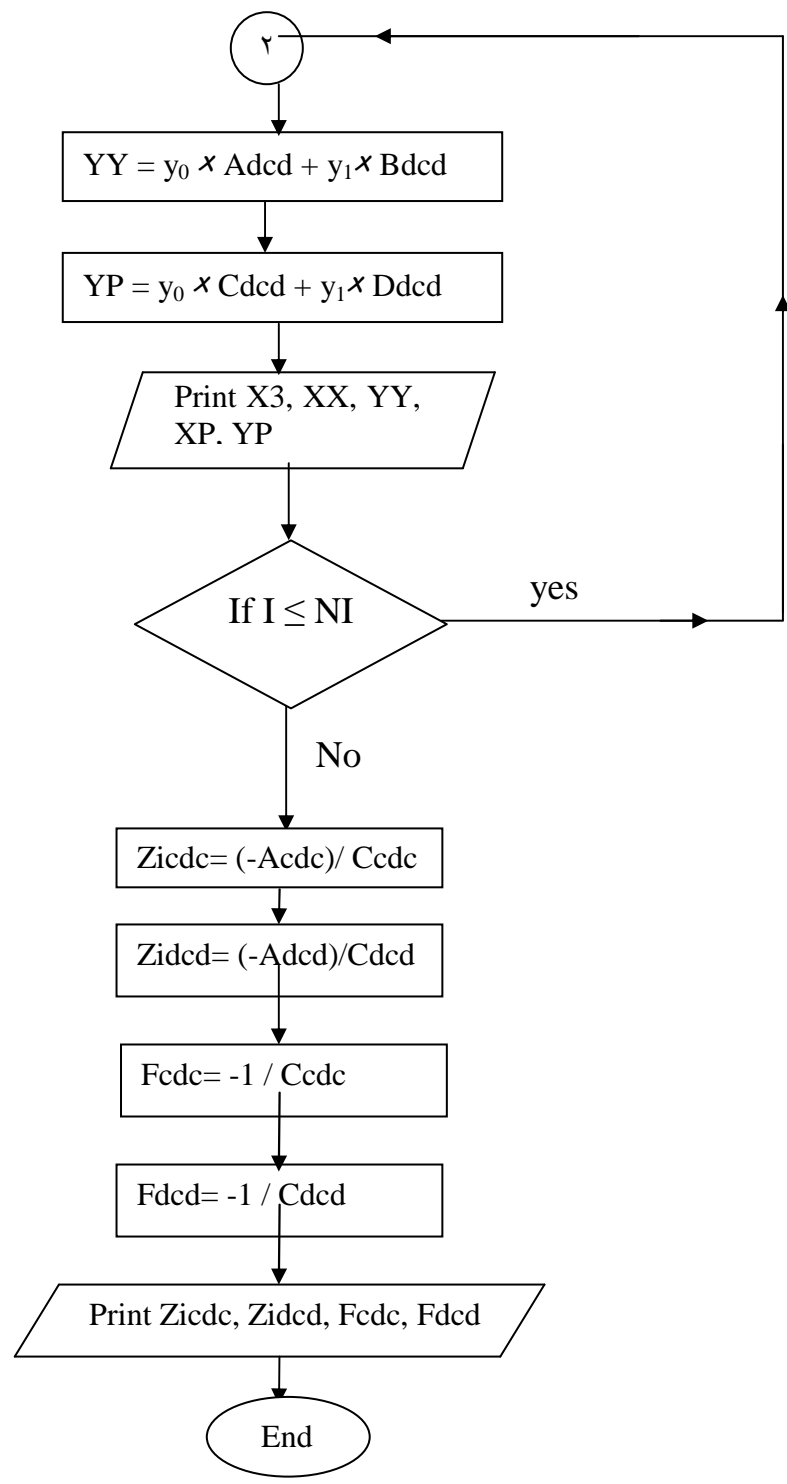
References

 A FLOW CHART FOR FORTRAN PROGRAM OF COMPUTING THE
 TRAJECTORY AND THE FIRST-ORDER OPTICAL PROPERTIES OF
 A QUADRUPOLE TRIPLET LENS

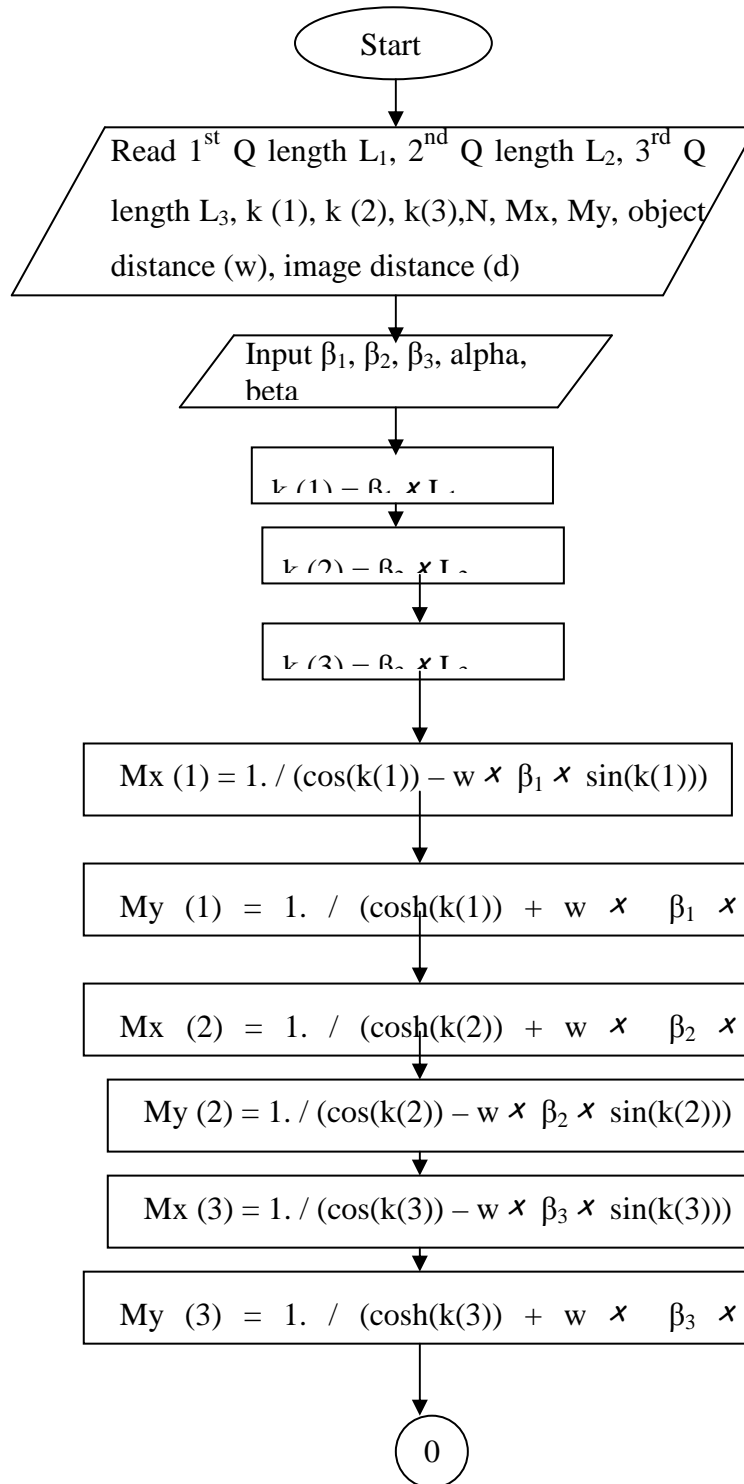


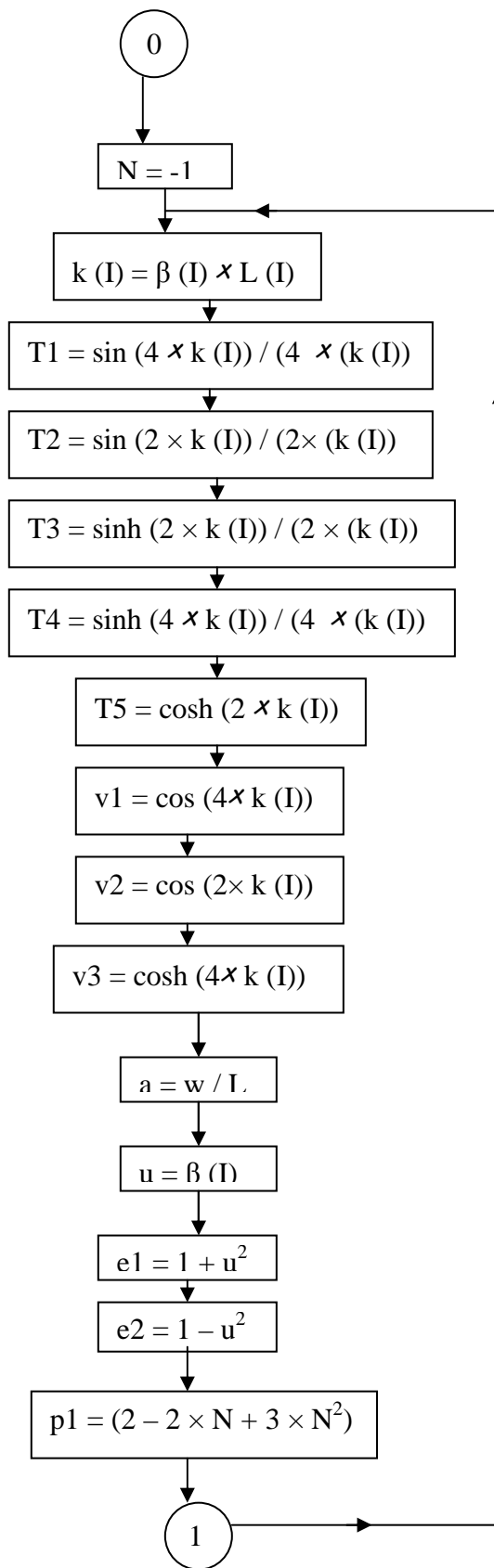


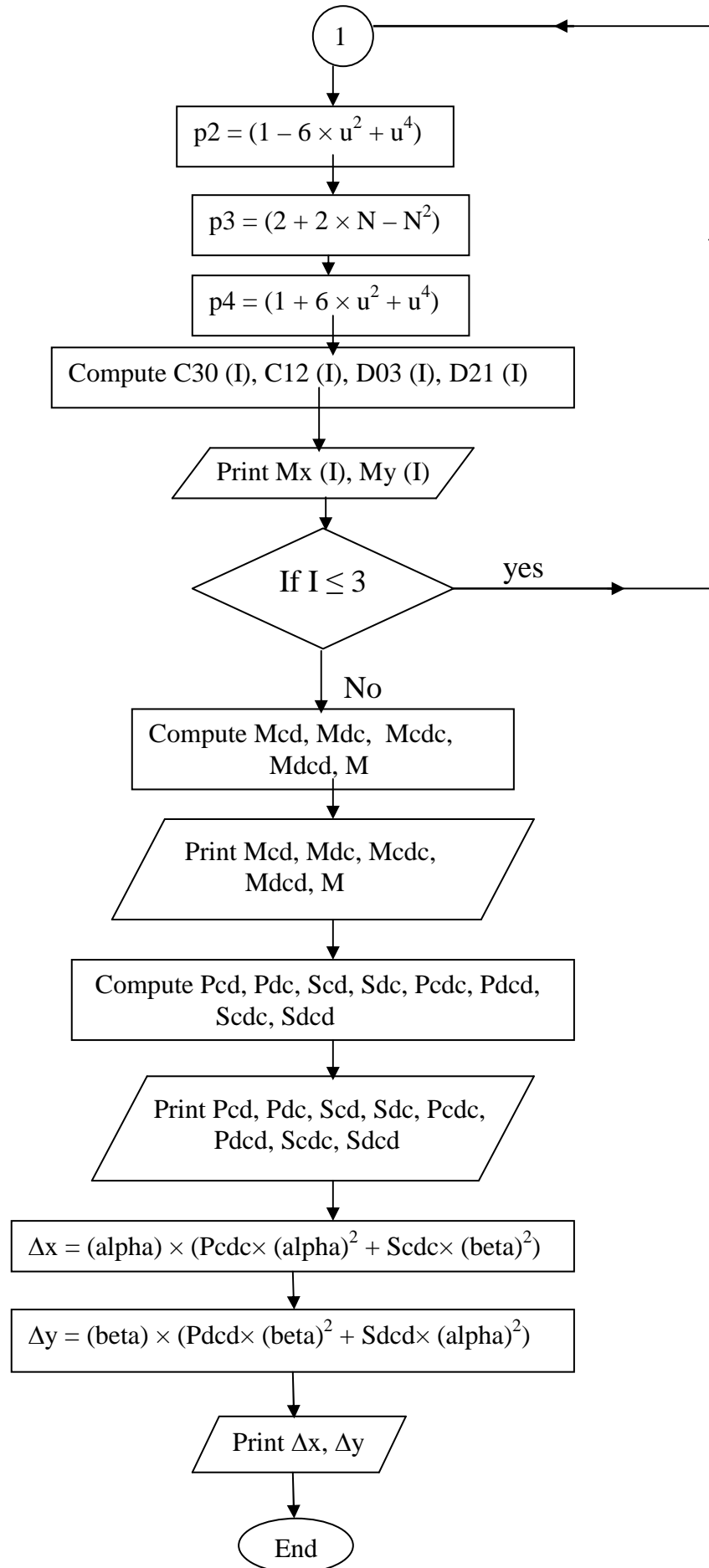




 A FLOW CHART FOR FORTRAN PROGRAM FOR COMPUTING THE
 SPHERICAL ABERRATION COEFFICIENTS OF A QUADRUPOLE
 TRIPLET LENS







List of Symbols

c	Aperture radius of the quadrupole lens (bore-radius).
C_{30}, C_{12}	Spherical aberration coefficients of the single quadrupole lens in the convergence plane.
CDC	Convergence–Divergence–Convergence plane.
DCD	Divergence–Convergence–Divergence plane.
D_{03}, D_{21}	Spherical aberration coefficients of the single quadrupole lens in the divergence plane.
F_{CDC}	Focal length of the quadrupole triplet lens in the Convergence–Divergence–Convergence plane.
F_{DCD}	Focal length of the quadrupole triplet lens in the Divergence–Convergence–Divergence plane.
F_i, F_o	Focal lengths in the image and object side respectively.
f_i, f_o	Focal points in the image and object side respectively.
$f(z)$	Potential function.
H_i, H_o	Principal planes in the image and object side respectively.
k	A coefficient accounting for the shape of the electrode.
L	Length of lens field.
L_1, L_2, L_3	Length of the first, second and third quadrupole lens respectively.
M	Total linear magnification.
M_{CD}	Magnification of the quadrupole doublet in the Convergence–Divergence plane.
M_{DC}	Magnification of the quadrupole doublet in the Divergence–Convergence plane.

M_{CDC}, M_{DCD}	Magnification of the quadrupole triplet in the Convergence–Divergence–Convergence and Divergence–Convergence–Divergence planes respectively.
P_{CD}	Spherical aberration coefficients of the quadrupole doublet lens in the Convergence–Divergence plane.
P_{CDC}	Spherical aberration coefficients of the quadrupole triplet lens in the Convergence–Divergence–Convergence plane.
P_{DC}	Spherical aberration coefficients of the quadrupole doublet lens in the Divergence–Convergence plane.
P_{DCD}	Spherical aberration coefficients of the quadrupole triplet lens in the Divergence–Convergence–Divergence plane.
Q_1	First quadrupole lens.
Q_2	Second quadrupole lens.
Q_3	Third quadrupole lens.
r	Radial displacement of the beam from the optical axis.
s_1	Distance between the first quadrupole lens Q_1 and the second quadrupole lens Q_2 .
s_2	Distance between the second quadrupole lens Q_2 and the third quadrupole lens Q_3 .
S_{CD}	Spherical aberration coefficients of the quadrupole doublet lens in the Convergence–Divergence plane.
S_{CDC}	Spherical aberration coefficients of the quadrupole triplet lens in the Convergence–Divergence–Convergence plane.
S_{DC}	Spherical aberration coefficients of the quadrupole doublet lens in the Divergence–Convergence plane.
S_{DCD}	Spherical aberration coefficients of the quadrupole triplet lens in the Divergence–Convergence–Divergence plane.

T_C, T_D	Transfer matrices of the single quadrupole lens in the convergence and divergence planes respectively.
T_{CDC}, T_{DCD}	Transfer matrices of the quadrupole triplet in the Convergence–Divergence–Convergence and Divergence–Convergence–Divergence planes respectively.
u	Object distance from starting point of the field of lens Q_1 .
$U = U(z)$	Axial potential distribution.
U_1	Electrode voltage.
U_0	Accelerating voltage.
v	Image distance from the end of the field of lens Q_3 .
z	Optical axis.
Z_{iCDC}	Focal plane in the image side of Convergence–Divergence–Convergence
Z_{iDCD}	Focal plane in the image side of Divergence–Convergence–Divergence.
Z_{oCDC}	Focal plane in the object side of Convergence–Divergence–Convergence.
Z_{oDCD}	Focal plane in the object side of Divergence–Convergence–Divergence.
α	Semi-aperture angle in the Convergence–Divergence–Convergence plane.
γ	Semi-aperture angle in the Divergence–Convergence–Divergence plane.
β	Lens excitation parameter ($\beta^2 = U_1 k / c^2 U_0$).
$\beta_1, \beta_2, \beta_3$	Lens excitation of the first, second, and third quadrupole respectively.

Synopsis

With the aid of transfer matrices method and personal computer a computational research has been carried out on the properties of a rectangular model representing the axial field of an electrostatic quadrupole triplet lens. The path of charged-particles beam traversing the rectangular fields has been determined by solving the trajectory equation of motion in Cartesian coordinates. A computer program has been written for this purpose.

The optical properties of the electrostatic quadrupole triplet lens have been computed with the aid of the beam trajectory along the lens axis. Computer programs in Fortran 77 have been written for determining the various optical properties. The computations have been mainly concentrated on determining the focal lengths and spherical aberration coefficients in both horizontal and vertical planes of the trajectory along the optical axis. The results have shown that the choice of the geometrical and operational parameters depends on the function of the electrostatic quadrupole triplet lens in a particular electron or ion-optical system.

CHAPTER ONE

ELECTROSTATIC QUADRUPOLE LENSES

CHAPTER TWO

PROPERTIES OF ELECTROSTATIC QUADRUPOLE LENSES

CHAPTER THREE

RESULTS AND DISCUSSION

CHAPTER FOUR

CONCLUSIONS AND RECOMMENDATIONS FOR FUTURE WORK

APPENDICES

REFERENCES

المستخلص

إستعانهُ بطريقتة المصفوفات الانتقاليه والحاسوب الشخصي فقد أجري بحث حاسوبي عن خواص نموذج مستطيلي يمثل المجال المحوري لعدسه ثلاثية كهروسكونيه رباعية الاقطاب، إن مسار حزمة الجسيمات المشحونه الماره خلال المجالات المستطيلية قد تم ايجاده بحل معادلة مسار الحركه بالاحداثيات الكارتيزيه إذ كتب برنامج حاسوبي لهذا الغرض.

لقد حسبت الخواص البصريه للعدسة الثلاثية الكهروسكونيه بالاستعانهُ بمسار الحزمه على امتداد محور العدسه. وكتبت برامج حاسوبيه بفورتران ٧٧ لايجاد مختلف الخواص البصريه. وتم تركيز الحسابات على ايجاد الابعاد البؤرية ومعاملات الزيوغ الكروية في كلا المستويين الافقي والعمودي للمسار على امتداد المحور البصري. وقد أظهرت النتائج أن إختيار المعلمات الهندسية والتشغيلية يعتمد على وظيفة العدسه الثلاثية الكهروسكونية الرباعية الاقطاب في منظومة بصريه ألكترونيه او أيونيه معينة.

References

Baartman, R. (1995)

Intrinsic third order aberration in electrostatic and magnetic quadrupoles

<http://www.triumf.ca/baartman/pap/pac97/quads.html>

Banford, A. P. (1966)

The transport of charged particle beams

(E. and F. N. Spon Limited, London)

Baranova, L. A. and Read, F. H. (1998)

Reduction of the chromatic and aperture aberrations of the stigmatic quadrupole lens triplet

Optik, **109**, 15–21

Baranova, L. A. and Read, F. H. (1999)

Minimisation of the aberrations of electrostatic lens systems composed of quadruple and octupole lenses

Int. J. Mass Spectrom, **189**, 19–26

Baranova, L. A. and Read, F. H. (2001)

Aberration caused by mechanical misalignment in electrostatic quadrupole lens systems

Optik, **112**, 131–138

Crewe, A.V., David, P.P., and Kopf, A. (1981)

United State Patent 4, 303, 864

Dymnikov, A. D., Fishkova, T. Ya., and Yavor, S. Ya. (1965)

Spherical aberration of compound quadrupole lenses and systems

Nucl. Instrum. Meth., **37**, 268–275

Enge, A. H. (1961)

Ion-focusing properties of a three-element quadrupole lens system

Rev. Sci. Instrum., **32**, 662–665

Fishkova, T. Ya., Baranova, L. A., and Yavor, S. Ya. (1968)

Spherical aberration of astigmatic doublet of quadrupole lenses
(rectangular model)

Sov. Phys. Tech. Phys., **13**, 520–525

Grime, G.W., and Watt, F. (1988)

Focusing proton and light ions to micron and submicron dimensions

Nucl. Instrum. Meth., **B30**, 227–234

Grivet, P. (1972)

Electron Optics

(Pergamon Press, Oxford and New York)

Hawkes, P.W. (1965/1966)

The electron optics of a quadrupole lens with triangular potential

Optik, **23**, 145–168

Hawkes, P.W. (1970)

Quadrupoles in electron lens design

Adv. Electronics and Electron Phys., Supplement 7, ed. Marton, L.

(Academic Press, New York and London)

Hawkes, P.W. and Kasper, E. (1989)

Principles of electron optics, vol.1

(Academic Press, London)

Jamieson, D. N. and Legge, G. J. F. (1987)

Aberrations of single magnetic quadrupole lenses

Nucl. Instrum. Meth., **B29**, 544–556

Larson, J. D. (1981)

Electrostatic ion optics and beam transport for ion implantation

Nucl. Instrum. Meth., **189**, 71–91

Martin, F. W. (1991)

Optical parameters of MeV ion microprobes

Nucl. Instrum. Meth., **B54**, 17–23

Nave, R. (2001)

Aberrations

<http://hyperphysics.phyastr.gsu.edu/hbase/geoopt/aberrcon.html#c2>

Okayama, S. (1989)

Electron beam lithography using a new quadrupole triplet
SPIE, Electron-beam, X-ray, and Ion-beam Technology: Submicrometer
Lithographies VIII, **1089**, pp 74–83

Okayama, S. and Kawakatsu, H. (1978)

Potential distribution and focal properties of electrostatic quadrupole lenses
J. Phys. E: Sci. Instrum., **11**, 211–216

Okayama, S. and Kawakatsu, H. (1983)

Line-focusing by means of a quadrupole lens
J. Phys. E: Sci. Instrum., **16**, 166–170

Regenstreif, E. (1967)

Focusing with quadrupole, doublet, and triplets
Focusing of Charged Particles, ed. A., Septier, pp 353–410
(Academic Press, New York)

Szilagyi, M. (1988)

Electron and ion optics
(Plenum Press, New York)

Republic of Iraq
Al-Nahrain University
College of Science



COMPUTATIONS ON THE OPTICAL PROPERTIES OF A TRIPLET ELECTROSTATIC QUADRUPOLE LENS

A Thesis

**Submitted to the College of Science at
Al-Nahrain University in Partial Fulfillment of the
Requirements for the Degree of
Master of Science**

in

Physics

by

Isra'a Lateef Mohammad Al-Omairi

(B.Sc. 2002)

in

Rabi'a Al-Aw'wal 1426 A. H.

April 2005 A. D.



جمهورية العراق
وزارة التعليم العالي والبحث العلمي
جامعة النهرين/كلية العلوم

حسابات عن الخواص البصريه لعدسه رباعيه الاقطاب كهروسكونيه ثلاثيه

رسالة

مقدمه الى كلية العلوم في جامعة النهرين

وهي جزء من متطلبات نيل درجة

ماجستير علوم

في

الفيزياء

من قبل

إسراء لطيفة محمد العميري

بكالوريوس ٢٠٠٢

في

نيسان ٢٠٠٥م

ربيع الاول ١٤٢٦هـ

Dedicated
To
My Parents
And
Brothers and Sisters

بِسْمِ اللّٰهِ الرَّحْمٰنِ الرَّحِیْمِ

(رَبِّ قَدْ أَتَيْتَنِي مِنَ الْمَلِكِ وَعَلَّمْتَنِي مِنْ تَأْوِيلِ الْأَحَادِيثِ

فَاطَرَ السَّمَاوَاتِ وَالْأَرْضِ أَنْتَ وَلِيِّ فِئَةِ الدُّنْيَا وَالْآخِرَةِ

تَوْفَنِي مُسْلِمًا وَأَلْحَقْنِي بِالصَّالِحِينَ)

صَدَقَ اللّٰهُ الْعَظِيمُ

يُوسُفُ ١٠١